PROGRESS REPORT NO. 23

covering the specific topic of

A CORRELATION OF PULSE COLUMN LIQUID-LIQUID HEAT TRANSFER

Contract No. AT-(40-1)-1320
The Performance of Contactors for
Liquid-Liquid Extraction

DEPARTMENT OF ENGINEERING RESEARCH

NORTH CAROLINA STATE COLLEGE

RALEIGH, NORTH CAROLINA

ORO-228

PROGRESS REPORT NO. 23

covering the specific topic of

A CORRELATION OF PULSE COLUMN LIQUID-LIQUID HEAT TRANSFER

Contract No. AT-(40-1)-1320
The Performance of Contactors for
Liquid-Liquid Extraction

TOPIC PERSONNEL

Graduate Committee

Dr. F. P. Pike, Dept. Chem. Eng., Chrm.
Dr. K. O. Beatty, Dept. Chem. Eng.
Dr. N. Underwood, Dept. Eng. Physics
Dr. L. S. Winton, Dept. Eng. Math.
Prof. J. F. Seely, Dept. Chem. Eng.

Department of Chemical Engineering

Dr. F. P. Pike
Mr. W. B. Barlage
Mr. Howard Prescott

Submitted by:
Frederick Philips Pike
Senior Investigator

DEPARTMENT OF ENGINEERING RESEARCH
NORTH CAROLINA STATE COLLEGE
RALEIGH, NORTH CAROLINA

October 23, 1959

A CORRELATION OF PULSE COLUMN LIQUID-LIQUID HEAT TRANSFER

William B. Barlage, Jr. and F. Philips Pike

PROJECT SUMMARY

This report is a continuation of the heat-transfer studies presented by S. C. Li and F. P. Pike in Progress Report No. 18, and those of R. P. Gardner and F. P. Pike, as presented in Progress Report No. 21. It was organized as a thesis program for Mr. William B. Barlage in partial fulfillment of the requirements for the Ph. D. Degree, in the area of Chemical Engineering.

It has been possible to obtain a good correlation of rate of heat transfer as a function of the same variables as influence mass transfer, plus the factors of magnitude and direction of the temperature difference. It is a significient point of theory that heat and mass transfer in the pulse column are influenced differently by the total throughput. The net result of this work is to demonstrate that for liquid-liquid systems, with their mobile interfaces, the traditional analogies between heat transfer and mass transfer break down.

A CORRELATION OF PULSE COLUMN LIQUID-LIQUID HEAT TRANSFER

by

WILLIAM BERDELL BARLAGE, JR.

A thesis submitted to the Graduate Faculty
of North Carolina State College
in partial fulfillment of the
requirements for the Degree of
Doctor of Philosophy

DEPARTMENT OF CHEMICAL ENGINEERING

RALEIGH

1959

APPROVED BY

Frederick Philips Pike

Chairman of Advisory Committee

To my Mother and Father whose faithful prayers and personal sacrifice have made my education possible.

BIOGRAPHY

William Berdell Barlage, Jr. was born September 1, 1932 in Philadelphia, Pennsylvania. All of his primary and secondary school training was received in Philadelphia public schools.

In September 1950, he entered Lehigh University, receiving his Bachelor of Science degree in Chemical Engineering from this institution in June 1954. In September 1954 he began graduate studies at the University of Virginia, and was a Memminger Fellow at this institution during the academic year 1954 to 1955. In September 1955 he completed all the requirements for the degree Master of Chemical Engineering at the University of Virginia, and began studies towards the Doctor of Philosophy degree at North Carolina State College. During his graduate studies at this institution, he was a teaching assistant during the academic year 1955 to 1956, and an Ethyl Fellow during the academic years 1956 to 1957, and 1957 to 1958.

He has been employed industrially by the Philadelphia Rust Proof Company, and by the Socony Mobil Oil Company. He presently holds the position of Assistant Professor of Chemical Engineering at Clemson College, Clemson, South Carolina.

He has been a student member of the American Chemical Society, and the American Institute of Chemical Engineers.

ACKNOWLEDGMENTS

The author would like to express here his sincere thanks and appreciation to Dr. F. P. Pike of the Department of Chemical Engineering for his helpful advice and guidance during the course of this investigation, and especially for the many hours of his personal time which he willingly and unselfishly gave of in the writing of this thesis.

Sincere thanks are also due to the other members of the Chemical Engineering staff, especially Dr. K. O. Beatty, Jr., for his helpful criticisms of various aspects of this investigation, and Professor R. Bright for his personal encouragement and advice given to the author during his graduate studies at North Carolina State College. In addition, the author would like to express his appreciation to Dr. N. Underwood of the Physics Department for his helpful criticisms of the thesis, and to the other members of his graduate and advisory committees.

The author would also like to express his sincere appreciation to the Ethyl Corporation for making available to him the Ethyl Corporation Fellowship during the last two years of his graduate studies, and to the U. S. Atomic Energy Commission for use of the equipment and supplies made available to the author for this investigation under contract number AT - (40 - 1)-1320.

Last but not least, the author wishes to acknowledge the loving encouragement and help given him by his wife, Linda.

1.0 TABLE OF CONTENTS

TABLE OF CONTENTS (continued)

TABLE OF CONTENTS (continued)

TABLE OF CONTENTS (continued)

TABLE OF CONTENTS (continued)

TABLE OF CONTENTS (continued)

2.0 LIST OF TABLES

3.0 LIST OF FIGURES

Page

4.0 SUMMARY

An extended study has been made of the rate of heat transfer between benzene and water in direct contact in a pulse column, and of the operating variables which controlled the behavior. In this mode of heat transfer the benzene was dispersed as a family of droplets into the water, which formed the continuous phase.

The pulse column unit was one employed previously by Li and Gardner on similar and earlier work. The column itself was 1.92-inches in inside diameter, and contained 8 stainless steel perforated plates spaced 2.00 inches apart. These plates were perforated with 1/8-inch holes in a triangular 60° pattern, providing 24.6 percent free area.

The equipment was carefully insulated and modified in many details in order to permit precise heat transfer measurements. The necessary details are presented in full in Section 9.0. Compared to the prior work, several aspects were revised or reinterpreted, while one new factor was discovered - the existence of a heat loss due to evaporation of benzene during transit of the contactor. An evaluation of these aspects and phenomena is presented in detail in Section 11.0. The final manner of operation and treatment of the data gave heat balances that consistently agreed within 10 percent.

The operating conditions were varied so as to provide the following ranges of variables and heat transfer responses:

Operating Variables

Variable	Symbol	Units	Range
Rate of Pulsing	$\overline{\Pi}_D$	ft/hr.	50 to 1200
Velocity ratio	V_D/V_C	none	0.35 to 4.0
Temperature Difference	$\triangle T_{lm}$	°C	1.4 to 13.7
Grashof component	$\triangle T_{lm}/\gamma_D^2$	$\frac{(°C)(lb\text{-}mass)^2}{(ft\text{-}lb\ force)^2(sec)^2}$.	3.0 to 40.0
Total flow rate	$(V_D + V_C)$	ft/hr.	26 to 90

Responses

Response	Symbol	Units	Range
Continuous phase heat transfer unit	$H\Theta U_{OC}$	ft.	0.207 to 2.89
Discontinuous phase heat transfer unit	$H\Theta U_{OD}$	ft.	0.226 to 0.632
Overall volumetric heat transfer coefficient	Ua	$Btu/(hr)(°F)(ft^3)$.	712 to 6353

The study was so carried out as to explore some points important to theory. A study of temperature differences at the ends of the column, augmented by several temperature probes within the column, led to the definite conclusion that rather large end-effects existed. The temperature probings also settled a major point by proving that the ln-mean temperature difference was valid over the contacting region of the perforated plates themselves.

A limited series of runs showed conclusively that the reversal of the direction of heat transfer made a rather large difference in the results, indicating that internal circulation and natural convection within the drops were prominently involved in the heat transfer mechanisms.

The extended range of the study disclosed new variables beyond those found by Li and Gardner. One new variable was the sum of the two flow rates, or the total flow rate. The other was the kinematic viscosity of the discontinuous phase, indicative of the temperature level.

The final correlations, uncorrected for any end-effects, are as follows for heat transfer from water to dispersed benzene,

$$H\Theta U_{OC} = 1.0(V_D/V_C)^{-1.58}(V_D + V_C)^{-0.262}(\overline{\mu}_D)^{0.117}(V_D/V_C)^{0.762}\left(\frac{\Delta T_{lm}}{V_D^2}\right)^{0.133}$$

$$= \text{ft.}$$

$$H\Theta U_{OD} = 0.38(V_D/V_C)^{-0.58}(V_D + V_C)^{-0.262}(\overline{\mu}_D)^{0.117}(V_D/V_C)^{0.762}\left(\frac{\Delta T_{lm}}{V_D^2}\right)^{0.133}$$

$$= \text{ft.}$$

and

$$Ua = 8.9\ V_D\left[(V_D/V_C + 1)\right]^{1.376}(\overline{\mu}_D)^{-0.039-\text{Log}(V_D/V_C)^{0.423}}\left(\frac{\Delta T_{lm}}{V_D^2}\right)^{-0.133}$$

$$= \frac{\text{Btu}}{(\text{hr})(^{\circ}\text{F})(\text{ft}^3)}.$$

For the reversed case, heat transfer from the dispersed benzene to water, approximate correlations are as follows,

$$H\Theta U_{OC} = 0.098(V_D/V_C)^{-1.58}(V_D + V_C)^{-0.262}(\overline{\mu}_D)^{0.117}(V_D/V_C)^{0.762}\left(\frac{\Delta T_{lm}}{V_D^2}\right)^{1.30}$$

$$= \text{ft.}$$

$$H\Theta U_{OD} = 0.035(V_D/V_C)^{-0.58}(V_D + V_C)^{-0.262}(\overline{\mu}_D)^{0.117}(V_D/V_C)^{0.762}\left(\frac{\Delta T_{lm}}{V_D^2}\right)^{1.30}$$

$$= \text{ft.}$$

and

transfer, is also an argument for the importance of natural convection and internal circulation.

The correlations as presented above are dimensional with the exception of the V_D/V_C ratio. However, it is thought that the present terms are actually components of dimensionless groups, similar to the following:

$$\left(\frac{H\Theta U}{D_p}\right) = \text{form of Nusselts number}$$

$$\left(\frac{\overline{\rho} D D_p \rho_D}{\mu_D}\right) = \text{form of Reynolds number}$$

$$\left(\frac{L^3 g \beta \Delta T_{lm}}{(V_D)^2}\right) = \text{form of Grashof number}$$

and

$$\left(\frac{V_D + V_C}{C_F}\right) = \text{form of relative flooding capacity.}$$

5.0 PURPOSE OF INVESTIGATION

It was the purpose of this thesis to refine and to extend the previous heat-transfer studies of Li and Gardner, to the point where the results could be generalized into a mathematical correlation valid over a reasonably wide range of variables.

The type of heat transfer involved was that of direct contact of one liquid with another immiscible with it in a vertical, countercurrent contactor agitated by pulsing of the continuous phase. In this case, the two fluids were benzene and water. To meet the purpose stated above, it would be necessary to give some thought and study to the concepts of the mechanisms involved.

6.0 MOTIVATION

The primary motivation for this study has been the intriguing nature of the novel physical circumstances influencing the mechanics involved in heat transfer. Practically all other heat transfer studies have involved solid boundaries where the fluid resistances are in part fixed by the rigid nature of the solid surface. In contrast, with direct contact between two fluid phases, additional influences are brought to bear, such as those related to mobility of the interface, and the formation of waves and oscillation. Additional properties such as interfacial tension and perhaps interfacial viscosity, old behavior patterns in new guise, such as mass circulation with the drops and the influence theron of frictional drag, are also important factors. Thus all of these factors provide the fascination of exploration into a new area of heat transfer.

Another consideration has been the possibility that for the case at hand, the heat transfer behavior might eventually turn out to be simply related to the mass transfer behavior, with the one being predictable from the other. There are many circumstances in which temperature measurements, compared to analytical measurements of the concentration of matter, are much more rapid and convenient besides being more accurate and more easily arranged for. In such cases, heat transfer measurements could provide answers for mass transfer problems. This type of inquiry has in fact already been carried out, in mixer-settler design studies by Mottel (32), who used a measure of the rate

of heat transfer to guide him in the selection of optimum stirrer proportions and speeds, for the purposes of intended mass transfer.

Finally, heat transfer by direct liquid-liquid contact avoids the ineffective presence of a temperature gradient across the separating walls normally present, and also avoids certain corrosion problems. Its attractiveness for these reasons had led to some studies in recent years of this mode of heat transfer, and gives this study a practical meaning with reference to the problem of removal of heat from certain reactor designs.

7.0 Definition of Important Variables

7.1 Variables Defining Flow Terms

7.11 Superficial Velocities. One important variable considered in almost all types of liquid-liquid contactors, in both heat and mass transfer studies, is that of superficial velocity. It is simply defined as the volume of fluid flowing per unit time, per unit superficial cross-sectional area in the contactor. The symbol V is generally used to represent superficial velocity, with subscripts being used to designate the particular liquid phase to which V refers.

In this investigation, superficial velocities have been defined as follows:

$$V_D = \frac{v_D}{A} \times 60 \qquad (1)$$

where

V_D = superficial velocity of discontinuous phase, $ft^3/(hr)(ft^2) = ft/hr$.

v_D = volumetric flow rate of discontinuous phase, ft^3/min.

A = superficial cross-sectional area of contactor, ft^2.

Also

$$V_C = \frac{v_C}{A} \times 60 \qquad (2)$$

where

V_C = superficial velocity of continuous phase, $ft^3/(hr)(ft^2) = ft/hr$.

A = superficial cross-sectional area of contactor, ft^2.

It is well to note here that the superficial cross-sectional area of a contactor is defined as the cross-section of the empty contactor

in the region where the major portion of contacting occurs. In general, the ends of liquid-liquid contactors, where entrance and discharge of the phases take place, are larger in cross-sectional area than in the major contacting region, and should not be considered in the determination of superficial area. For packed and pulsed columns, the superficial cross-sectional area would be defined as the cross-sectional area of empty column in the region where the packing and perforated plates were located. In addition, the cross-sectional area of any mechanical supports within the column, such as plate spacers in a pulse column, are not included here in the calculation of superficial cross-sectional areas.

As a matter of comparison, it is interesting to note, that superficial velocities are lower in value than "true" or actual velocities within the column. This is due to the fact that the actual cross-sectional area in the major contacting region of a contactor which is available for fluid passage is less than the superficial area. Thus for a given volumetric flow rate within a column, superficial velocities will be lower than "true" or actual velocities, both velocities being taken relative to the contactor wall.

7.12 Pulse Frequency-Amplitude Term.

7.121 Use of Frequency-Amplitude Product. It is obvious that in any pulse column studies, the effect of pulse amplitude and frequency upon the operating characteristics of the column must be considered. Although some investigators have considered both pulse frequency and amplitude as independent variables in studying the flooding and mass

transfer performance of pulse columns, most studies show the frequency-amplitude product as a more important variable.

Cohen and Beyer (6), in studying the extraction of boric acid from isoamyl alcohol with water in a perforated plate pulse column, found their data could be better correlated by considering the frequency-amplitude product as a variable rather than considering frequency and amplitude as independent variables. Wiegandt and Von Berg (56), in summarizing the results of other investigators, mention the frequency-amplitude product as an important variable. Sege and Woodfield (43), use the frequency-amplitude product in correlating their results on the extraction of uranyl nitrate from tributyl phosphate with water. Recently, Li and Newton (26) have used the frequency-amplitude product in calculating phase velocities through the plate holes in a pulse column, for the system benzoic acid, toluene, and water.

7.122 Use of the $\overline{fl}_D$ term. In studying the flooding characteristics of the pulse column used in this investigation, Pike, et al (35), found that the major controlling variables were an average rate of pulsing, represented by the symbol $\overline{fl}$, and the ratio of superficial velocities, V_D/V_C. Two different values of $\overline{fl}$ have been considered, and are defined as follows:

$\overline{fl}_D$ = Average flow rate of total material past the plates in the direction of the discontinuous phase flow, averaged over the actual time of flow in that direction, ft/hr.

$\overline{fl}_C$ = Defined the same as $\overline{fl}_D$, only for a direction the same as that of the continuous phase, ft/hr.

In the definitions just presented, the total material pulsed through the plates is, in general, an emulsion of unknown composition. The difference between $\overline{\Pi}_D$ and $\overline{\Pi}_C$ determines the magnitude and direction of the net pumping action of the puke pump.

The physical significance of the $\overline{\Pi}$ variables and its relation to pulse frequency, amplitude, V_D and V_C, may be better understood by considering the case where the pulse is sinusoidal in nature. A plot of the instantaneous column fluid velocity, U, versus time is shown in Figure 1 for a perfectly sinusoidal pulse, under the special and simplifying case where $V_D = V_C$. The velocity term, U, refers to the flow of both phases through the plate perforations, yet is calculated on a superficial basis.

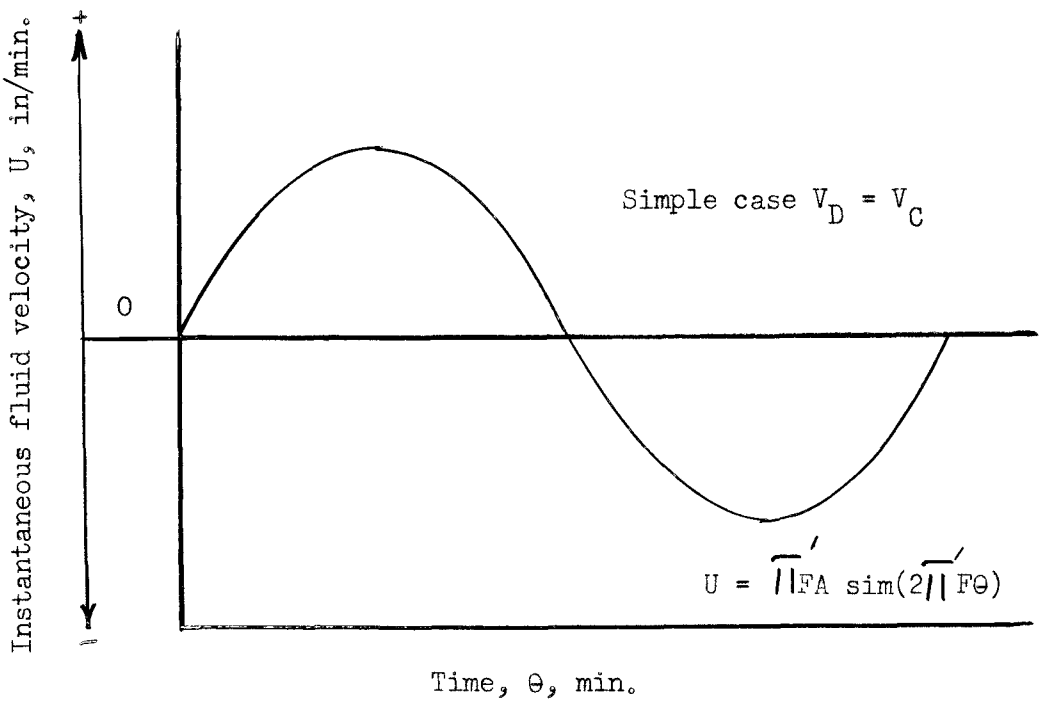

Figure 1. Velocity pattern in a pulse column

If the superficial velocity difference is defined as

$$\triangle V = V_D - V_C \tag{3}$$

where $\triangle V$ = superficial velocity difference, ft/hr.

then for the special and simplifying case above, where $V_D = V_C$, $\triangle V = 0$. Under these conditions, the instantaneous column fluid velocity, U, at any time, θ, is given by the simple expression, as developed by Pike (35),

$$U = \overline{\pi}' FA \sin(2\overline{\pi}' F\theta) \tag{4}$$

where $\overline{\pi}' = 3.1416$

θ = pulse time, min.

F = pulse frequency, 1/min.

A = pulse amplitude, in.

$F\theta$ = dimensionless product

U = instantaneous fluid velocity, in/min.

When there is a superficial velocity difference within the column, i.e., $V_D/V_C > 1$, or $V_D/V_C < 1$, a plot of instantaneous column fluid velocity vs. time is somewhat different than shown in Figure 1. If, for example, $V_D/V_C > 1$, then there will be a superficial velocity difference in the column in the direction of the discontinuous phase flow. This superficial velocity difference will be constant, and defined by equation (3). A plot of U vs. θ for the situation where $V_D/V_C > 1$, combined with a perfectly sinusoidal pulse, is shown in Figure 2. It will be noted

from Figure 2 that this particular situation, the flow pattern is shifted upwards as compared to the case where $V_D = V_C$.

From Figure 2 it can be seen that for $V_D/V_C > 1$, the instantaneous fluid velocity, U, at any time, θ, is given by the expression,

$$U = \overline{/\!/}' FA \sin(2\overline{/\!/}' F\theta) + \triangle V \qquad (5)$$

Sinilarly, it can be shown that when $V_D/V_C < 1$, the instantaneous fluid velocity at any time will be given by equation (5) also. However, in this case, $\triangle V$ will be negative in sign, and the flow pattern shifted downwards as compared to the case where $V_D = V_C$.

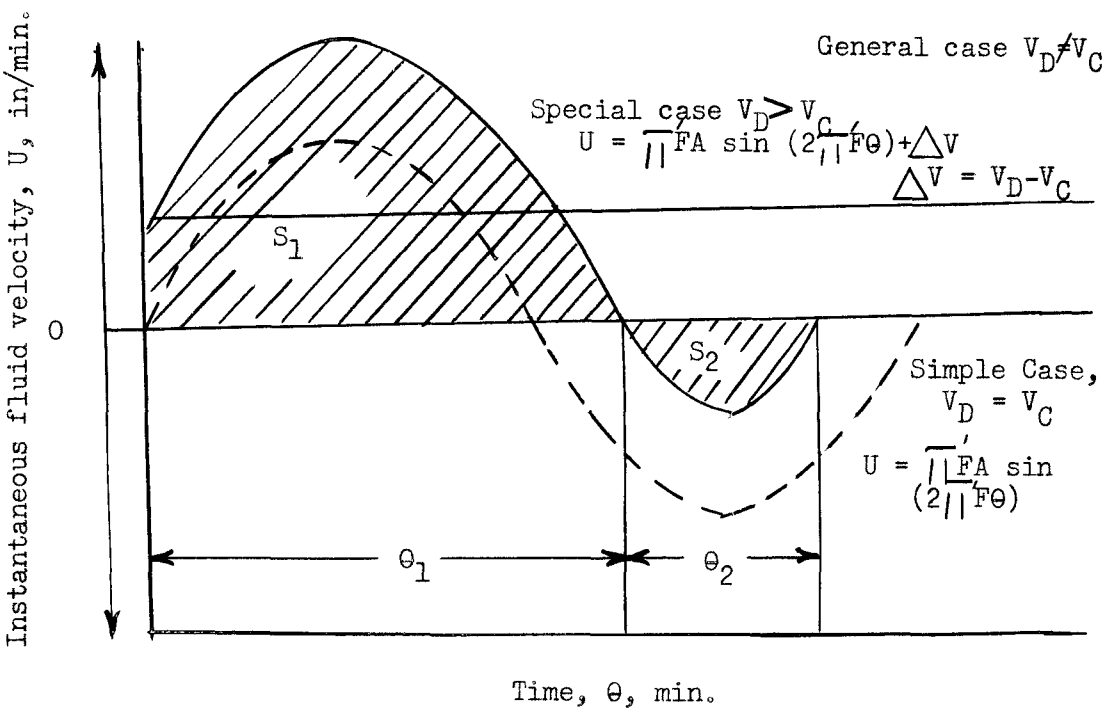

Figure 2. Velocity patterns in a pulse column

If S_1 and S_2 represent the areas under the curves in Figure 2 for pulse strokes in the direction of flow of the discontinuous and continuous phases respectively, and θ_1 and θ_2 represent the duration of the pulse stroke in these directions respectively, then $\overline{\Pi}_D$ and $\overline{\Pi}_C$ are defined as follows:

$$\overline{\Pi}_D = \frac{S_1}{\theta_1} \tag{6}$$

$$\overline{\Pi}_C = \frac{S_2}{\theta_2} \tag{7}$$

In order to calculate $\overline{\Pi}_C$ and $\overline{\Pi}_D$ as a function of FA and $\triangle V$, it is necessary to know the exact nature or form of the pulse used in the column. Generally, because of mechanical imperfections in the pulsing mechanism, it is necessary to determine this relationship between $\overline{\Pi}_C$, $\overline{\Pi}_D$, FA, and $\triangle V$ experimentally. This is true even when the pulsing mechanism has been designed to give a pulse of some given form.

Such an experimental relationship for the column used in this investigation has been determined by Pike, et al (35), and is shown in Figure 3.

In the development of Figure 3, is was found that for a given value of $\triangle V$, $\overline{\Pi}_D$, and $\overline{\Pi}_C$ were dependent only upon the product FA, and were independent of the individual values of F and A used.

Although the variables $\overline{\Pi}_D$, $\overline{\Pi}_C$, and V_D/V_C were developed and defined from studies of the flooding characteristics of the pulse column used in this investigation, it was felt that these variables would also be important in describing other responses of the pulse column, such as

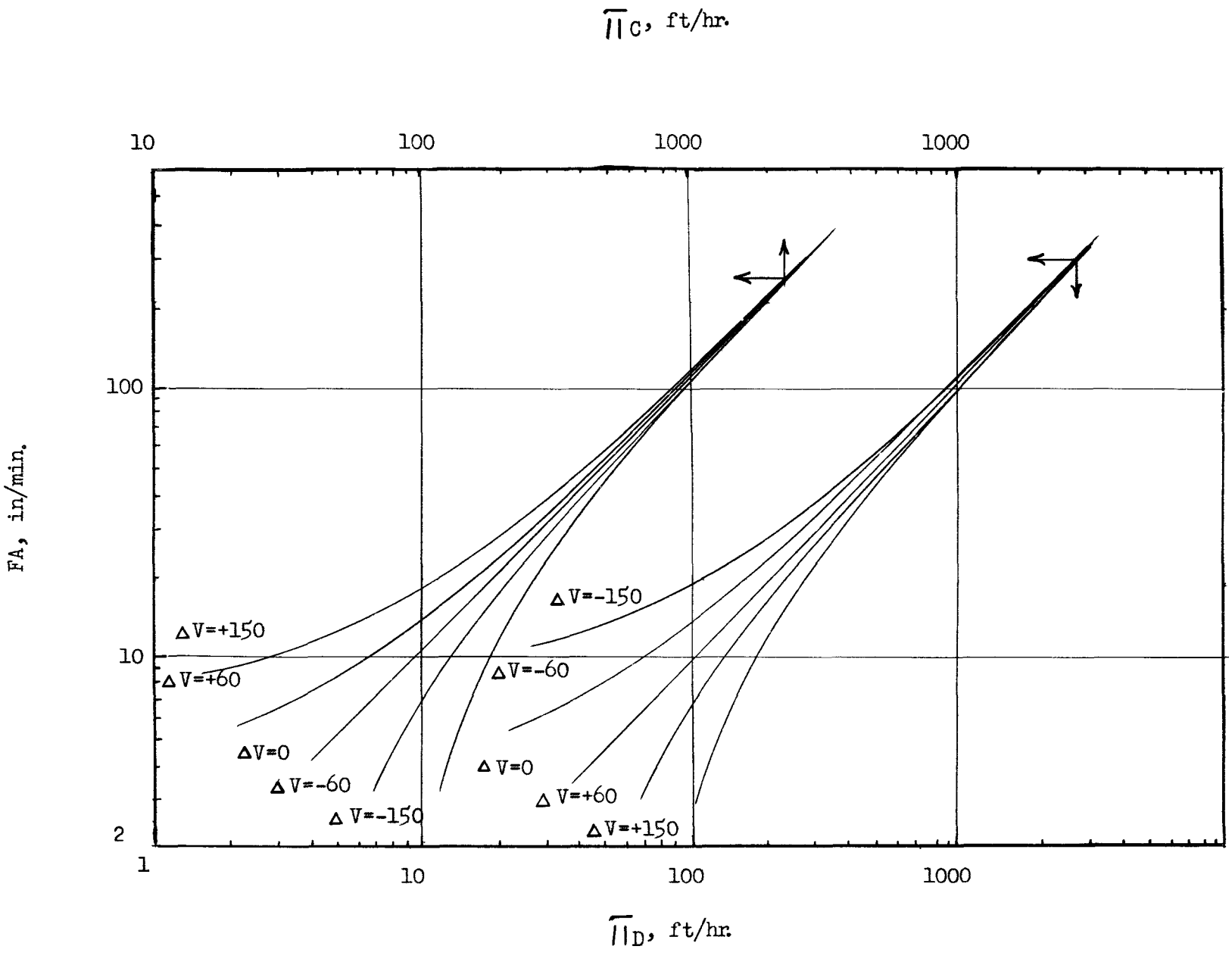

Figure 3. Relation between rates of pulsing and frequency-amplitude product

rates of heat and mass transfer, and pressure drop. These variables have been used by other investigators quite successfully in describing responses of the pulse column, as will be shown later.

7.2 Variables Defining Mass Transfer

7.21 The Number of Mass Transfer Units. A useful method for computing the height of a liquid-liquid contactor is based on the idea of calculating the number of a certain kind of contact unit required for a given separation, and multiplying the number of such units by the height requirement for a single unit. This idea of a contact transfer unit was developed by Chilton and Colburn (5), and has the advantage of expressing the relative difficulty of an extraction process in terms of a dimensionless quantity, which increases in numerical value as the difficulty of separation of the process increases. Based on the two-film theory of Whitman (55), the following definitions of the number of mass transfer units are used for columns employing a continuous and discontinuous phase. The equations defined below are for single component diffusion, with the solute diffusing from the discontinuous to the continuous phase.

$$N_D = \int_{X_{D2}}^{X_{D1}} \frac{(1 - X_D)_M \, dX_D}{(1 - X_D)(X_D - X_{Di})} \qquad (8)$$

where

N_D = number of discontinuous phase mass transfer units

X_D = mole fraction of solute in bulk of discontinuous phase

X_{Di} = mole fraction of solute in discontinuous phase at interface between phases.

$(1 - X_D)_M$ = ln-mean difference between $(1 - X_D)$ and $(1 - X_{iD})$

or

$$(1 - X_D)_M = \frac{X_D - X_{Di}}{\ln(1 - X_{Di}/1 - X_D)}$$

$$N_C = \int_{X_{C2}}^{X_{C1}} \frac{(1 - X_C)_M \, dX_C}{(1 - X_C)(X_{Ci} - X_C)} \qquad (9)$$

where

N_C = number of continuous phase mass transfer units

X_C = mole fraction of solute in bulk of continuous phase

X_{Ci} = mole fraction of solute in continuous phase at interface between phases

$(1 - X_C)_M$ = ln-mean difference between $(1 - X_C)$ and $(1 - X_{Ci})$

or

$$(1 - X_C)_M = \frac{X_{Ci} - X_{Ci}}{\ln(1 - X_C/1 - X_Ci)}$$

$$N_{OD} = \int_{X_{D2}}^{X_{D1}} \frac{(1 - X_D)_{OM} \, dX_D}{(1 - X_D)(X_D - X_C^*)} \qquad (10)$$

where

N_{OD} = number of overall discontinuous phase mass transfer units

X_C^* = mole fraction of solute in bulk of continuous phase which would be in equilibrium with X_D

$(1 - X_D)_{OM}$ = ln-mean difference between $(1 - X_C^*)$ and $(1 - X_D)$

or

$$(1 - X_D)_{OM} = \frac{X_D - X_C^*}{\ln(1 - X_C^*/1 - X_D)}$$

$$N_{OC} = \int_{X_{C2}}^{X_{C1}} \frac{(1 - X_C)_{OM}\, dX}{(1 - X_C)(X_C^* - X_C)} \qquad (11)$$

where

N_{OC} = number of overall continuous phase mass transfer units

X_D^* = mole fraction of solute in bulk of discontinuous phase that would be in equilibrium with X_C

$(1 - X_C)_{OM}$ = ln-mean difference between $(1 - X_D^*)$ and $(1 - X_C)$

or

$$(1 - X_C)_{OM} = \frac{X_D^* - X_C}{\ln (1 - X_C/1 - X_C^*)}$$

The subscripts 1 and 2 refer to the bottom and top of the contactor, respectively, in all of the above definitions. If dilute concentrations of the solute are used, then the terms $\frac{(1 - X)_M}{(1 - X)}$ and $\frac{(1 - X)_{OM}}{1 - X}$ in the above equations may be assumed to be unity for both phases, and the equations somewhat simplified.

In general, values of N_{OD} and N_{OC} are determined experimentally since measurements of N_D and N_C entail the determination of values of X_{Di} and X_{Ci}, which are extremely difficult, if not impossible, to obtain. However, by careful choice of the system used and concentrations of the solute, it is possible to experimentally determine values of N_{OD} and N_{OC} which are approximately equal to N_D and N_C. In addition, by proper treatment of experimental values of N_{OD} and N_{OC}, it is sometimes possible to calculate values of N_D and N_C from the data correlations.

7.22 The Height of Mass Transfer Units. In the preceding section, it was indicated that the height of a mass transfer or contact

unit was that quantity by which the number of transfer units was multiplied in order to get the total contactor height. From this simple concept comes the following definitions for the heights of mass transfer units in liquid-liquid contactors employing continuous and discontinuous phases.

$$HTU_D = \frac{Z}{N_D} \tag{12}$$

where

HTU_D = height of a discontinuous phase mass transfer unit, ft.

Z = height of contactor, ft.

It is well to note here that the definition of Z is arbitrary, and will be discussed in more detail in Section 7.4.

$$HTU_C = \frac{Z}{N_C} \tag{13}$$

where

HTU_C = hieght of a continuous phase mass transfer unit, ft.

$$HTU_{OD} = \frac{Z}{N_{OD}} \tag{14}$$

where

HTU_{OD} = height of an overall discontinuous phase mass transfer unit, ft.

$$HTU_{OC} = \frac{Z}{N_{OC}} \tag{15}$$

where

HTU_{OC} = height of an overall continuous phase mass transfer unit, ft.

It is sometimes desirable to know the relationship between heights of the individual mass transfer units, HTU_D and HTU_C, and heights of the overall mass transfer units, HTU_{OD} and HTU_{OC}. For a single component diffusing, these relationships have to be shown to be by Sherwood and Pigford (45):

$$HTU_{OD} = HTU_D \frac{(1 - X_D)_M}{(1 - X_D)_{OM}} + HTU_C \frac{m V_D \rho_D M_C}{V_C \rho_C M_D} \frac{(1 - X_C)_M}{(1 - X_D)_{OM}} \qquad (16)$$

where

M_C = molecular mass of continuous phase

M_D = molecular mass of discontinuous phase

m = average slope of the equilibrium curve averaged over the continuous film,

thus

$$m = \frac{X_{Di} - X_D^*}{X_{Ci} - X_C} \qquad (17)$$

Also,

$$HTU_{OC} = HTU_C \frac{(1 - X_C)_M}{(1 - X_C)_{OM}} + HTU_D \frac{V_C \rho_C M_D}{m V_D \rho_D M_C} \frac{(1 - X_D)_M}{(1 - X_C)_{OM}} \qquad (18)$$

When dilute solutions are employed for both phases, the above equations may be reduced to the more simple forms,

$$HTU_{OD} = HTU_D + HTU_C \frac{m V_D \rho_D M_C}{V_C \rho_C M_D} \qquad (19)$$

and

$$HTU_{OC} = HTU_C + HTU_D \frac{V_C \rho_C M_D}{m V_D \rho_D M_C} \qquad (20)$$

7.3 Variables Defining Heat Transfer

The information presented in the following section by no means represents all of the possible variables defining heat transfer in liquid-liquid contactors. Only variables which are pertinent to this and related investigations are presented here.

7.31 Rates of Heat Transfer Between Phases. One of the most important entities in heat transfer studies in liquid-liquid contactors is the net rate of heat transfer between phases, represented by the symbol q. When a continuous and discontinuous phase are employed, and there is no heat of solution, heat of agitation, etc., q may be simply defined by the equation

$$q = v_D \rho_D C_D \Delta T_D \times 60 \times 1.8 \qquad (21)$$

where

q = net rate of heat transfer between the continuous and discontinuous phases, Btu/hr.

v_D = volumetric flow rate of the discontinuous phase, ft^3/min.

C_D = heat capacity of the discontinuous phase, Btu/(lb)(^oF).

ρ_D = density of the discontinuous phase, lbs/ft^3.

ΔT_D = temperature change in the discontinuous phase, ^oC.

and, similarly

$$q = v_C \rho_C C_C \Delta T_C \times 60 \times 1.8 \qquad (22)$$

where

v_c = volumetric flow rate of the continuous phase, ft^3/min.

C_C = heat capacity of the continuous phase, Btu/(lb)(^oF).

ρ_C = density of the continuous phase, lbs/ft^3.

ΔT_C = temperature change in the continuous phase, ^oC.

It would be well to emphasize here that ΔT_D and ΔT_C are temperature changes in the discontinuous and continuous phase respectively which results from a net rate of heat transfer, q, between the two phases. Actually, there can be heat effects present in each phase other than just q, which effect the inlet and outlet temperatures of the phases. If so, it is necessary to take these other heat effects into consideration before true values of ΔT_D and ΔT_C may be calculated, as will be shown later.

7.32 The number of heat transfer units. In a manner very much analogous to that employed in mass transfer studies, it is possible to define expressions for the number of heat transfer units for heat transfer in a liquid-liquid contactor. Assuming a true counter-current flow pattern between the discontinuous and continuous phases, the sensible heat effect over a differential height, dZ, of the contactor is expressed by the following equation:

$$dq = v_C \rho_C \; C_C \; S dT_C \times 1.8 \qquad (23)$$

where

S = superficial cross-sectional area of column, ft^2.

dT_D = differential temperature change in the continuous phase resulting from the rate of heat transfer, dq, between phases, ^oC.

and

$$dq = v_D \rho_D \; C_D \; S dT_D \times 1.8 \qquad (24)$$

where

dT_D = differential temperature change in the discontinuous phase resulting from the rate of heat transfer, dq, between phases, ^oC.

For this analysis, it is assumed that all heat effects other than heat

transfer between phases are negligible. Therefore, assuming the direction of heat transfer to be from the continuous to discontinuous phase, the rate of heat transfer between the discontinuous and continuous phases over a differential height of the contactor is given by the expression

$$dq = Ua\ S(T_C - T_D)(1.8)dZ \qquad (25)$$

where

U = overall heat transfer coefficient for heat transfer between phases, Btu/(hr)(^oF)(ft^2).

S = as defined for equation (23).

a = interfacial heat transfer area between phases per unit volume of contactor, ft^2/ft^3.

T_C = bulk temerature of continuous phase in column height dZ, ^oC.

T_D = bulk temperature of discontinuous phase in column height dZ, ^oC.

dZ = differential column height, ft.

In general, it is very difficult to evaluate quantitatively the interfacial heat transfer area per unit volume of contactor, a. Thus U and a are usually conbined together into one term, Ua, which may be considered as an overall heat transfer coefficient per unit volume of column, with the dimension of $\frac{Btu}{(hr)(^oF)(ft^3)}$.

Equating and rearranging equations (23) and (25), we have that

$$\frac{dT_C}{T_C - T_D} = \frac{Ua\ dZ}{V_C \rho_C\ C_C} \qquad (26)$$

Similarly, equating and rearranging equations (24) and (25) we have that

$$\frac{dT_D}{T_C - T_D} = \frac{Ua\ dZ}{V_D \rho_D C_D} \tag{27}$$

From equations (25) and (26), the number of overall heat transfer units are defined as follows:

$$\overline{N}_{OD} = \int_{T_{D2}}^{T_{D1}} \frac{dT_D}{T_C - T_D} \tag{28}$$

where

$\overline{N}_{OD}$ = number of overall discontinuous phase heat transfer units

T_{D_2} = inlet temperature of discontinuous phase, ^oC.

T_{D_1} = outlet temperature of discontinuous phase, ^oC.

$$\overline{N}_{OC} = \int_{T_{C2}}^{T_{C1}} \frac{dT_C}{T_C - T_D} \tag{29}$$

where

$\overline{N}_{OC}$ = number of overall continuous phase heat transfer units

T_{C_1} = inlet temperature of continuous phase, ^oC.

T_{C_2} = outlet water temperature, ^oC.

Thus $\triangle T_D$ and $\triangle T_C$ in equations (21) and (22), respectively, may be defined as,

$$\triangle T_D = T_{D_1} - T_{D_2} \tag{30}$$

and

$$\triangle T_C = T_{C_1} - T_{C_2} \tag{31}$$

Although equations (23) through (29) were used in defining overall heat transfer units, individual phase heat transfer units, analogous to

individual-phase mass transfer units, may also be defined. Using equations analogous to (28) and (29), we have that

$$\overline{N}_D = \int_{T_{D2}}^{T_{D1}} \frac{dT_D}{T_i - T_D} \tag{32}$$

where

$\overline{N}_D$ = number of discontinuous phase heat transfer units

T_i = interfacial temperature between discontinuous and continuous phase, °C.

and

$$\overline{N}_C = \int_{T_{C2}}^{T_{C1}} \frac{dT_C}{T_C - T_i} \tag{33}$$

where

$\overline{N}_C$ = number of continuous phase heat transfer units.

In liquid-liquid contactors employing a continuous and discontinuous phase, no one has yet been able and it may be impossible, to measure directly the values of interfacial temperature T_i. Similar difficulties, it will be remembered, are encountered in the determination of interfacial concentrations in mass transfer studies. For this reason, only values of the overall heat transfer units $\overline{N}_{OD}$ and $\overline{N}_{OC}$, have been measured to date. It may be possible, however, to derive values of the individual-phase heat transfer units $\overline{N}_D$ and $\overline{N}_C$ from the manipulation and correlations of measured values of $\overline{N}_{OD}$ and $\overline{N}_{OC}$, and some assumptions.

In the derivation of the above equations, it was assumed that steady conditions without backmixing between phases are maintained. If it is

also assumed that Ua, the mass flow rate of each phase, and the physical properties of each phase also remain constant throughout the contactor, then the temperature of each phase will vary linearly throughout the column as a function of q, and may be expressed as a linear function of either phase temperature, T_D or T_C.

If the above assumptions are valid, then equations (28) and (29), for $\bar{N}_{OD}$ and $\bar{N}_{OC}$, respectively, may be integrated to yield.

$$\bar{N}_{OD} = \frac{T_{D_1} - T_{D_2}}{(\triangle T)_{lm}} \tag{34}$$

and

$$\bar{N}_{OC} = \frac{T_{C_1} - T_{C_2}}{(\triangle T)_{lm}} \tag{35}$$

where

$$(\triangle T)_{lm} = \frac{\triangle T_2 - \triangle T_1}{\ln(\triangle T_2/\triangle T_1)} = \frac{\triangle T_1 - \triangle T_2}{\ln(\triangle T_1/\triangle T_2)} \tag{36}$$

and

$$\triangle T_1 = T_{C_1} - T_{D_1} \tag{37}$$

$$\triangle T_2 = T_{C_2} - T_{D_2} \tag{38}$$

7.33 The Height of Heat Transfer Unit. Once the number of heat transfer units have been defined, the height of such a unit may be determined in a manner exactly analogous to that employed in mass transfer. The height of a heat transfer unit is simply that quantity by which the number of heat transfer units must be multiplied in order to get the total contactor height. Again, as in the case of mass transfer, the

height of the contactor, Z, is somewhat arbitrary, and will be discussed in more detail in Section 7.4. Thus, the height of heat transfer units are defined as follows:

$$H\Theta U_D = \frac{Z}{\bar{N}_D} \tag{39}$$

where

$H\Theta U_D$ = height of a discontinuous phase heat transfer unit, ft.

$$H\Theta U_C = \frac{Z}{\bar{N}_C} \tag{40}$$

where

$H\Theta U_C$ = height of a continuous phase heat transfer unit, ft.

$$H\Theta U_{OD} = \frac{Z}{\bar{N}_{OD}} \tag{41}$$

where

$H\Theta U_{OD}$ = height of an overall discontinuous phase heat transfer unit, ft.

and

$$H\Theta U_{OC} = \frac{Z}{\bar{N}_{OC}} \tag{42}$$

where

$H\Theta U_{OC}$ = height of an overall continuous phase heat transfer unit, ft.

If the assumptions made in the derivation of equations (34) and (35) are again assumed valid, then equations (26) and (27) may be integrated to yield

$$N_{OC} = \int_{T_{C2}}^{T_{C1}} \frac{dT_C}{T_C - T_C} = \int_{Z=0}^{Z} \frac{Ua\ dZ}{V_C \rho_C C_C} = \frac{Ua\ Z}{V_C \rho_C C_C} \tag{43}$$

and

$$N_{OD} = \int_{T_{D2}}^{T_{D1}} \frac{dT_D}{T_C - T_D} = \int_{Z=0}^{Z} \frac{Ua\ dZ}{V_D \rho_D C_D} = \frac{Ua\ Z}{V_D \rho_D C_C} \tag{44}$$

Thus $H\Theta U_{DC}$ and $H\Theta U_{OC}$ may be defined by combining equations (41) and (44), and (42) and (43), respectively, to give

$$H\Theta U_{OD} = \frac{V_D \rho_D C_D}{Ua} \tag{45}$$

and

$$H\Theta U_{OC} = \frac{V_C \rho_C C_C}{Ua} \tag{46}$$

Equations (34) and (35) may also be combined with equations (41) and (42) respectively, to yield:

$$H\Theta U_{OD} = \frac{Z}{(T_{D1} - T_{D2})/(\triangle T)_{lm}} \tag{47}$$

and

$$H\Theta U_{OC} = \frac{Z}{(T_{C_1} - T_{C_2})/(\triangle T)_{lm}} \tag{48}$$

The relationship between heights of the individual heat transfer units, $H\Theta U_D$ and $H\Theta U_C$, and heights of the overall heat transfer unit, $H\Theta U_{OD}$ and $H\Theta U_{OC}$, are analogous to those of mass transfer, and have been shown to be

$$HOU_{OD} = HOU_D + HOU_C \frac{V_D \rho_D C_D}{V_C \rho_C C_C} \tag{49}$$

and

$$HOU_{OC} = HOU_C + HOU_D \frac{V_C \rho_C C_C}{V_D \rho_D C_D} \tag{50}$$

7.34 Overall Heat Transfer Coefficients. If the assumptions made in the derivation of equations (34) and (35) are again assumed valid, then equation (25) may be integrated to yield:

$$q = Ua\ S(\triangle T)_{lm} Z \tag{51}$$

Since the product SZ is the total volume of the contactor, V_T, Ft^3, then equation (51) may be rearranged as follows to define the overall heat transfer coefficient per unit volume of contactor, Ua,

$$Ua = \frac{q}{V_T\ (\triangle T)_{lm}} \tag{52}$$

7.4 End Effects

7.41 Definition of Contactor Height, Z. As was previously mentioned, the definition of column height for a liquid-liquid contactor is somewhat arbitrary. In general, the contactor height is defined as that portion of the apparatus in which the major portion of the phase contacting takes place. For packed columns, the contactor height is usually taken as the height of packing within the column. However, for spray towers the height is simply the distance between inlet discontinuous-phase nozzle and the interface of coalescence. For the pulse column used in this investigation, the column height has been arbitrarily defined as the number of plates multiplied by the plate spacing.

studies, has been that of measuring concentration profiles within the column. Thus when ever end effects are present, an abrupt change or discontinuity will appear in the concentration profile at the end or ends of the contactor. A method similar to the one above has also been utilized in the determination of end effects for heat transfer in liquid-liquid contactors. Abrupt changes, discontinuities, in the temperature profile within the column, determined by means of temperature probes, will occur when end effects are present.

End-effects may also be measured by experimentally determining some measure of the column effectiveness such as the number of mass or heat transfer units, as a function of column length or height. Theoretically, the contactor should have zero effectiveness at zero height. However, because of end-effects, some columns have a finite effectiveness at extrapolated zero height. Thus, the extrapolation of a plot of some measure of effectiveness versus some measure of column length to zero effectiveness results in a measure of the end-effect, expressed in terms of column length. Such a plot is shown in Figure 4, and has been prepared from mass transfer data obtained by Pike et al (36), with the system benzene-water, and the pulse column used in this investigation.

An examination of Figure 4 shows an end-effect equivalent to 3 plates.

7.44 Common Magnitude for End-Effects. For spray columns, Sherwood, Evans, and Langcor (44) assumed that the end-effects were located in the drop as they formed, causing 40-45 percent of the extraction in

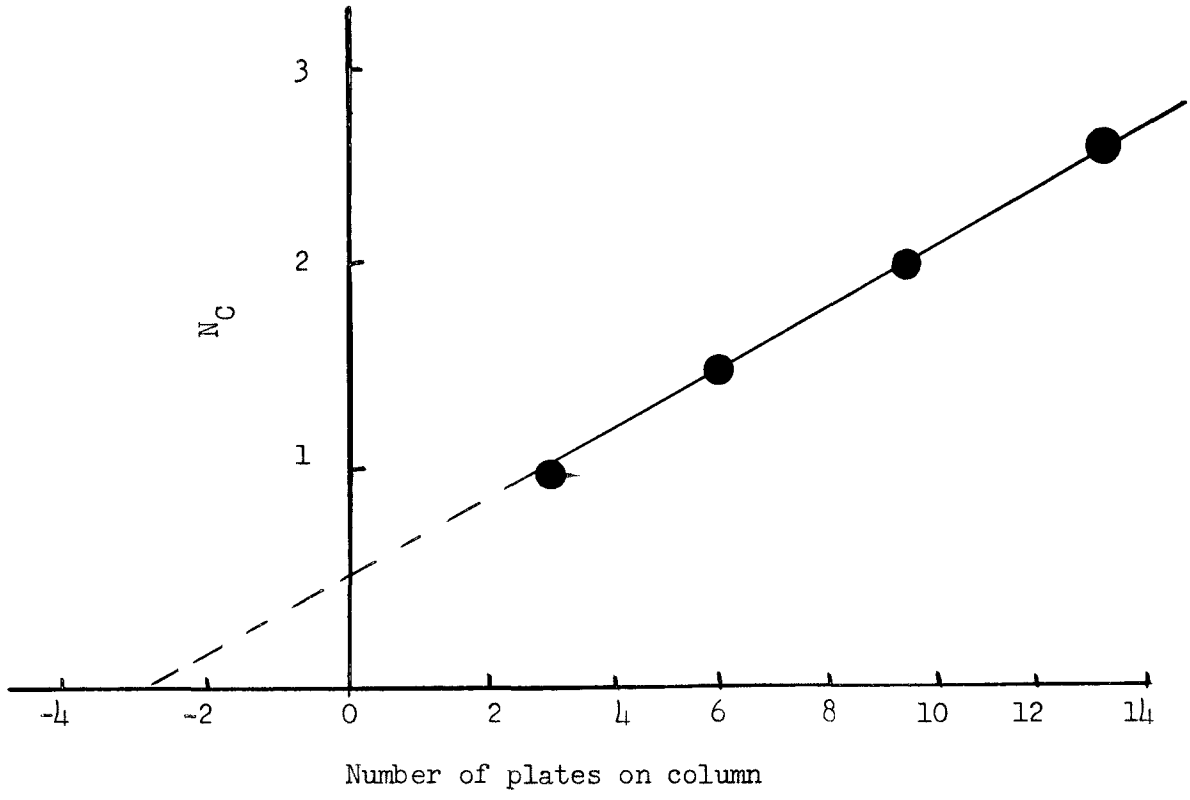

Figure 4. Effect of number of plates on number of mass transfer units

these towers. Farmer (12), found an effect of the same magnitude for the spray columns used in his investigations.

Although end-effects for mass transfer in packed columns will vary with tower design, the following data are reported for end-effects in packed columns. MacAdams, Pohlenz, and St. John (30) report an end-effect of 7 inches, while Surosky and Dodge (47) have reported an end-effect of 2.2 inches from their investigations.

For pulse-columns, as described previously, the end-effect for the continuous phase may be about 3 plates.

7.5 Analogy between Heat and Mass Transfer

7.51 Introduction. From the limited knowledge of turbulence in fluid streams, it should be evident that both eddy diffusion and heat transmission in a turbulent stream are dependent upon velocity gradients, and thus friction (momentum transfer), heat transfer, and mass transfer must be intimately related. As a result, the theoretical development in these three fields are somewhat analogous. Most of the theoretical and experimental work done in these areas has been in the study of turbulence and the connection between wall friction and the properties of the turbulent stream. However, some investigators have employed this background to develop expressions for analogy between heat, mass and momentum transfer. A few of the more important relations are given below.

7.52 The Reynolds Analogy. The first theoretical equation for an analogy relating heat and momentum transfer for turbulent flow in a pipe or tube was that developed by Reynolds (34). Assuming that the heat lost due to friction, divided by the momentum of the stream, was equal to the ratio of the actual heat transferred in a pipe section to the heat which would be transferred were the fluid to come to thermal equilibrium with the pipe wall, Reynolds developed the relation,

$$h = \frac{fC\rho U}{2} \tag{53}$$

where

h = heat transfer coefficient at pipe wall in contact with fluid flowing, Btu/(hr)(^{o}F)(ft^{2}).

f = Fanning friction factor, dimensionless

All other terms are as previously defined.

The Fanning friction factor is defined by the expression

$$f = \frac{1}{2} \frac{D}{\rho} \left(\frac{dP}{dL} \right) \frac{g_c}{U^2} \tag{54}$$

where

D = pipe or tube diameter, ft.

P = pressure, lbs-force/ft^2.

L = length of tube or pipe, ft.

g_c = constant, 32.17 $\frac{(\text{lbs-mass})(\text{ft})}{(\text{lb-force})(\text{sec})^2}$.

and all other terms are as previously defined

The above assumptions of Reynolds are equivalent to the assumptions that, for turbulent flow inside of tube or pipe,

$$E_M = E_H \tag{55}$$

where

E_M = eddy diffusivity of momentum transfer

E_H = eddy diffusivity of heat transfer

and

$$\frac{C\mu}{k} = 1 \tag{56}$$

where

μ = viscosity of fluid flowing, lb-force-hr/ft^2.

k = thermal conductivity of fluid flowing, Btu/(hr)(ft^2)($^\circ$F/ft).

Equation (53) above may be arranged in a more convenient form to give

$$\frac{h}{C\rho U} = \frac{f}{2} \tag{57}$$

where the dimensionless group, $\frac{h}{C\rho U}$, is defined as the Stanton number, St. Thus

$$St = \frac{h}{C\rho U} \tag{58}$$

Reynolds developed another expression, similar to equation (57), relating mass and momentum transfer, and based on the similarity of momentum of mass transfer in the turbulent core of a fluid flowing in a tube or pipe. This relation is given as follows:

$$k_c = \frac{fU}{2} \tag{59}$$

where

k_c = mass-transfer coefficient, lb mole/(hr)(ft^2)(lb mole/ft^3).

In the derivation of equation (59), Reynolds neglected, or did not allow, properly for the gradual change in the relative importance of D_V and E_M in going from the pipe or tube wall to the center of the stream, where

D_V = diffusion coefficient, ft^2/hr.

Thus Reynolds assumed D_V and μ negligible in comparison with ε and E_m, where

ε = eddy viscosity, lb force hr/ft^2.

7.53 The Von Karman Analogy. Von Karman (53) modified the Reynolds analogy between mass and momentum transfer by assuming that the variation of μ, and the shear stress, τ, are similar across the fluid stream such that τ/N is a constant, where

τ = shear stress in flowing fluid, lb force/ft^2.

N = rate of diffusion of diffusing component, lb mole/(ft^2)(hr).

In addition to the above assumption, Von Karman also assumed that and D_v were negligible in comparison to ε and E_M, as did Reynolds, and developed the relation

$$k_c = \frac{\alpha f U}{2} \tag{60}$$

where

$$\alpha = E_M \rho / \varepsilon \tag{61}$$

It has been found that α varies from 1.0 to 2.0 in the turbulent core of the stream for fluid flowing in tubes or pipes.

If E_M and ε are assumed negligible in comparison with D_v and μ, the Von Karman's relation takes the form

$$k_c = (\rho D_v / \mu)(fU/2) \tag{62}$$

indicating the possible importance of the dimensionless group, $(\rho D_v / \mu)$. This group is called the Schmidt group, Sc, and is defined as,

$$Sc = \frac{\mu}{\rho D_v} \tag{63}$$

7.54 Other Modification of the Reynolds Analogy. The first important modification of the Reynolds analogy was made by Prandtl (38) and Taylor (48), who considered heat transfer to take place through two resistances in series. These resistances were a laminar layer at the tube wall and the turbulent layer to which the Reynolds analogy applied.

A corresponding analogy between mass and heat transfer, based on the above assumptions, was also developed from the Reynolds analogy by Colburn (7). Both of the above analogies for mass and heat transfer, and heat and momentum transfer, were modified even further by Chilton and Colburn (4) as will be discussed in Section 7.55.

7.55 The Chilton-Colburn Analogy. Probably the most important and useful analogy between mass, heat, and momentum transfer are those developed by Chilton and Colburn (4).

By use of dimensional analyses, the following familiar dimensionless relation has been developed for correlating heat transfer coefficients for fluids being heated as they pass through tubes or pipes in turbulent flow.

$$\frac{hD}{k} = a(D\rho U/\mu)^b \quad (\mu C/k)^c \tag{64}$$

The above dimensionless groups are defined as follows:

$$\text{Nusselt number} = Nu = \frac{hD}{k} \tag{65}$$

$$\text{Reynolds number} = Re = \frac{D\rho U}{\mu} \tag{66}$$

$$\text{Prandtl number} = Pr = \frac{\mu C}{k} \tag{67}$$

and a, b, and c are experimentally determined constants. All other terms are as previously defined.

A similar expression has been developed by means of dimensional analysis, for the correlation of mass transfer through the gas phase flowing in turbulent flow through a wetted-wall column. This correlation is given by the following dimensionless relation.

$$\frac{k_c D}{Dv} = a'(D\rho U/\mu)^{b'} \quad (\mu/\rho Dv)^{c'} \tag{68}$$

In this case, the dimensionless group, $\frac{k_c D}{Dv}$, is defined as,

$$\text{Sherwood number} = Sh = \frac{k_c D}{Dv} \tag{69}$$

All other dimensionless groups and terms are as previously defined, with a', b' and c' again being experimentally determined constants.

An examination of equation (64) and (68) above, shows that both equations may be arranged to give a function of the Reynolds number equal to the product of a pair of dimensionless groups as follows:

$$a(D\rho U/\mu)^{b-1} = \frac{h}{U\rho C} (\mu C/k)^{1-c} \tag{70}$$

and

$$a'(D\rho U/\mu)^{b'-1} = \frac{k_c}{U} (\mu/\rho Dv)^{1-c'} \tag{71}$$

Chilton and Colburn (4) have defined the above functions of the Reynolds number in equations (70) and (71) as the "j factor" for heat and mass transfer respectively, and are defined as follows:

$$j_H = a(D\rho U/\mu)^{b-1} = \frac{h}{U\rho C} (\mu C/k)^{1-c} \tag{72}$$

and

$$j_M = a'(D\rho U/\mu)^{b'-1} = \frac{kc}{U} (\mu/\rho Dv)^{1-c'} \tag{73}$$

where

j_H = j factor for heat transfer, dimensionless

j_M = j factor for mass transfer, dimensionless

When heat, mass and momentum transfer in fluids are intimately related and are accomplished by similar mechanism, the constants associated with the two functions of the Reynolds number are equal, i.e., $a = a'$ and $b = b'$. Thus, under such conditions, the j factor for heat and mass transfer are equal, and related to the Fanning friction factor as follows:

$$j_H = j_M = \frac{f}{2} \tag{74}$$

Furthermore, if the mass, heat and momentum transfer processes are operating through the same paths, or accomplished by similar mechanisms, then the j factor concept and equation (74) can be used to predict any two of these transfer processes from a third.

In using the j factor concept for the prediction of mass transfer from heat transfer, or vice versa, it is necessary to assume that coefficients and exponents of the Reynolds number are equal, i.e., $a = a'$ and $b = b'$. In general, this has been found to be true for mass and heat transfer in most solid-gas or liquid-solid contactors, with the same values of these constants being experimentally determined for each type of contactor. Values of these constants have been found to be,

$$a = a' = 0.023$$

and

$$b = b' = 0.80$$

Values of c' have been found experimentally to be approximately 0.44, with values of c ranging from 0.3 to 0.4. In developing the j factor concept, Chilton and Colburn arbitrarily assumed c and c' to be equal, and to have the value 2/3.

The above j factor equations have been used rather successfully in correlating data on absorption and evaporation in wetted-wall columns, absorption on cylinders placed at right angles to a gas stream, and vaporization from a plane surface. Recently, Calderbank and Korchinski (3) used the j factor analogy successfully in predicting heat transfer to liquid drop in a continuous liquid phase from mass transfer data for an analogous situation where the dispersed phase resistance was assumed negligible.

In the past, most success has been achieved with the j factor analogy in predicting heat transfer from mass transfer, or vice-versa, rather than in predicting heat or mass transfer from the Fanning friction factor. This seems to be due to the fact that the friction factors are commonly calculated from measurements of total drag, including both skin friction and the normal pressure drag, whereas the analogy holds only when skin friction alone is considered. Such cases thus result in the inability to characterize properly the state of motion of the fluid by a simple term such as the Reynolds number.

8.0. LITERATURE REVIEW

8.1 Heat Transfer in Liquid-Liquid Contactor

8.11 Background. Although this section of the Literature Review deals mainly with heat transfer in liquid-liquid contactors, it is felt that a section of the more important work in the field of mass transfer and fluid hydrodynamics should be presented here as background material. This is especially true for the material which will be presented in section 8.12, Heat Transfer Between Single Drops and Continuous Liquid Phases.

For quite some time the "two-film" theory of Whitman (refer to Sherwood and Pigford(45)) has been the accepted model for interpretation of both heat and mass transfer data in gas-liquid or liquid-liquid systems. Here it is assumed that the fluid in the region on either side of the interface is essentially laminar in its structure and that heat and mass can traverse these regions only by a diffusional process. It is now known that this picture is an oversimplification, yet two-fluid systems are often successfully treated as if two adjacent finite resistances of this sort do exist.

Higbie (21) diverges from the Whitman "two-film" theory to assume that for a given fluid phase, the interface is continually being renewed in some manner by fresh phase brought from the interior to the surface. When and where it reaches the interface, this fresh material creates an unsteady-state absorption pattern as solute penetrates into the relatively fresh layers; hence the generation of the term "penetration theory". This concept is being steadily developed in recent

years, particularly by Toor and Marchello (51), by Danckwerts (9,10), and by E. Ruckenstein (41). Unfortunately, no clear, convenient and unambiguous treatment has yet been demonstrated for this basic model of unsteady-state penetration.

Another concept of interest is the rate of heat or mass transfer to a drop follows different mechanisms in the period of formation, the period of rise and upon drop coalescence. Light and Conway (27) provide a good illustration of this situation for the case of mass transfer to and from drops.

Probably one of the most significant theoretical contributions made in the field of mass transfer was that of Kronig and Brink (23). By modifying the results of Hadamard (18) on the hydrodynamics of rising droplets, they were able to calculate a theoretical circulation pattern within a shperical drop, as shown in Figure 5, due to viscous drag between the drop and the surrounding medium.

By applying diffusion theory to the circulation pattern, considering the streamlines as lines of constant solute concentration, they were able to show that the time of circulation of matter was small compared with the time of diffusion, except at the boundary surface of the drop. However, as the droplets became sufficiently large, 0.1 mm in radius or larger, this effect became less important. In applying their theory to rates of extraction, Kronig and Brink were able to show theoretically that the rates of extraction were 2.5 times as large for droplets with internal circulation, as compared to stationary droplets in a surrounding medium with an infinite diffusion coefficient. This

The existance of circulation patterns similar to these described by Kronig and Brink have been shown to occur, and have been varified experimentally in several different ways. Spells (46) made photographs of the striae in glycerine-water drops which clearly showed the circulation pattern. Heertjes, et al (20), allowed drops of isobutanol, colored blue with $Co\ Cl_2$, to rise through water, and measured the amount of isobutanol transfered to the continuous water phase. When the concentration of isobutanol reached a certain value, color changes from blue to pink occured within the drop in a manner to give evidence for the existance of circulation patterns. Heertjes actually found that the last remaining portion of original color had the shape of a ring at positions A, as shown in Figure 5. If no circulation had occurred in the drop, the original color would have been expected to remain longest in the center of the drop. It has also been found that in some mass transfer studies on liquid drop, that the rapid rates of extraction determined experimentally were difficult to explain unless internal circulation within the drop was assumed.

The assumptions of Kronig and Brink require that a moving drop circulate no matter what its size. In practice, it has been observed that for a given system, drops smaller than a certain size (about 1 mm) tend not to circulate at all, for reasons yet unclarified. Garner and Skelland (14) review some of this information. Non-circulating drops are found to absorb heat and matter entirely by diffusional processes, whereas circulating drops are a different case. Schwindt and Stuke (42) demonstrate transition cases where drops show various degrees of partial

internal circulation. Linton and Sutherland (28) both review and demonstrate the fact that internal circulation of drops can be controlled either by surface absorption of molecules or by absorption of particulate matter like dust.

In addition to internal circulation as a factor in heat and mass transfer, drop oscillation and the presence of surface waves and distortion above been observed.

The net effect of all of these hydrodynamic complications is that there is at present no satisfactory mathematical model for either heat or mass transfer to or from drops.

8.12 Heat Transfer Between Single Drops and Continuous Liquid Phases. Conkie and Savic (8) appear to be the first investigators who studied heat transfer to single drops considering internal circulation within the drops. The results of Kronig and Brink were not used directly due to the fact that they assumed the motion took place in the Stokes' regime, and therefore no boundary layer in the classical hydrodynamical or thermal sense existed. Conkie and Savic, however, felt that a boundary layer did exist, and therotically examined the influence of circulation on its thickness and extent. From this they were able to determine the effect of circulation on the value of the local heat transfer coefficient, and compare their results with experimental results of other investigators.

McDowell and Myers (31) experimentally determined the temperature rise of liquid drops rising through another liquid, and compared their results with those predicted from three assumed heat transfer mechanisms. The three mechanisms considered were; (1) non-circulating drop being

heated by pure radial conduction with no outside film resistance, and surface temperature equal to that of the surrounding medium; (2) a non-circulating drop being heated by pure radial conduction with an outside film resistance; (3) a circulating drop of the type described by Kronig and Brink in which the streamlines are assumed to be isotherms, and outside film resistances assumed negligible. They conclude that in systems where the viscosity of the drops is low compared to that of the continuous phase, circulation will take place in the drop, and mechanism (3) above controls. Also, if the thermal conductivity of the continuous phase is low compared to that of the liquid drop, and no circulation within the drop is present, then an appreciable part of the resistance to heat transfer will be in the film outside the drop, and mechanism (2) controls.

Calderbank and Korchinski (3) determined values of the continuous phase heat transfer coefficient for mercury drops falling through hotter or colder aqueous solution of glycerol held at constant temperatures. They were able to correlate their data with that published for heat transfer to solid spheres along with data from analogous mass transfer situations where the dispersed-phase resistance was negligible. The correlation was good up to Reynolds numbers of 200 where all experimental data departed from that for solid spheres. It was noted, however, that at Reynold's numbers above 200, drop oscillations were observed to occur. Since internal drop circulation has been shown to be present at Reynold's numbers below 200, it was concluded that internal circulation has no appreciable effect on the continuous phase heat transfer coefficient.

Calderbank and Korchinski also were able to show that the ratio of an effective mass or thermal diffusivity for circulating drops, based on the model of Kronig and Brink, to that for a rigid sphere in a continuous phase medium of constant temperature and negligible resistance, was 2.25. Using data from bromobenzene drops falling in aqueous glycerol solution, along with much literature data, they were able to show that this ratio varied from 1.8 to 3.3 in the circulating regime. However, in situations where the experimental data indicated the presence of drop oscillations, values of the above ratio were much higher.

Handlos and Baron (19) have developed a schematic drop model which takes into account vibrational patterns as well as circulation patterns within the drop for regions of highly turbulent motion (Reynolds number about 1000). They assumed that the tangental motion caused by circulation is combined with the assumed random radial motions due to vibration in the evaluation of an eddy diffusivity. By combining this motion with the single circulation patterns of Kronig and Brink, Handlos and Baron were able to derive single expressions for the dispersed phase mass transfer for coefficients, or the inside drop coefficients. By using the results of West et al, (54) for the determination of a continuous phase mass transfer coefficient, and assuming the simple substitution of thermal diffusivity for mass transfer diffusivity, they were able to calculate values of the overall heat transfer coefficient for the system benzene-water. These data were correlated with the experimental results of Garwin and Smith (15). They were also able to correlate their experimental values of overall mass transfer coefficient for the system benzene-water, using various substances as the

solute, with calculated values of the overall coefficients. This was also true with experimental mass transfer data reported by other investigators.

Elzinga and Banchero (11) adopted three drop models to describe the mechanism of heat transfer within drops, and used these models in conjunction with their experimental data to determine the continuous phase heat transfer coefficient. The three drop models considered were: (1) a completely mixed drop in which there were no temperature gradients; (2) a circulating drop with flow patterns similar to those predicted by Kronig and Brink. However, in the solution of Kronig and Brink's equations, finite values of the continuous phase heat transfer coefficient were assumed rather than infinite. By comparing the heat transfer data calculated from the experimental results with those calculated from the experimental results with those calculated assuming a given drop model, and with the aid of the limiting maximum and minimum values of the heat transfer coefficient, Elzinga and Banchero were able to determine which drop model best described the mode of heat transfer. They were also able to develop a general correlation from which values of the continuous phase heat transfer coefficient could be calculated for systems in which the ratio of the discontinuous to continuous phase viscosities was equal to or less than unity. However, in systems where this ratio is greater than unity, circulation ceases to become an important factor, and the above mentioned correlation gives high results. Also, if oscillations are noted within the drop, the results from the correlation will be low.

8.13 Heat Transfer in Liquid-Liquid Spray Columns. It appears that the first heat transfer studies performed in a spray column were made by Allen, et al (1), in studying the continuous hydrolysis of fats. Value of the overall heat transfer coefficient-total heat transfer area product, UA, are reported. However, the author states that the data are not sufficiently complete to draw conclusive relationships between operating conditions and UA. Also values of a mean temperature difference are reported, but the exact nature of this mean temperature difference is not clearly defined.

Rosenthal (40) carried out heat transfer studies in a spray column using the system toluene and water. In addition to the heat transfer studies, he also determined some of the flooding and hold-up characteristics of the column for two different types of spray distributors. For transfer of heat from the continuous water phase to dispersed toluene drops, Rosenthal found that values of $H\Theta U_{OD}$ increases linearly and decreased linearly as a function of V_C and V_D respectively when plotted on logarithmic coordinates. Values of V_D or V_C were used as parameters, and were shown to effect appreciably the values of $H\Theta U_{OD}$. The data were correlated by an equation of the form

$$H\Theta U_{OD} = \frac{(V_C)^a}{(V_D)^b} \qquad (75)$$

where K, a, and b are experimentally determined constants. However, for V_D/V_C ratios greater than 1.2, values of $H\Theta U_{OD}$ decreased faster than predicted by the above equation.

For heights of overall discontinuous phase units, it was found that values of $H\Theta U_{OD}$ decreased slightly, in a linear fashion, as a

function of V_D or V_C on logarithmic coordinates. Values V_D or V_C as parameter seemed to have no appreciable affect upon $H\Theta U_{OD}$, and the data was correlated by an equation of the form

$$H\Theta U_{OD} = \frac{K}{(V_D)^a (V_C)^b} \tag{76}$$

Equation (76) was also limited to values of V_D/V_C less than 1.2. Treybal (52) has taken the above data of Rosenthal and presented values of $H\Theta U_{OD}$ and $H\Theta U_{OC}$ as functions of the superficial velocity ratio, V_D/V_C.

Values of the overall volumetric heat transfer coefficient, Ua, were also determined by Rosenthal. It was found that Ua increased linearly as a function of V_D or V_C on logarithmic coordinates, but V_D was only important as a parameter when V_C was the independent variable. V_C as a parameter had little affect on Ua when V_D was the independent variable. It was found that values of Ua could be correlated by the expression,

$$Ua = K V_C^a V_D^b \tag{77}$$

Rosenthal made two runs in which the direction of heat transfer was reversed, but could detect no effect upon the results.

Garwin and Smith (15) studied drop size and rise in spray columns, using the system benzene-water. From these studies, using benzene as the dispersed phase, holdup calculations were made from which values of the overall heat transfer coefficient, U, were determined. Also, from profile data of the continuous phase, rigorous values of U were

calculated and compared with those calculated using a ln-mean temperature difference. It was found that the ratio of the rigorously to logarithmicly calculated values of U increased from slightly less than unity at low holdup, to 1.2 at high holdups. This behavior of the ratio was considered as evidence for recirculation of the continuous phase at high flow rates of the discontinuous phase. It was also found that U decreased with increasing flow rates of the continuous and discontinuous phases, and with increasing holdup. However, Ua increased with increased flow rates of both phases.

Garwin and Smith made studies with heat transfer in both directions between phases. They found that the rates of heat transfer were greater from the discontinuous to continuous phases than when the reverse was true. The difference was of the order of 25 to 30-percent, but no reason was set forth to explain it by Garwin and Smith. This point is discussed later.

Barbouteau (2) experimented with heat transfer from water to hydrocarbons both in small laboratory equipment and in commerical equipment. By measuring the size of the drops in auxilary equipment, he was able to estimate the surface area exposed, and from that the individual film coefficients for the continuous phase outside the drop. Both mathematical analysis and his correlations of data involved the same dimensionless numbers, the Nusselt number, the Reynolds number, and the Prandtl number, as employed by Calderbank and Korchinski. His results, applying to the aqueous phase, invite comparison with those of Calderbank and Korchinski, and other reviewed by them. However, results of Barbouteau are much lower and tend to rise much more rapidly as the

Reynolds number increases. If the results of Barbouteau are extrapolated above a Reynolds number of 1000, the extrolation tend to agree in magnitude and slope with the experimental results of Calderbank and others in the corresponding region of Reynolds number.

Johnson, et al (22), in addition to mass transfer studies, investigated the effect of varying physical properties of solvent pairs on the operation of a spray column. To accomplish this, heat was transferred in both directions between a continuous water and discontinuous phases of carbon tetrachloride-naphtha mixtures of varying properties. Although the authors present their results in terms of the heights of individual phase heat transfer units, $H\Theta U_D$ and $H\Theta U_C$, no where do they indicate how they were calculated from the experimental data. It is therefore believed that the results are actually in terms of $H\Theta U_{OD}$ and $H\Theta U_{OC}$ rather than $H\Theta U_D$ and $H\Theta U_C$.

The $H\Theta U_C$ data were correlated with V_D/V_C on logarithmic coordinates, and the $H\Theta U_D$ data correlated as a function of V_D/V_C on rectangular coordinates, as was done by Traybal. It was found that the rates of heat transfer were again higher for heat transfer from the discontinuous to continuous phase. Internal circulation within the drop, similar to that described by Cronkie and Savic, was set forth as a possible explaination for the difference.

The most recent published work on heat transfer in spray columns was done by Pierce, et al (34), using the system mercury dispersed in water. From studies of drop sizes and velocities in the column, calculations of holdups were made in addition to the calculations of

interfacial heat transfer areas per unit volume of contactor. Also values of U and Ua were determined, and found to decrease with increased column length. From temperature profile data, it was found that a plot of q versus $\triangle T$ was not linear, and therefore the use of a logarithmic temperature difference not justified. It was also found that recirculation of the continuous phase caused a discontinuity in its temperature at the bottom of the column, which accounted for 80-percent of the total temperature rise of the continuous phase. Also high speed movies showed water clinging to the mercury drops as they flowed downward, along with oscillations within the drops, but with little horizontal mixing. Results indicated that the major heat transfer resistance was not at the water-mercury interface, but between the surface of the drops and the bulk of the phase.

8.14 Heat Transfer in Other Liquid-Liquid Contactors. Grover and Knudsen (17) have determined the rates of heat transfer between a petroleum solvent and water flowing in a horizontal circular pipe. Three methods of solvent injection were employed to determine the effect of mixing. Values of UA/V, where V represents the volume of the contactor, were correlated with the total liquid mass flow rates for various degrees of mixing. Calculation showed that for the same flow rates and temperatures used in the investigation, heat transfer is more effective by direct contact than with a double tube co-current heat exchanger. Also a general correlation between a Nusselts number and Reynolds number was developed.

Mottel (32), in evaluating the effectiveness of mixing two liquids in a mixer-settler utilizing a shrouded paddle, measured heat transfer rather than mass transfer in the evaluations.

8.2 Heat and Mass Transfer Studies on Pulse Column Used in this Investigation.

8.21 Introduction. The heat and mass transfer studies discussed in this section are, without a doubt, the ones most pertinent to this investigation. This is due to the fact that the studies presented herein have all been made on the same basic equipment. In addition, the same system, benzene dispersed in water, was employed in all, along with similar operating conditions of flow and pulsing rates.

8.22 Heat Transfer for Studies of Li. In addition to making major modifications on the pulse column, such that it could be used for heat transfer studies in addition to mass transfer studies, Li (25) also made some preliminary investigations on the heat transfer responses of the column. These included an evaluation of heat losses from the column, and heat generated within the column due to the pulsing action. Also, Li made a limited number of heat transfer runs on the system benzene-water, to demonstrate the effectiveness of the modified unit. Heat was transfered from a continuous water phase to a discontinuous benzene phase flowing countercurrently through the column.

Li operated at a V_D/V_C ratio of 1.0, with $V_D = V_C = 20$ ft/hr. These relatively low flow rates of the benzene and water phase were chosen to permit a wide range of pulsing rates, $\overline{fl}_D$, to be used before flooding was reached in the column. Pulsing rates vary from a low of $\overline{fl}_D = 50$ ft/hr, to a high near the flooding point of $\overline{fl}_D = 1200$, were used. Li

used benzene inlet temperatures approximately equal to room temperature, and water inlet temperatures of approximately 60° C. Three runs were made using a water inlet temperature of approximately 45° C. A complete summary of Li's data and recalculated results are given in tables 2A through 2F of the appendix.

8.23 Heat Transfer Studies of Gardner. The studies of Gardner (13) were simply a continuation of the work of Li. However, in all of his heat transfer runs, Gardner used only one value of the rate of pulsing, $\overline{fl}_D$ = 150 ft/hr and a constant V_C superficial velocity of 20 ft/hr, even through V_D/V_C ratios greater than unity were sometimes employed.

Gardner also used a benzene inlet temperature approximately equal to room temperature. However, several different inlet water temperatures were employed in his studies.

By varying the V_D/V_C ratio, and the inlet water temperature, Gardner was able to correlate Ua, H_{OC} and H_{OD} as a function of V_D/V_C and ΔT_{lm}. In addition, he was also able to determine from photographs hold-ups within the column, from which he was able to derive and correlate U values as a function of V_D/V_C and ΔT_{lm}. Gardner also made three runs in which the V_D/V_C ratio was so adjusted as to give approximately the same measured temperature differences between phases at each end of the column. In this way Gardner was able to calculate an average temperature difference between phases throughout the column. From these three runs he was able to show that result calculated using the known temperature difference through the column, correlated with those calculated using a ln-mean temperature difference. In so far as these

few runs could, they supported the appropriateness of the use of a ln-mean temperature difference. Gardner was also able to show that values of $H\Theta U_{OC}$, $H\Theta U_{OD}$, and Ua, were dependent only upon the product FA, and independent of the individual values of F and A used.

From his limited data, Gardner was able to develop the following correlations for the pulse column heat transfer responses.

$$H\Theta U_{OC} = 0.55\ (V_D/V_C)^{-1.12}\ (\triangle T_{lm})^{0.146} = \text{ft.} \tag{78}$$

$$H\Theta U_{OD} = 0.24\ (V_D/V_C)^{-0.18}\ (\triangle T_{lm})^{0.146} = \text{ft.} \tag{79}$$

$$U = 44(V_D/V_C)^{0.51}\ (\triangle T_{lm}^{-0.146} = \text{Btu/(hr)(°F)(ft}^2\text{)}. \tag{80}$$

and

$$Ua = 2000(V_D/V_C)^{1.15}\ (\triangle T_{lm})^{0.146}$$

$$= \text{Btu/(hr)(°F)(ft}^3\text{)}. \tag{81}$$

8.24 Mass Transfer Studies of Pike, et, al. Pike, et al (36), using the system benzene and water, were able to experimentally determine values of N_C and N_D for the pulse column used in this investigation in mass transfer response. This was done by careful choice of solute concentrations used in their investigations. Thus it was possible to calculate values for the heights of individual phase transfer units, HTU_C and HTU_D.

Values of $\overline{\Pi}_D$ from 50 to 1200 ft/hr were used. In addition, V_D/V_C ratios of approximately 1/3, 1.0, and 3.0 were employed.

9.0 MATERIALS AND APPARATUS

9.1 Materials

9.11 Water. All water used in this investigation was a good grade of distilled water, prepared in the Department of Chemical Engineering, North Carolina State College. The distilled water was stored and transported in clean stainless steel drums at all times. Although most of the water passing through the column during operation was collected in stainless steel drums, none of it was ever recycled to the column except during start-up. Recycled water was used during the start-up period and until thermal equilibrium was reached in the column in order to conserve the freshly distilled water for later use during the course of a run.

9.12 Benzene. A thiopene-free, 1°-grade of benzene was used in this investigation. It is the purest commercial grade produced by the Barrett Division of Allied Chemical and Dye Corporation. Although this benzene had been used previously in mass transfer and other heat transfer studies, it was redistilled in departmental facilities, and stored in stainless steel drums. All benzene collected during operation of the column was stored in clean stainless steel drums, and reused in subsequent operations. For this reason, it was assumed that all benzene employed was water saturated, at least at room temperature.

9.2 Apparatus

9.21 Background. The apparatus used in this investigation was originally constructed under an Atomic Energy Commission contract, No. AT-(40-1)-1320, for the study of various performance patterns,

particularly mass transfer, in a pulse column. At the completion of the mass transfer studies, the equipment was modified by Li (25) for heat transfer studies, and its performance evaluated. Modification of the apparatus consisted mainly of insulations of component parts, and the installation of stream heaters and temperature measuring devices. For a more detailed description of the column modifications, refer to Li (25).

9.22 General Description. The pulse column apparatus used in this investigation is shown schematically in Figure 6. An examination of Figure 6 shows that the less dense discontinuous phase, benzene, is pumped from a 55-gallon stainless steel feed tank, through a benzene "Rotameter"* and an adjustable constant-temperature bath, by means of a Milton-Roy, variable speed, "Constameter" piston pump. These pumps are specifically designed to produce a constant rate of flow by suitable synchronization of twin pistons. From the constant temperature bath, the less dense phase enters the bottom of the pulse column proper through the benzene inlet nozzle. The benzene thus flows up the column as the discontinuous phase, coalescing at the water-benzene interface, and overflowing by gravity into a stainless steel storage drum. The contents of the column as pulsed by means of a Milton-Roy "Simplex" pump equipped with a special micro-adjustment of the stroke length.

---

*Quotation marks have been used to set-off commercial trade names of all materials and apparatus used in this investigation. A complete listing of these trade names is given in the nomenclature, Section 14.0, along with more detailed information on the materials and apparatus.

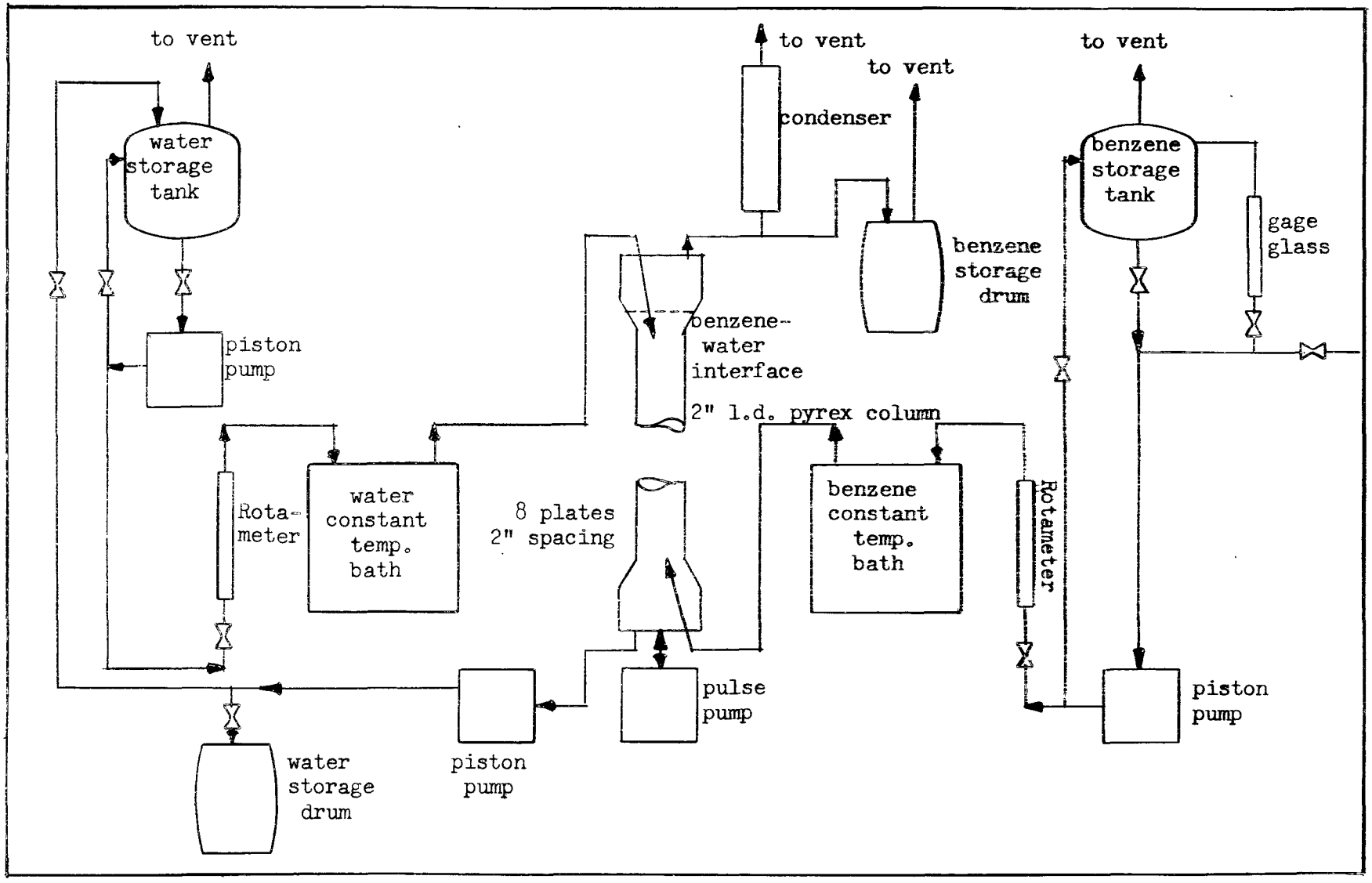

Figure 6. Schematic diagram of apparatus

Figure 6 also shows the continuous water phase pumped from a 55-gallon stainless steel storage tank, through a "Rotameter" and second constant-temperature bath, by means of another Milton-Roy variable speed "Constametric" pump. However, after passing through the column, the water phase is pumped from the bottom of the column by means of a third Milton-Roy "Constametric" pump into a stainless steel storage drum, or into a more convenient measuring container. The benzene-water interface level was controlled by adjusting the speed of the water inlet pump, while the actual flow rate of the continuous water phase through the column was determined by the speed of the water discharge pump.

A more detailed description of the component parts of the apparatus used is given in Section 9.4.

9.3 Modifications of Apparatus

9.31 Additional Stream Heaters. When the original equipment was modified by Li, only one constant temperature tank was installed. This tank was installed such that it could be used to heat either the benzene or water feed streams, but not both at the same time. In all the heat transfer studies made on the pulse column by Li and by Gardner, this single constant temperature bath was used to heat the water feed stream, while the benzene feed stream entered the column at room temperature. However, as a result of their investigations, both Li and Gardner recommended the installation of a benzene stream constant temperature bath to control the inlet temperature of the benzene more accurately. This was found necessary due to relatively large fluctuations in room

diameter. Again, a 1/2-inch diameter stainless steel tube, 5-1/4 inches in length, was soldered to the outside of the nozzle to give an air space of approximately 1/8-inch thick, and 5-1/4 inches long. In addition, a 1-inch diameter "Teflon" sleeve was placed around the outside of the 1/2-inch diameter tube. It was hoped that the smaller area of the new distributor, plus the increased air space thickness, would give lower temperature rises than observed by Li and Gardner. However, results of this investigation indicated temperature rises in the benzene feed stream, at the inlet, comparable to those observed by Li and Gardner under similar operating conditions. This might indicate that metal conduction was supplying most of the unwanted heat transfer.

9.33 Temperature Probe. At the conclusion of Li's heat transfer studies, a question was raised concerning the validity of the use of a ln-mean temperature driving force in his calculations. Although this point was investigated to some degree by Gardner, it was felt that more information on the behavior of the temperature driving forces in the pulse column was needed. For this reason a stainless-steel temperature probe was installed in order to permit exploration of the temperature profiles within the column. The temperature probe was installed in such a way that it could be raised or lowered to any point in the column through a packing gland located at the bottom of the column. A more detailed description of the temperature probe is given in Section 9.47.

9.4 Components of Apparatus

9.41 Feed Storage Tanks. The apparatus used in this investigation was equipped with two 55-gallon, stainless-steel, feed storage tanks.

Although both of these storage tanks could have been used in storing the benzene and water feeds, only the benzene tank was used. This was due to the manner in which the benzene flow rates were determined. In actual operation of the column, it was found more convenient to pump the continuous-water phase directly from the 55-gallon steel drum in which it was transported, rather than pump it from this drum to the stainless steel storage tank.

9.42 Feed Stream Measuring Devices. Both the benzene and water feed streams were each equipped with two Fisher and Porter "Stabl-Vis Rotameter" of different ranges, and calibrated for specific benzene and water temperatures. However, these "Rotameters" were only used for flow indication and adjustment of the two phases, and not for flow measurements. In addition to the "rotameters", each feed stream included a set of three calibrated gage glasses. These gage glasses were all approximately 48-inches long, and had internal diameters of 0.75, 1.5, and 3.0 inches. By means of a three-way quick-acting valve, it was possible to measure accurately the flow from any desired gage glass for short periods of time.

Benzene flow-rates were determined by using the 1.5-inch diameter glass standpipe, while water flow rates were obtained by actually collecting and determining the mass of water discharged from the column in a given time. A more detailed description of flow measurements is given in Section 10.21.

9.43 Feed Stream Constant Temperature Baths. As was mentioned previously, two feed stream heaters were used in this investigation, controlling the inlet temperatures of both the benzene and water streams to

the pulse column. Since both constant temperature tanks were identical in construction, the following description applies to both.

9.431 Heat Exchangers. Each heat exchanger, or constant-temperature bath, consisted essentially of a 55-gallon steel drum (22 inches in diameter and 36 inches high), in which was coiled one hundred feet of 3/8-inch outside diameter, (0.032-inch wall thickness) copper tubing. The inside of the drum was painted with a pigmented epoxy resin, "DEL" white E-Z. This paint is reported to be capable of dry service at temperatures up to 450°F. Maximum wet service temperatures used in this investigation were approximately 190°F. The protection provided was not quite adequate in that some peeling of the paint was noted.

The copper tubing was arranged in a 75-turn helical coil of about 16 inches in diameter. It conveyed the stream being heated. The outside heating area of the immersed copper coil was 9.8 square feet. The drum was filled to within 2 inches of the top with about 460 pounds of water, and insulated with a 1-inch blanket of "Ultralite" insulation. To help maintain a uniform temperature in the bath, a 1/4-h.p., 1725 rpm, explosion-proof "Lightning" mixer was mounted in the tank. It was inserted through a drum cover which served to reduce evaporation losses.

The heat exchangers were installed as close as possible to the pulse column to minimize heat transfer between the feed line and the surroundings.

9.432 Heaters and Wiring. In recognition of the heavy heat loads imposed by start-ups, heaters with a total rating of 6.0 kilowatts (20,500 Btu/hr) were installed in the constant temperature bath.

Table 1. Characteristics of electrical heaters

Number of heaters Employed	Voltage	Rating (k.w.)	Manufacturer's Catalog No.
1	118	1 kw	MT-110
1	236	2 kw	MT-120
2	236	1.5 kw	MT-115

All "Chromalox" Immersion Heaters employed were manufactured by the Edwin L. Wiegand Company, and are listed in Table 1.

The heaters were equipped with 1-1/4 inch standard pipe thread screw connections. The heater and one drain valve were installed through the use of five couplings brazed into the drum side about 6 inches from the bottom of the drum. The four heaters were equally spaced around one-half the circumference, with the drain valve opposite.

The 2 kw heater was connected directly to an off-on power supply, while the other three heaters were used in conjunction with "Variac" Transformers which permitted fractional use of the heaters by permitting the off-on load to be adjusted to small values. In addition, the power supply to the "Variac" connected with the 1 kw heater came from the power output of a Fisher "Electronic or Transistor Relay". The net results of such fine control of power input to the heaters was the practical elimination of fluctuations in the temperature of the reservoir water. For a more detailed wiring diagram of the heaters, refer to Li (25).

9.433 Thermostats. The temperature of each constant-temperature bath was controlled by a sensitive thermostat and relay which operated the 1 kw heater. Power from the heater came from a "Variac"

autotransformer which was directly connected with the power output of a Fisher "Electronic or Transistor Relay". This relay was in turn actuated by means of a Fisher "Micro-Set" thermostat, which was sensitive within 0.01°C.

9.434 Auxiliaries. For additional safety, two boxes were constructed from 3/4-inch plywood to house all the "Variacs", switches, and relays for both constant temperature baths. These boxes were made safe by keeping a small positive pressure, above atmospheric, within the boxes with compressed safe air. Thus, it was impossible for any benzene vapors to be transported into the boxes and cause an explosion resulting from an electrical spark within the boxes.

9.44 Pumps and Isolation Chamber.

9.441 Feed and Discharge Pumps. Both the benzene and water feed-stream pumps, and the water-discharge pump were "Constrametric" piston pumps controlled by D.C. motors and "Thymotrol" controls. These pumps possessed dual pistons so geared that the resultant flow was supposed to be constant. By means of an auxiliary wet of gears, the speed range of the pumps was rated to be 58 fold downward from the maximum capacity. To further lower the minimum capacity, the pump motors were equipped with 100 Ohm resistors which could be switched in series with the series fields of the D.C. drive motors. Flow rates were adjusted by means of "Helipots" which controlled motor speeds, and provided the desired flow rates.

The packing for these pumps was stated to be "pure" Teflon.. It was installed practically without the use of lubricant, and was leached by many months of operation.

Flow capacities for these pumps are indicated in Table 2.

Table 2. Capacities of the pumps employed

Material Pumped	Gal/hr	Ft/hr[a]
Benzene (feed)	0.72[b] - 57.0[d]	5 - 394
Water (with feed end discharge)	0.46[c] - 32.5[d]	8 - 225

[a]Using a 1.917-inch diameter column with a 0.377-inch diameter spacers for the plates. Some convenient conversion factors for such a column are:

GPH = 6.938 x FPH = gallons per hour

GPH = 0.1337 x CFH = gallons per hour

FPH = 0.0003211 x CFM = feet per hour

CFM = 3114 x FPH = cubic feet per minute

[b]Minimum without irregular action, with the added control provided in motor field.

[c]Minimum without irregular action, as rated.

[d]Rated maximum of pump.

9.442 Pulse Pump. The pulse pump was a Milton-Roy "Simplex" pump equipped with a special microadjustment for stroke length, thus permitting the piston stroke to be changed during operation from 0 to 4-inches. This is equivalent to a range of amplitude in the 1.92-inch diameter column of 0 to 2.54-inches. The pulse pump speed was also controlled by a "Thymotrol" unit in conjunction with a D.C. drive motor. Pulse frequencies could be varied from about 7 to 110 strokes per minute by means of a "Helipot" variable resistor. The pulse pump was also packed with "Teflon".

9.443 Isolation Chamber. An isolation chamber was installed between the pulse pump and the column, and fitted with a double thickness of a 4-mil, 4-inch chamber "Kel-F" diaphragm. It had been found in practice that the so-called "pure" Teflon packing rings were not pure Teflon, but instead possessed a small percentage of some substance, probabily a binder, that slowly leached from the packing into the fluid pulsed. This contaminant tended to affect the degree of dispersion in the pulse column. The isolation chamber served to eliminate this factor from at least the major source of trouble, the pulse pump.

The pump side of the isolation chamber was equipped such that this side of the chamber could be filled with water under a head of approximately ten feet. This was done to insure complete filling of this side of the isolation chamber after changes in stroke length were made, and to make-up for water losses due to leakage around the packing gland of the pump. If such a provision were not made, incomplete filling of the pump side of the isolation chamber might result, leading in turn to incomplete transmission of the pulse stroke through the diaphragm.

Prior to this investigation, isolation chamber diaphragms were merely cut to the diameter of the chamber flanges, and bolted into place. This resulted in stretching of the diaphragm during the pulse stroke in addition to tearing around the flange bolts, all of which resulted in rapid failure of the diaphragm, especially at high values of pulse amplitude.

During the course of this investigation, it was necessary to replace a broken isolation chamber diaphragm. Instead of installing the new diaphragm as described above, enough diaphragm material was cut and

preformed to allow the diaphragm to move a total distance, in the chamber, slightly greater than that of the maximum pulse stroke to be used. This procedure resulted in less stretching and tearing of the diaphragm, and greatly increased diaphragm life.

9.45 Pulse Column.

9.451 Description. A scale drawing of the pulse column is shown in Figure 7. The column consists of a precision-bore tube of chemical-grade (No. 7720) "Pyrex", 1.92-inches in inside diameter and 18-inches in length. Eight perforated plates of 20 gage stainless steel were held together on a 1/4-inch stainless steel center tie rod the same length as the column, the plate spacing being maintained by 2.00-inch sections of 3/8-inch outside diameter stainless steel tubing slipped over the central tie rod. By tightening nuts on the tie rod ends, the plates and spacers could readily be squeezed enough to cause the plate assembly to bind against the column wall with a force sufficient to withstand the pulsing action.

The precision-bore section of the column tube was 1.917-inches in internal diameter, thus giving 2.886-square inches of cross-sectional area. After subtracting the cross-sectional area of the 0.377-inch diameter spacers, which was 0.112-inches, the superficial cross-sectional area was 2.774-square inches, or 0.01926-square feet.

Attached to each end of the column were 2 x 3-inch Corning "Double Tough" Pyrex pipe reducers, which served as settling zones and to which the feed and exit lines were attached, as shown in Figure 7. Five 1/8-inch "Ameripol" (a solvent-resistant synthetic rubber) gaskets were used to all glass-to-glass, or glass-to-metal connections of the column

installation. These gaskets had been exposed for several years to the action of benzene and water, and therefore were thought to be thoroughly leached of all extractable substances.

The top of the column was designed such that the benzene overflow was vented to a glass condenser. Thus any benzene vapors, coming from the hot benzene discharge, would be condensed and returned to the benzene overflow before leaving the column. This is shown in Figure 6.

9.452 Plate design. The plates used in the pulse column were made of 20 gage stainless steel, perforated with 1/8-inch holes in a 60-degree triangular patterns, providing 24.6 percent free area. Figure 8 shows a plate in detail.

Four of the eight plates used were commercially punched, and four were drilled. The first plate, starting from the bottom of the column, was drilled, and plates 2 through 8 alternated between punched and drilled plates. All punched plates were positioned with the round edge upward. The characteristics of the perforated plates are given in Table 3.

Table 3. Details of perforated plates

Plate diameter	1.912-inches
Plate thickness	0.0317±0.00122-inches
Hole diameter	0.127±0.0163-inches
Hole spacing	0.244±0.0789-inches
Percent free space	24.6
Diameter/spacing ratio	0.521
Plate gage	21.8 U. S. Std. (interpolated)

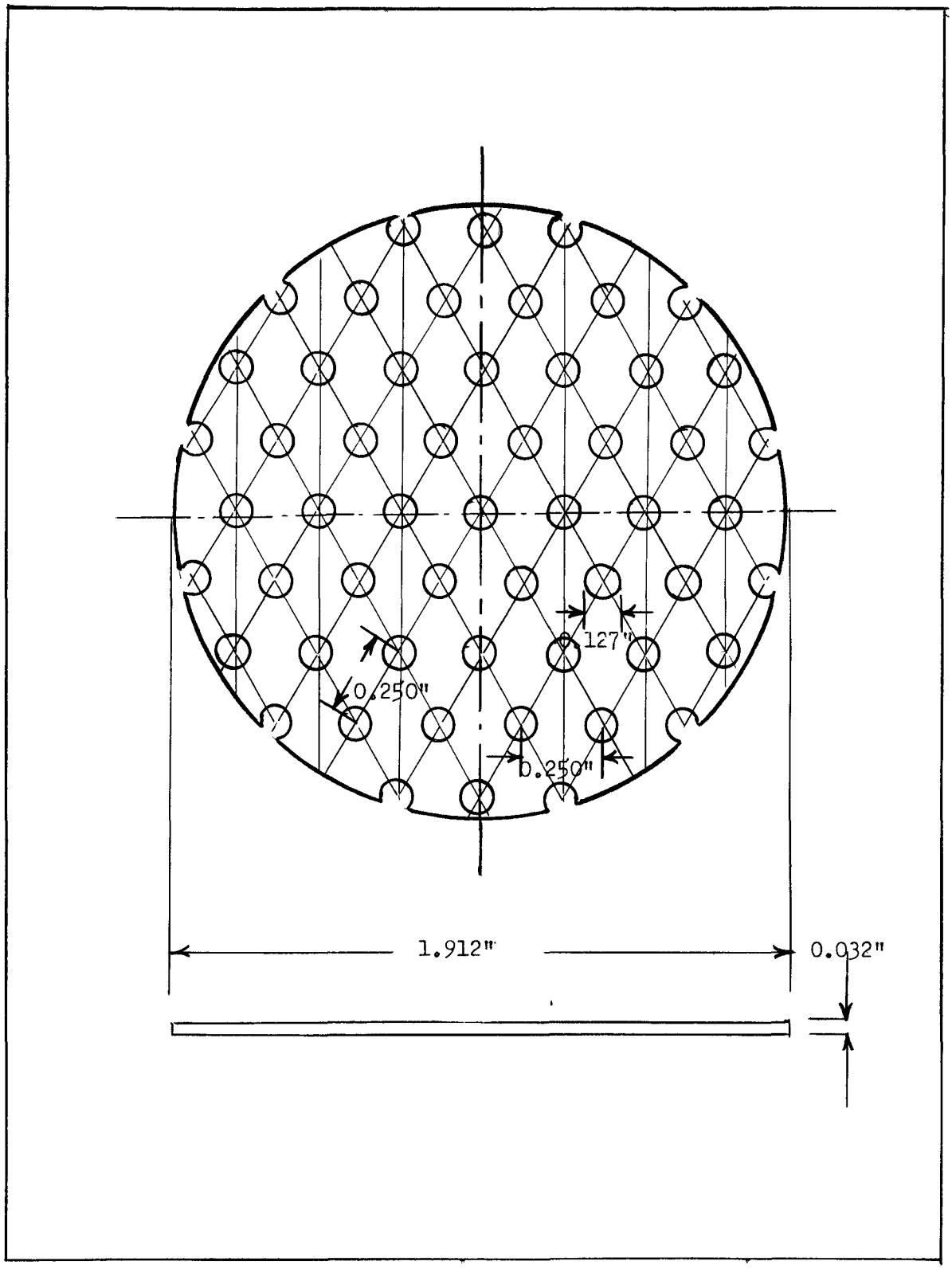

Figure 8. Plate detail

9.46 Insulation.

9.461 Column Insulation. The pricision-bore tube of the pulse column and the two "Pyrex" reducers located at each end of the tube were all insulated with six pieces of "styrofoam" plastic insulation. The six pieces of insulation were cut such that they formed three matching pairs which enclosed the column with a layer of styrofoam between 3 and 5 inches thick, averaging about 4 inches. Each pair was mounted around the column by two bolts holding them together, and arranged in such a way that the central section, around the precision-bore tube, could be removed readily without interferring with other parts of the insulation. The top and bottom support plates of the column, including the pulse isolation chamber, were more easily insulated with 3 to 4 layers of 1-inch thick "Ultralite".

9.462 Other Insulation. As was previously mentioned, both the benzene and water constant temperature baths were insulated with a 1-inch thick layer of "Ultralite" insulation. In addition, both the benzene and water stainless steel feed storage tanks were similarly insulated with a 1-inch layer of "Ultralite".

All piping, feed and discharge lines, and connecting tubing were insulated with "Protekto-Flex" pipe insulation. This insulation consisted of a 1-inch glass-fiber liner with an integral plastic jacket. Irregular joints were covered with conventional fiber-glass material, tapped with a polyvinyl chloride tape.

For a more detailed description of the column insulation, and properties of the various insulating materials used, refer to Li (25).

9.47 Temperature Measuring Devices.

9.471 General Description and Locations. When the pulse column was modified for heat transfer studies, four thermopiles were installed to measure the inlet and outlet temperature of both the benzene and water phases. Thermopiles were located in the two feed stream inlet nozzles, water discharge line, and in the benzene coalescing section above the benzene-water interface at the top of the column, as shown in Figure 7. In addition, a sensitive mercury-in-glass thermometer was located in the benzene feed line about one foot from the column. This thermometer was so located as to enable a correction to be made in the heat balances for heat transfer to the benzene via conduction through the benzene inlet nozzle.

Another thermometer was hung within a yard of the column, and was used to record room temperature. Thus fluctuations in room temperature could be noted and related to heat losses from the column.

9.472 Thermopile Assembly. For sensitive temperature measurements, an iron-constantan thermopile with four terminals was constructed. The four terminals were made from thermocouple-grade, No. 30 B. and S. Gauge enameled wire, and inserted in 1/8-inch outside diameter stainless steel tubes selected as the thermowells. The thermopile terminals were welded together with an electric arc, and to the other terminals, each junction was coated with "Glyptal" and covered with a plastic film of "Mylar". In addition, to further insure against short circuiting, and to avoid airfilm heat transfer resistances, the thermowells were partly filled with a molten heat resistant plastic, known as "Westcoat Clear", which upon cooling forms a tough, rubbery solid.

Constantan extension wires carried the thermopile circuit through a selector switch to a Leeds and Northrup, type K, precision portable potentiometer. The selector switch was a rotary, totally-enclosed, low-contact resistance switch made especially for use with thermocouple and thermopiles. It was a two-pole, twelve-position, type 31-3-0-2 switch, manufactured by Leeds and Northrup.

The cold junction for the thermopiles was an ice bath made with distilled water, and kept in a Dewar flask, which in turn was kept in a larger Dewar flask. The potentiometer and selector switch were both kept at room temperature.

9.473 Thermowells. As was mentioned above, the thermowells for the four thermopil terminals were made from 1/8-inch outside diameter stainless steel tubing, with a 1/64-inch wall thickness. Ends of the thermowells containing the terminals were closed by soldering with silver-solder.

The water-inlet thermowell tip was located at the discharge slots in the water inlet nozzle. The benzene inlet thermowell tip, however, was located only 1/4-inch inside the column to minimize the magnitude of corrections necessary due to heat transfer from the continuous phase to benzene in the inlet nozzle. The thermowell used in measuring benzene discharge temperatures extended down from the top of the column 1-inch, reaching to about 1.5-inches above the benzene-water interface. The bottom thermowell, used in measuring water discharge temperatures, extended about 2-inches into the column, along the axis of the exit water line.

9.474 Feed Line and Room Thermometers. As was mentioned previously, mercury-in-glass thermometers were used to measure room temperature, and benzene temperatures in the benzene feed line, about one foot from the column.

Room temperatures were measured using a conventional 2 to 52°C thermometer, graduated in 0.2°C increments for 100 mm immersion. Benzene temperatures in the feed line were measured with a -2 to 50°C thermometer, graduated in 0.1°C increments for total immersion, and manufactured by The Brooklyn Thermometer Company. By using a magnifying slide, temperatures could be estimated to 0.01°C on this thermometer.

9.475 Temperature Probe. The temperature probe, for determination of temperature profiles within the column was constructed by installing an iron-constantan thermocouple in a stainless steel thermowell. The wire used was thermocouple grade, No. 30, B. and S. gauge enameled wire, the junctions being welded together with an electric arc. The measuring junction was soldered into a 3/32-inch outside diameter stainless steel tube, 26-inches in length. Constantan extension wires were used to connect the temperature probe with the same selector switch and potentiometer as was used for the thermopiles. A cold junction, consisting of an ice-bath made with distilled water and kept in a Dewar flask, was again used for the reference junction.

The temperature probe was installed in the column through the 8 x 8 x 3/8 stainless steel bottom end plate by means of a "Koncentrick" Teflon packed packing gland. Perforated plates in the column were so arranged that all holes approximately 1/4-inch from the plate edges were in the same vertical line. In this way it was possible to locate the

packing gland such that the temperature probe could be moved up and down in column through these holes. The temperature probe installation is shown schematically in Figure 7. Holes 3/4-inch in diameter were cut in the styrofoam insulation around the column so the position of the probe could be visibly observed.

9.5 Process Piping

All lines used on the pulse column equipment were of type 316 stainless steel tubing, with the tubing being joined with "Teflon"-seated "Koncentrik" fittings of the same alloy. In addition, all valves and packing glands were made of 316 stainless steel, with "Teflon" packing. A few valves and other items, not in direct contact with either phase, were of brass or polyethylene. Except for five synthetic rubber gaskets (well extracted with benzene) in the pulse column, all liquid contact was with stainless steel, brass, glass, Teflon, polyethylene, and Kel-F.

9.6 Safety Provisions

Since benzene is both high flammable and toxic, much attention has been paid to the provisions of safety. In addition to the explosion-proof boxes constructed for housing the constant-temperature bath controls, and the vent and condenser on the hot benzene discharge line, the room containing the equipment was ventilated with two large explosion-proof fans. One fan exhausted to the outside, while the other circulated air within the room. All pumps, wiring and fixtures were of explosion-proof construction. Any equipment capable of sparking, such

as some control switches, were installed in a separate, isolated room. Also adequate warning signs and indoctrination of all personnel were employed.

10.0 EXPERIMENTAL PROCEDURES

10.1 Calibration of Instruments

10.11 Thermopiles. Each of the four thermopiles was calibrated against a set of precision mercury-in-glass thermometers, themselves calibrated to 0.01°C. by the National Bureau of Standards. The calibration was carried out in a Fisher "Isotemp Bath", a water bath maintaining the temperature constant within less than 0.01°C. The thermometers were totally immersed. The thermopiles, in their respective thermowells, were immersed as far as possible. A wiring unit similar to that employed with the column installation was used.

The calibration was carried out at approximately 5°C. intervals from 20°C to 75°C. The calibrations are presented in Table 4 for each of the four thermopiles. To illustrate the results, the data were plotted in Appendix Figure 1. However, in actual use, the data were plotted on a larger scale plot to permit temperatures to be estimated to 0.01°C. For temperatures above 75°C., the calibration curves were extrapolated linearly.

10.12 Temperature Probe. The temperature probe was calibrated in the pulse column against the previously calibrated thermopiles, using only hot water in the column. The calibration data are presented in Table 5 from which the calibration curve, shown in Appendix Figure 2 was obtained.

10.13 Flow Measuring Devices. Although all rotameters and gage glasses had been previously calibrated for the pulse column apparatus, only one of the benzene gage glasses was actually used for any flow measurement. None of the rotameters were utilized because of the low flow rates employed in this investigation, and it was found more accurate to determine water flow rates directly from the water discharge, rather than from any gage glass readings. This was due to the fact that changes in the water inlet flow rate were made to maintain the water-benzene interface within the column at some given position. All benzene flow rates were determined using the 1-1/2 inch diameter gage glass, the calibration curve for which is given in Appendix Figure 3.

10.2 Measurements of Variables

10.21 Flow Rates.

10.211 Benzene. As mentioned above, a 1-1/2 inch diameter calibrated gage glass was used in the measurements of benzene flow rates. Use of a quick-acting three-way valve allowed prompt switching from the benzene storage tank to the gage glass, and vice versa. By noting the initial gage glass reading and the time required to reach a final reading, it was possible to calculate the volume of benzene pumped from the glass per unit time. All times observed in pumping from the gage glass were determined with a stopwatch. Initial and final benzene volumes in the glass were obtained from the calibration curve shown in Appendix Figure 3. For the range of pump settings used in this investigation, a time lapse of approximately 60 seconds was allowed for pumping from the gage glass.

10.212 Water. Water flow rates in the column were determined by actually collecting and determining the mass of water discharged from the column in a given time. The discharge water was simply collected in a 800 ml. glass beaker over a period of approximately 1-1/2 minutes and weighed. By also noting the temperature of the water discharging into the beaker, it was possible to calculate the volumetric flow rates of water in the column. Again all times were determined with a stop-watch.

For both the benzene and water stream, it was found that the flow rates were reproducible within ± 1 percent by use of the aforementioned methods of measurements. Unfortunately, flow rate drifts of ± 10 percent were sometimes observed over periods of several hours, due in some manner to the pump action at low speeds. However, flow rates were checked about every 30 minutes during the course of a run to keep the drift to a minimum.

10.22 Rate of Pulsing.

10.221 Pulse Frequency. The speed of the pulse pump motor was controlled by means of a precision variable resistance "Helipot", with the actual frequency of a pulse cycle determined by timing the number of cycles observed in about one minute. Such frequency measurements were found to be reproducible to within ± 0.1 cycles per minute. No drift of frequency rate was noted after a warm-up period of about one hour.

10.222 Pulse Amplitued. Amplitude has been defined as the maximum fluid displacement in the column during a pulse cycle, under conditions such that the travel of the liquid level stayed between plates. This, of course, was not true for 2 and 2-1/2 inch amplutides where one

plate was traversed. Pulse amplitudes were originally determined by use of a cathetometer under conditions of very low frequency rates. It was found that the overall reproducibility was about ± 0.01 inches. Amplitudes were set by use of a micro-adjustment arm and the following calibration data given in Table 6.

Table 6. Pulse amplitude calibration data

For a column 1.917 inches in diameter.

Micro-adjustment arm setting on pulse pump	Amplitude in column inches
1/4 + 0.0	0.20
3/8 + 6.05	0.25
3/8 + 13.0	0.30
1/2 + 13.0	0.40
5/8 + 13.0	0.50
7/8 + 13.5	0.63
1-1/8 + 1.0	0.75
1-1/2 + 5.0	1.00
2-1/4 + 8.0	1.50
3 + 7.0	2.00
3-7/8 + 1.0	2.50

10.23 Temperature.

10.231 Thermopile. Temperatures of the inlet and outlet streams of both the benzene and water phases were determined by means of thermopiles. Readings were obtained by introducing the proper thermopile into the potentiometer circuit by means of the selector switch, and reading the resulting e.m.f. of the thermopile. Temperatures could then be readily obtained from calibration curves for the thermopiles. Thermal e.m.f.'s were measured using a Leeds and Northrup Precision Portable, type K, potentiometer, on which values of e.m.f. could be estimated to within 0.001 millivolts.

10.232 Temperature Probe. Temperature profiles within the column were determined by means of a temperature probe in a manner exactly analogous to that employed with the thermopiles. It was found that once the probe was located in a desired position, only a few seconds were required for the measuring junction of the thermocouple in the probe to reach a form of dynamic thermal equilibrium with the surrounding liquid. Actually, the temperature probe measured an average fluid temperature due to the fact that the surrounding liquid temperature was continually increasing and decreasing because of the pulsation within the column. However, once a form of dynamic or average thermal equilibrium was reached, thermal e.m.f.'s were again estimated to 0.001 millivolts on the potemtiometer.

10.233 Thermometers. In addition to the thermopile and temperature probe readings, room temperature and the temperature of benzene in the feed line about one foot from the column were also recorded. This

was done by simply reading these temperatures directly from the mercury-in-glass thermometers.

10.3 Operating Procedure

10.31 Start-up. Initially all valves were closed, except for by-pass around the pumps, and all electrical switches open. All heaters in the constant temperature baths were turned on at full power until the baths reached the desired constant temperatures. This usually required one to two hours, depending on the temperatures on the baths. It was found that the bath temperatures had to be 1 to 10°C. higher than a given inlet stream temperature due to heat losses in the feed lines. The exact magnitude of this temperature difference was dependent upon the operating temperature of the bath, and the feed stream flow rate.

Once the water phase constant temperature bath had reached temperature, the by-pass valves around the water pumps were closed, and water started through the column. The bath controls were then set to maintain a given constant temperature. A flow rate equivalent to a superficial velocity of approximately 20 ft/sec was used. Once through discharge water form previous runs was used during start-ups in order to conserve the freshly distilled water for the actual run.

At the end of a two hour period, the pulse amplitude was set and the pump side of the isolation chamber filled with water, from a relatively high water head as described in Section 9.443. The pulse pump was then set into operation at the desired frequency, and fresh distilled water started into the column from the stainless steel storage drum at the desired flow rate. By-pass valves around the benzene pump were

closed, and benzene started into the column at the proper flow rate. The benzene constant-temperature bath controls were then set to maintain a given constant temperature. Since the flow rates of both streams were found not to be independent, it was necessary to make minor flow rate adjustments after both phases had been introduced into the column.

Thirty minutes after the benzene stream had been started through the column, temperature readings were taken and flow rates checked. In addition, the pulse pump frequency was also checked. From this point on, temperature measurements were made every 10 minutes, with pulse frequency and flow rates being checked every 30 minutes. This procedure was followed until the last three readings for at least two of the thermopiles agreed within 0.01 millivolts, and the last two readings for all thermopiles agreed within 0.01 millivolts. When this agreement between readings for the individual thermopiles was obtained, the run was assumed complete.

10.32 Change of Conditions. Since both temperatures and flow ratios of the benzene and water streams were set during the start-up of a series of runs, the only variables that required major changes during the heat transfer runs were pulse amplitude and/or frequency. Changes in pulse amplitude necessitated a brief shut-down of the pulse pump while the amplitude was changed and the isolation chamber filled with water on the pump side. Both phases were allowed to continue flowing into the column during such changes. Variations in pulse frequency were simply made by changes in the "Helipot" setting of the pulse pump, and checked by means of a stopwatch as previously described.

Once the changes in pulse frequency and/or amplitude were made, 30 minutes were allowed to pass before any temperature readings were taken. From this point on, temperature measurements were made very 10 minutes, with pulse frequency and flow rates being checked every 30 minutes, as was described above, until completion of the run.

10.33 Shut-downs. At the completion of a run or series of runs, both water pumps and the benzene pump were shut-off, and by-pass valves around these pumps opened. All other valves were closed, and the pulse pump shut down. Finally, all heaters in the constant temperature tanks were shut off.

11.0 ANALYSIS OF BEHAVIOR PATTERNS

11.1 Heat of Pulsing in the Column

11.11 Introduction. The pulsing action has the effect of imparting mechanical energy to liquid charged to the column. This mechanical energy degenerates into heat energy as the fluid in the column is pulsed through the perforated plates, thus contributing to temperature changes in the column liquid, and is known as the heat of pulsing. In addition, some mechanical energy is also degenerated into heat energy due to friction around the packing gland of the pulse pump, which affects liquid temperatures in the column if not properly controlled.

It was, therefore, necessary to quantitatively evaluate the magnitude of this heat of pulsing before any interpretation of the heat transfer data could be made. Such an evaluation was made by Li (25) in his preliminary heat transfer studies on the pulse column.

11.12 Results of Li.

11.121 Interpretation of Li. In principle, the heat of pulsing is simply measured by filling the well-insulated column with the fluid to be pulsed, and then pulsing at some desired rate. Care must be taken, however, to ensure that the pulse pump packing gland is loose enough so that resulting heat effects can only come from the degeneration of mechanical energy as the fluid is pulsed through the plates, and not result from friction at the pump packing gland, As the heat of pulsing develops, the temperature of the batch of liquid rises, and is measured.

Li determined heats of pulsing by introducing weighed amounts of benzene or water into the column at temperatures close to those of the

column materials and surroundings. After waiting 15 minutes to ensure thermal equilibrium between the column liquid and its surroundings, an average pulsing rate denoted by the symbol $\overline{|\,|}\,a$, was imposed on the column. The pulse pump packing gland was loosened to eliminate heat effects at this source. The $\overline{|\,|}\,a$ term is merely the average flow rate, in feet per hour, of a pulse, considering both the up and down pulse. For the case of no superficial velocity difference in the column, $\overline{|\,|}\,a$ has been shown by Pike (35) to be simply expressed as,

$$\overline{|\,|}\,a = 10\ FA \tag{82}$$

where the number 10 includes a factor for conversion of units, and

$\overline{|\,|}\,a$ = average flow rate, or the volume of liquid pulsed past a plate during a stroke, divided by the product of the column cross-sectional area and actual time of flow in that direction, ft/hr.

F and A are the same as previously defined. (See Section 7.122)

Li's results showed that temperatures at the top and bottom of the column increased linearly as a function of time for the first 30 to 60 minutes of pulsing and then began to increase in a non-linear fashion with decreasing rates of temperature rise. This decrease in the rate of temperature rise as a function of time was attributed to increased heat-transfer through the column glass-and-metal parts. However, when the temperature of the surroundings was about the same as inside the column, only a constant rate of temperature rise was noted. This led to the conclusion that only the initial constant rate of temperature rise was a measure of the heat of pulsing.

Li also found that the initial rate of temperature rise, and the average, was 15 percent higher at the bottom of the column than at the top. This behavior has led to the conclusion that frictional losses, hence heat generation, was higher in the pulse line than in the column proper. However, by averaging the two initial rates of temperature rise, Li calculated heats of pulsing by the following expression:

$$q_{PB} = E_B \, (dT/d\Theta)_B \times 1.8 \tag{83}$$

where

q_{PB} = heat of pulsing for batch system in 8-plate column, Btu/hr.

E_B = heat equivalent of batch of liquid and of solids in immediate contact with the liquid, Btu/°F.

$(dT/d\Theta)_B$ = average of two initial rates of temperature rise, measured at the top and bottom of the column, °C/hr.

When the column was filled with benzene to the level actually used under operating conditions, 4.4 pounds of benzene were contained in the column, and E_B had a value of 4.92 Btu/°F. Similarly, when the column was filled to the operating level with water, 5.0 pounds of water were contained in the column, and E_B had the value 8.12 Btu/°F.

Using q_{PB} as defined above, Li was able to show a relation with a as follows:

$$q_{PB} = 1.02 \times 10^{-8} \, \overline{\Pi a}^{2.83} \tag{84}$$

It is well to note here that Li used the symbol q_P for the batch system heat of pulsing, q_{PB}, defined by equation (84).

11.122 Predicted values from pressure-drop data. Pike, et al, (37) studied the pressure-drop through the pulse column as a function of a, and developed the following correlation for 22-plates in the column.

$$\triangle P = 3.31 \times 10^{-5} \overline{/\!/a}^{1.83} \qquad (85)$$

where

$\triangle P$ = pressure-drop across 22 plates, expressed as inches of fluid flowing (water).

From the above pressure-drop relationship, Li was able to derive an expression predicting what is here called the heat of pulsing for a flow system in the column, with 8 plates, denoted by the symbol, q_{PF}, and defined as

$$q_{PF} = 0.155 \times 10^{-8} \overline{/\!/a}^{2.83} \qquad (86)$$

where

q_{PF} = heat of pulsing for flow system in 8-plate column, Btu/hr.

Li made no distinction between the heats of pulsing actually measured for a batch system, q_{PB}, and those predicted from pressure drop data for a flow system, q_{PF}. Thus when Li made a simple comparison of equations (84) and (86), he found that for the particular apparatus used in this investigation, and its adjustments, the measured heats of pulsing were about 6.5 times that predicted from pressure drop data. This difference was interpreted to mean that far more heat was generated in the pulse line than among the plates in the column.

11.13 Reinterpretation of Li's Data. Although Li's experimental method and the data obtained for the determination of heats of pulsing were assumed to be essentially correct, comparison of his experimental results with those predicted from pressure drop data was considered to be in error, as was indicated in the previous section.

Li's heat of pulsing data were essentially for a batch system. His data were calculated from the initial rates of temperature rise of a given mass of material, resulting from the collective influence of many pulsations.

The pressure drop data, however, represents the energy dissipated across a given number of plates during just one pulse cycle, and is not the total result of many pulsings. In other words, the pressure drop data may be thought of as energy degraded as fluid flows through the column as a result of one pulse cycle. Thus, heat of pulsing data predicted from pressure drop data may be considered to apply essentially to a flow system. Therefore, Li's data must be interpreted for a flow system before any comparison of the two can be made.

In reinterpreting Li's data for a flow system, the central point involved is that, for the batch system, the resident material in the column received heat at a constant rate, and rose in temperature indefinitely. However, for the flow system, there was a finite residence time during which the material entered and left the system. Only during this residence time was it exposed to the heat of pulsing. In this case, the given rate of heat generation was continually expended into different batches of the liquid as it flowed through the column.

Considering a fluid flowing through the column at some superficial velocity V, the time required for a given fluid element to pass from one end of the column to the other is given by the expression

$$\triangle \theta_R = Z/V \tag{87}$$

where

$\triangle \theta$ = resident time of fluid element in column, hr.

Z = column length, ft.

V = superficial fluid velocity, ft/hr.

Assuming the rate of heat generation expended to this fluid element due to pulsing in a flow system, to be equal that expended to a similar fluid element in a batch system, then the total amount of heat generated in the element, Q_F, is given by the expression

$$Q_F = q_{PB} \triangle \theta_R \tag{88}$$

where

Q_F = total amount of heat generated in fluid element passing through the column due to the heat of pulsing, Btu.

It is reasonable to assume that the heat equivalent of the batch system, E_B, over an infinitesimal increment of time, is the same as the heat equivalent for the flow system, E_i for an infinitesimal increment of flow. Hence, in spite of the different temperature profiles within the column for the batch and flow system, it is assumed that

$$E_i = E_B \tag{89}$$

where

E_i = heat equivalent for flow system of infinitesimal increment of flow, Btu/°F.

Thus, Q_F may be expressed as

$$Q_F = E_i \triangle T_P = E_B \triangle T_P = q_{PB} \triangle \theta_R \tag{90}$$

where

$\triangle T_P$ = increase in temperature of fluid element due to heat of pulsing, °C.

However, from equation (83), we have that

$$q_{PB} = E_B \, (dT/d\theta)_B \times 1.8 \tag{83}$$

Therefore, equations (83) and (90) may be combined and rearranged to yield

$$\triangle T_P = (dT/d\theta)_B \triangle \theta_R \tag{91}$$

Thus for any given value of the average rate of pulsing, $\overline{\Pi}a$, the heat of pulsing for a flow system, q_{PF}, may then be determined by the following expressions for the heat imparted to a flowing system.

$$q_{PF} = VA \rho C(\triangle T_P) \times 1.8 = VA \rho C(dT/d\theta)_B \triangle \theta_R \times 1.8 \tag{92}$$

or combining with equation (87)

$$q_{PF} = A \rho C(dT/d\theta)_B (Z) \times 1.8 \tag{93}$$

where

A = superficial column cross-sectional area, ft^2.

ρ = fluid density, lbs/ft^3.

C = specific heat of fluid, Btu/(lb)(^{o}F)

and all other terms are the same as previously defined.

Using equation (93) above and Li's data for the initial rates of temperature rise, heats of pulsing were calculated which were applicable to a flow system, and are shown as a function of $\overline{f}a$ in Figure 9. Also shown on Figure 9 are values of the heat of pulsing predicted from pressure drop data using equation (86). Excellent agreement between the experimental and predicted results is now noted, with the experimental results being used in this investigation, and in the recalculation of the heat transfer results of Li and Gardner.

11.2 Heat Losses from the Column

11.21 Introduction. Although the column was well insulated, measured and calculated rates of heat transfer to the surroundings turned out to be too large to neglect. Thus, heat losses through the column insulation were simply determined by passing hot water through the column, at a constant flow rate and inlet temperature, and measuring the difference between the inlet and outlet temperatures.

11.22 Results of Li.

11.221 Experimental. Li (25) pumped water steadily at a superficial velocity of about 20 ft/hr into the top of the column, and out the bottom. The water flow rate and direction matched that for the heat transfer runs. Except for one run, the column was not pulsed. Results showed that a slow pulsing rate ($\overline{f}a$ = 143), seemed to have no effect

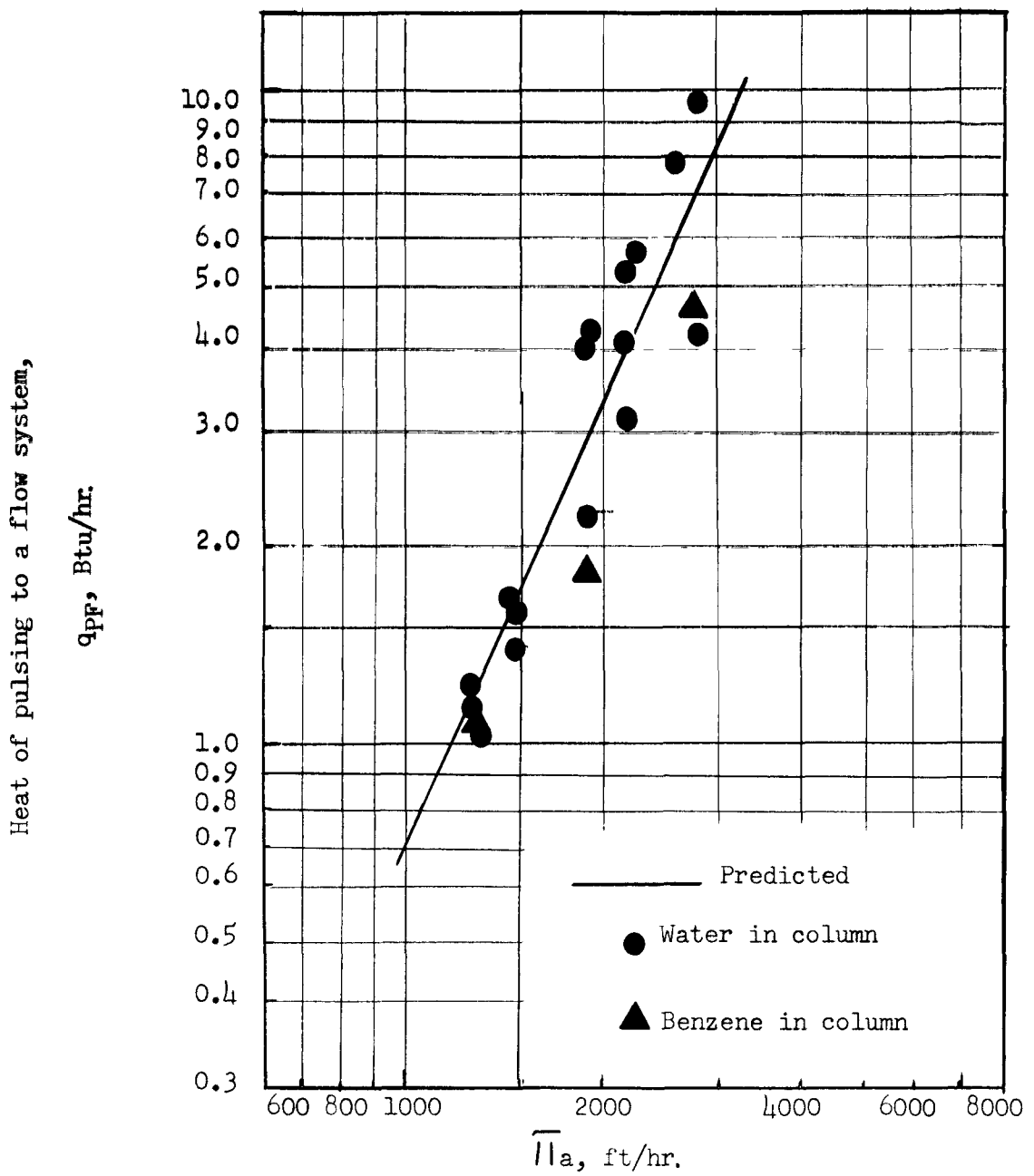

Figure 9. Heat of pulsing as a function of $\overline{\Pi}a$

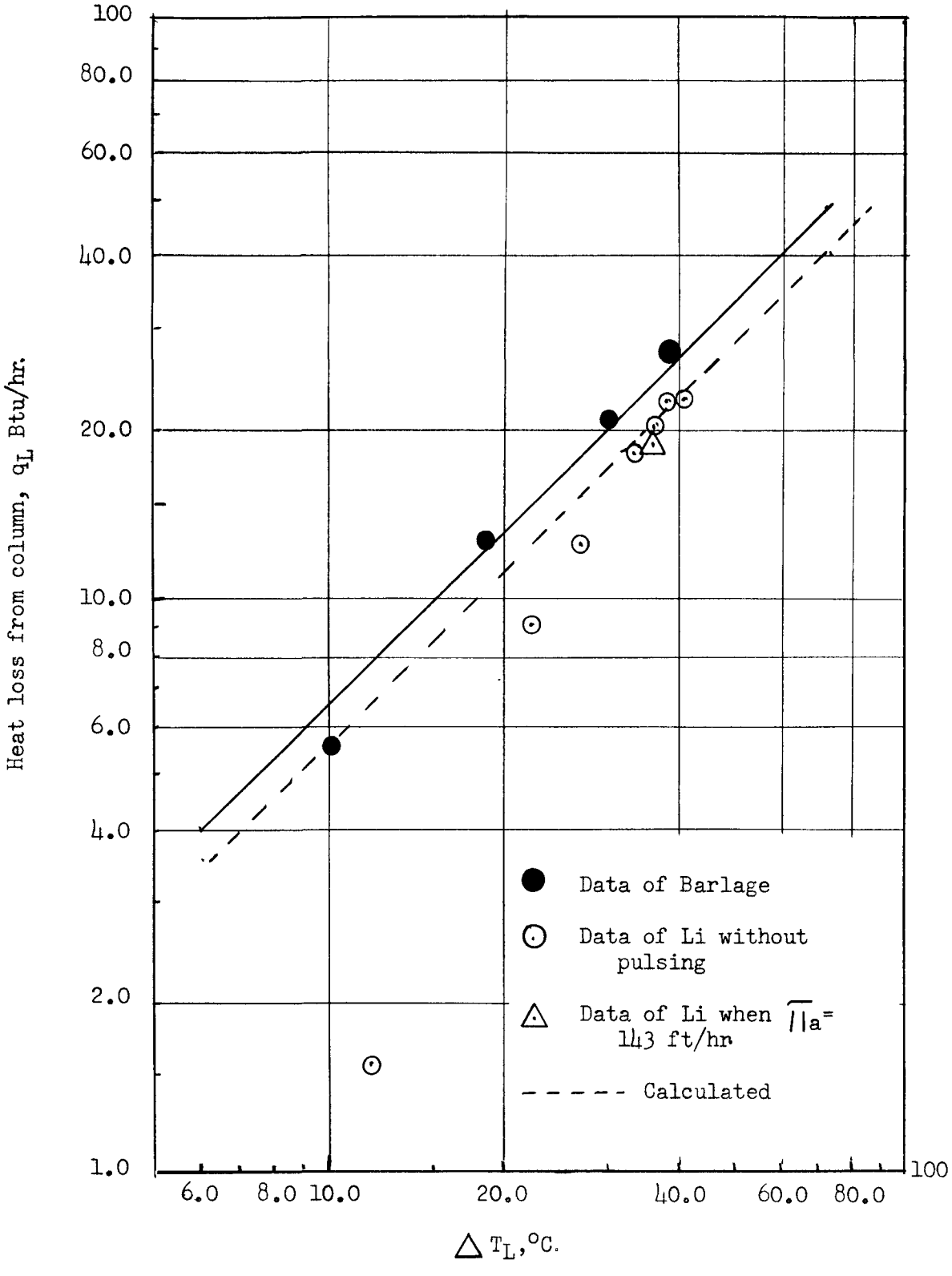

Figure 10. Heat losses under run conditions

11.23 Results of this Investigation. Preliminary to the major heat transfer studies of this investigation, heat losses from the column were again determined with water, using the same method of procedure and flow conditions employed by Li. However, in all heat loss runs, a period of three to five hours was allowed for the column to reach a state of thermal equilibrium. All runs were made starting with the column at room temperature. Results of these heat transfer studies are listed in Table 7, and are plotted on Figure 10 also.

Table 7. Heat loss data

	Water Flow Rate		Temperature Data, °C.				Heat Losses
Run No.	v_c ft³/min.	V_c ft/hr.	inlet TC_1	outlet TC_2	room T_R	Diff. ΔT_L	q_L Btu/hr.
126	0.00612	19.1	64.00	63.35	24.0	39.7	26.4
127	0.00664	20.7	53.60	52.93	25.6	27.7	29.6
128	0.00690	21.5	40.93	40.68	22.9	17.9	11.6
129	0.00682	21.3	35.11	34.99	24.5	10.6	5.5
130	0.00677	21.2	54.38	53.96	22.8	31.4	19.0

An examination of Figure 10 now shows excellent agreement between values of heat losses predicted by equation (94) and those observed in this investigation as compared to losses observed by Li.

Although the exact reasons for the discrepancy between Li's data and those predicted by equation (94) are not clearly understood, it is felt that he did not always allow sufficient time for the column to reach a state of thermal equilibrium. A careful examination of his run data sheets revealed that in almost every run where his results were

lower than those predicted by equation (94), a change from a higher to a lower value of inlet water temperature had been made. Thus, if only 30 minutes were allowed for thermal equilibrium, it is felt that the column had not reached equilbrium in this time, and observed values of heat losses would be low. This would be due to the fact that the surroundings of water in the column would be at a higher temperature than under true equilbrium conditions, and measured heat losses would be reduced below equilibrium values.

11.24 Conclusions. Li used his measured values of heat losses from the column rather than those predicted by equation (94) in all of his calculations. This was due to the fact that his measurement of heat loss was made under the same operating conditions that were used during the actual heat transfer studies, and therefore were judged to be suitable for correcting heat balance of the heat transfer runs. However, because of the agreement between measured heat losses from the column obtained in this investigation, and those predicted by equation (94), results of this investigation were used in all calculations, and in the recalculations of Li's data. In addition, the heat loss data of this investigation were also used by Gardner in all of his heat transfer calculations.

11.3 Heats of Solution

11.31 Introduction. When two pure liquids are brought into contact, both dissolve some of the other, no matter how insoluble they are considered to be. With each increment dissolved, there is a heat effect which can be large or small. Since such an effect could conceivably be

important in heat transfer studies in liquid-liquid contactors, it was felt that some quantitative evaluation was necessary of the heats of solution.

11.32 Calculation of Li. Preliminary estimates indicated that it would be virtually impossible to measure heats of solution in a static calorimeter for the system benzene-water, because of the time required for equilibrium to be reached without stirring. If stirring was employed to enhance equilibrium, heat effects due to the stirring would be greater than those of solution. It was also concluded that the heats of solution could not be measured with insulated pulse column, considering it to be a flow calorimeter, because of the precision with which the heat effects must be determined. It was, therefore, decided to calculate the heat of solution effects from known solubility data, thermodynamic relations, and estimates of the degree of saturation obtained.

Assuming water entering the pulse column at 30°C with no benzene content, and leaving at 50°C saturated, Li was able to show that the heat effect would be 1.6 Btu/hr across the water phase for a flow rate of 0.0055 ft^3/min. Similarly, for benzene entering the column at 30°C with 5 percent of its saturation content, and leaving at 95 percent saturated at 50°C, Li showed that the heat effect would be 12.6 Btu/hr added to the benzene phase for a benzene flow rate of 0.006 Ft^3/min. Application of the above heats of solution in the calculations of this investigation is discussed in detail in Section 11.524.

11.4 Heats of Evaporation

11.41 Evidence for Evaporation. During the course of his preliminary heat transfer studies on the pulse column used in this investigation, Li detected the odor of benzene in the room containing the equipment. The unit was operated at atmospheric pressure. It was concluded that this odor resulted, primarily, from the evaporation of benzene within the column, with the benzene vapors escaping into the room through the benzene discharge vent at the top of the column. The pulsing action also pulses air back and forth in the vent system. For this reason, the benzene overflow vent was equipped with a glass condenser, as described in Section 9.451, and vented to the outside. Thus, any benzene vapors, coming from a hot benzene discharge, would be condensed and returned to the benzene overflow, excepting for that portion which is displaced in a mixture with air by the pulsing action.

Although neither Li nor Gardner reported any signs of benzene condensation in the glass condenser, both indicated to Pike (37) that they thought a small amount of benzene evaporation was taking place and reducing the indicated values for the rate of heat transfer, when measured on the benzene side. This presence of evaporation was somewhat substantiated by the fact that Li (25) and Gardner (13) reported average percent deviations in their heat balance (discussed in Section 11.51) of 6.6 and 12.5 percent respectively, the benzene phase values being low.

During the course of this investigation, however, condensation of benzene vapors in the glass condenser was observed, especially at operating conditions of high benzene outlet temperatures, and low V_D/V_C

ratios. In addition, bubbles of benzene vapor were actually seen within the column under these extreme operating conditions mentioned above. As a result of this benzene evaporation the column, the average percent deviation in the heat balances of this investigation was 15.0 percent, with percent deviations as high as 70 percent being noted at operating conditions of high benzene outlet temperatures, low V_D/V_C ratios, and high rates of pulsing. Thus, it was felt that some procedure or method of calculation should be developed for an approximate quantitative evaluation of the heat effects associated with the evaporation of benzene, both within the major contacting area of the column, and at the benzene discharge vent. Such a method of calculation is described below in Section 11.42.

11.42 Development of Heat of Evaporation Relation.

11.421 Assumptions. It was believed that a certain portion of the discrepancies noted between the net rates of heat transfer between phases, uncorrected for heats of evaporation, Δq^*, (defined in Section 11.51) was directly related to the heat of evaporation of benzene in the column. The remaining portion of the heat balance discrepancy was attributed to certain random errors inherent in the operation of the column. One source for such random errors are end-effects, and will be discussed in some detail in Section 11.63.

After some deliberation, it was decided that heat losses within the column, resulting from the evaporation of benzene, should be dependent upon three major operating variables. These variables were the pulse frequency-amplitude product, FA; the sum of the benzene and water

vapor pressures measured at the outlet benzene temperature; and the V_D/V_C ratio.

The sum of the benzene and water vapor pressures were used as a measure of the total vapor pressure of the system since the benzene and water are essentially immiscible. Thus, it was considered more correct to use the sum of the vapor pressure, rather than that of the benzene alone, evaluated at the outlet benzene temperature. Although the V_D/V_C ratio was assumed to have little effect upon the evaporation of benzene in the benzene discharge vent, it was considered to be an important factor in the evaporation of benzene within the column proper. Finally, it was believed that the FA product should in some way effect the evaporation of benzene both within the column proper, and in the benzene discharge vent, due to pulse agitation.

11.422 Correlation of Variables. It was assumed that the heat of evaporation of benzene in the column was represented by an equation of the form,

$$q_e = k(FA)^m \ (\Sigma P/100)^n \ (V_D/V_C)^p \qquad (95)$$

where

q_e = heat of evaporation losses from the column, Btu/hr.

ΣP = summation of benzene and water vapor pressures evaluated at the benzene outlet temperature, mm Hg.

FA = pulse frequency-amplitude product, in/min.

V_D/V_C = ratio of superficial velocities, dimensionless.

and

k, m, n, and p are experimentally determined constants.

A value of the constant, m, was determined by plotting values of log $\triangle q^*$ versus log FA for constant values of outlet benzene temperatures, and a V_D/V_C ratio of one. Data of Li, Gardner, and of this investigation were used. Although the pattern obtained was not precise, due to random heat effects, a linear dependence of $\triangle q^*$ upon FA was clearly evident, and reasonably approximated by m = 0.533. This was especially true for the runs in which the benzene temperatures were high, and the heat of evaporation effect was relatively large in comparison to the random effects.

The next step in the correlation was to plot log $\triangle q^*/(FA)^{0.533}$ versus log $(\Sigma P/100)$ for a V_D/V_C ratio of one. Again a linear behavior pattern was noted, with the slope yielding a value of the exponent, n, of 2.64. The data of Li, Gardner, and of this investigation were again used in the correlation.

Although the values of $\triangle q^*/(FA)^{0.533}$ scattered over a wide range, five logarithmic averages of these values were used, and showed a very definite dependence upon $(\Sigma P/100)$, as shown in Figure 11.

Since the low values of $\triangle q^*$ are inherently much less precise than the higher values, more weight was given to the higher average values of $\triangle q^*/(FA)^{0.533}$ in drawing the above curve.

Similarly, the exponent of the (V_D/V_C) ratio, p, was determined by plotting the log (V_D/V_C) versus log $\triangle q^*/(\Sigma P/100)^{2.64}(FA)^{0.533}$. Only the data of this investigation at the higher temperature levels were used in this particular correlation. Because of the wide scatter of values of $\triangle q^*$, an arithmetic average of values of $\triangle q^*/(FA)^{0.533}(\Sigma P/100)^{2.64}$ were used, which yield linear relationship as shown in Figure 12.

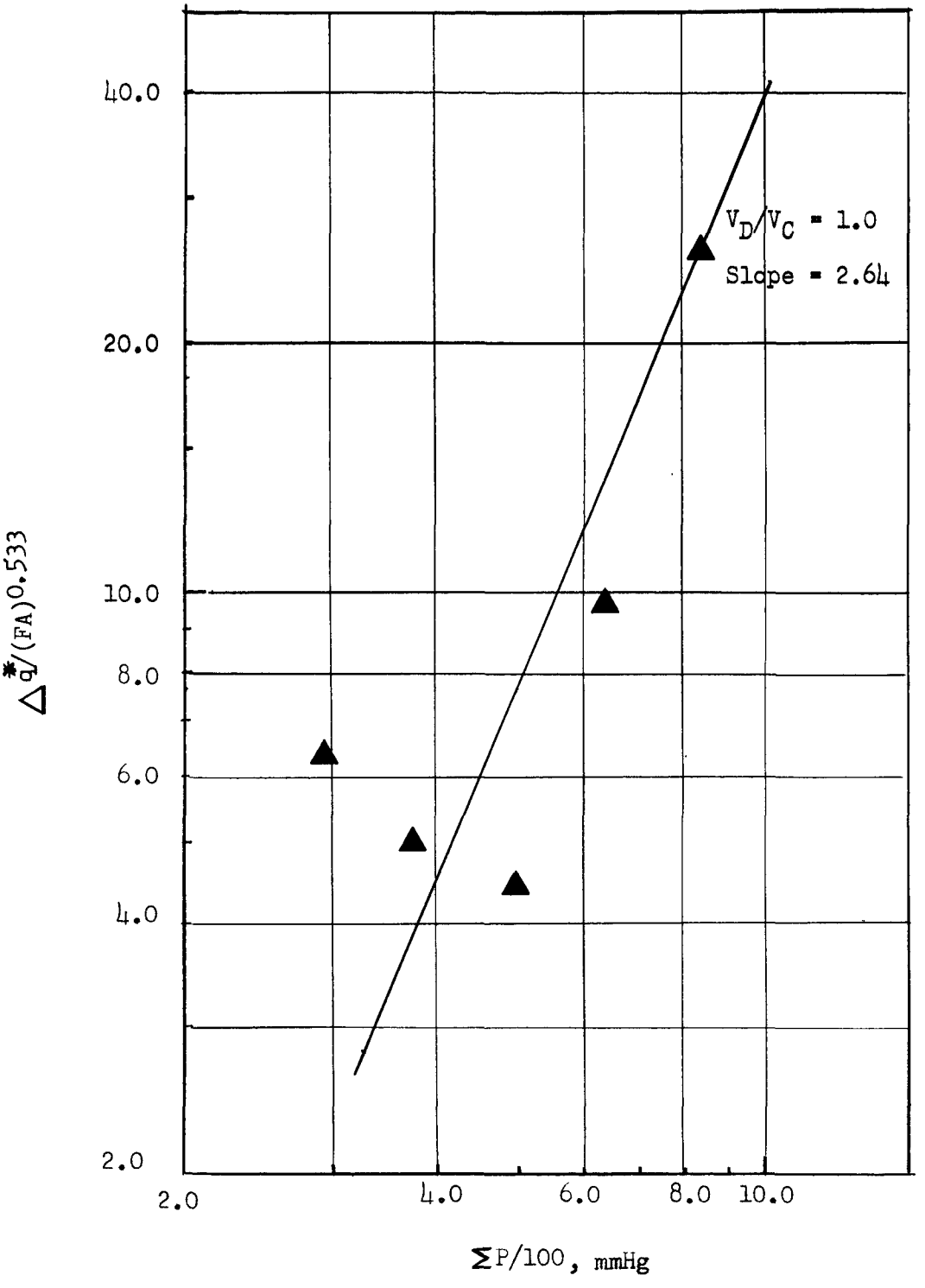

Figure 11. Effect of vapor pressure upon heat of evaporation

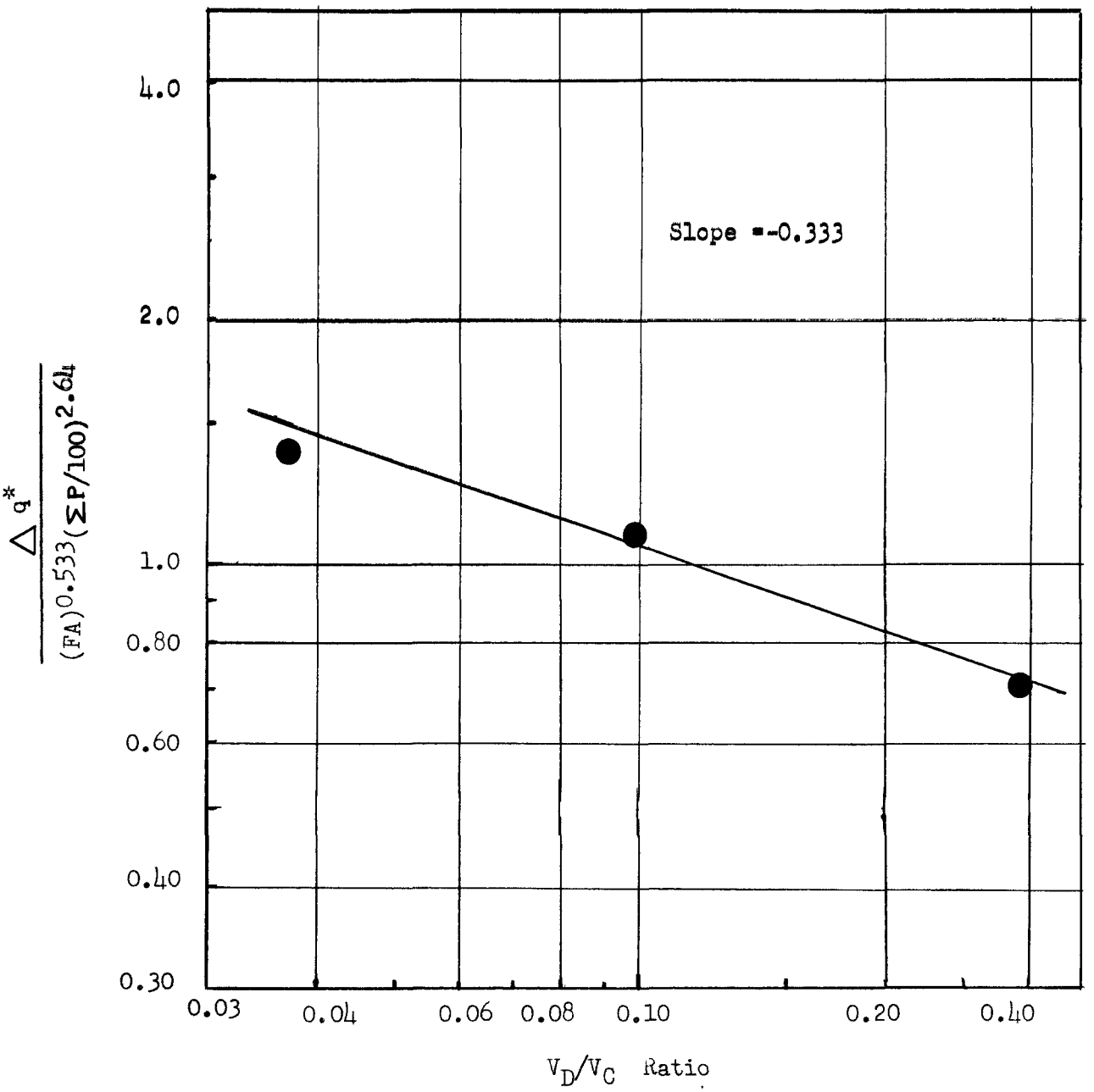

Figure 12. Effect of superfical velocity ratio upon heat of evaporation

Figure 12 clearly shows the dependence of $\triangle q^*/(FA)^{0.533}(\Sigma P/100)^{2.64}$ upon the V_D/V_C ratio, and is reasonably approximated by a value of -0.333 for the exponent, p.

It was arbitrarily assumed that the sum of the random errors inherent in $\triangle q^*$ must be zero for all heat transfer runs used in the determination of the above exponents. Thus, under such an assumption, the sum of all the $\triangle q^*$s must be equal to the sum of all the heat of evaporation effect, or

$$\Sigma \triangle q^* = \Sigma q_e = k(FA)^{0.533}(\Sigma P/100)^{2.64}(V_D/V_C)^{-0.333} \qquad (96)$$

Using equation (96) above, a value k was determined from the experimental data used in the evaluation of the above exponents with the exception of Gardner's data. This value of k was found to be 0.0814. Thus, heat losses due to evaporation in the pulse column used in this investigation, using benzene dispersed in water as the system, may be quantitatively evaluated from the expression

$$q_e = 0.0814\ (FA)^{0.533}\ (\Sigma P/100)^{2.64}\ (V_D/V_C)^{-0.333} \qquad (97)$$

11.43 Conclusion. An examination of equation (97) indicates that the correlation predicts large values of heats of evaporation at operating conditions of high benzene outlet temperatures, and low V_D/V_C ratios. Such high predictions, however, are in agreement with experimental observations, since under the operation conditions mentioned above, benzene condensation in the glass condenser and benzene vapor bubbles in end column were observed. Similarly, under operating conditions where

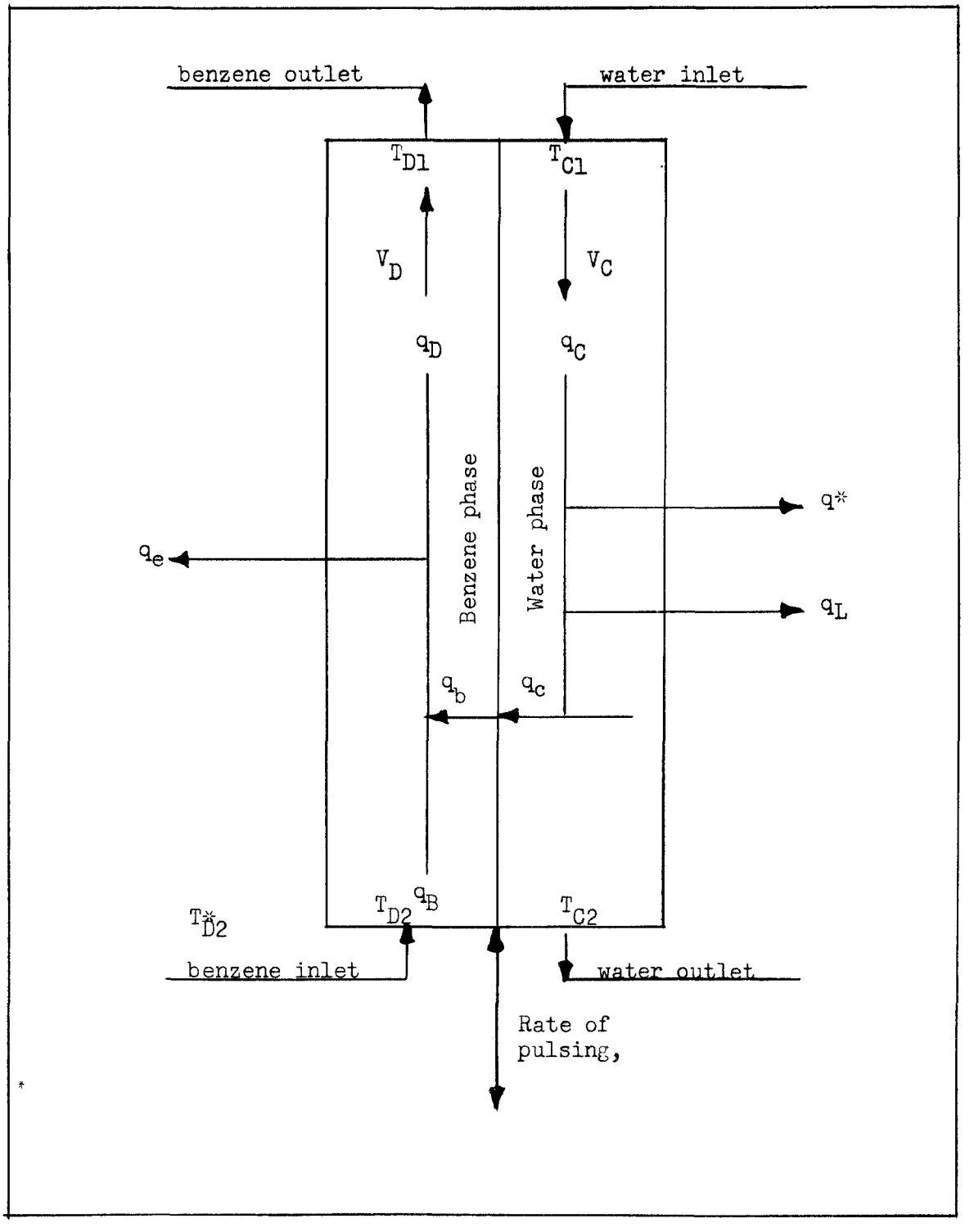

Figure 13. Schematic diagram for heat balance in pulse column

$$q_b = q_c$$

or combining equations (100) and (101),

$$q_D - q_B = q_e = q_c + q_{PF} - q_L - q^* \tag{103}$$

In practice, it has been found that the measures of q_b and q_c are not, in general, equal. Therefore, an average measure of heat transfer between phases has been defined as follows:

$$q_a = (q_b + q_c)/2 \tag{104}$$

where

q_a = average net rate of heat transfer between phases, Btu/hr.

Also, as a measure of discrepancies in the heat balances, the percent deviation from q_a has been defined as,

$$\% \text{ deviation} = \triangle q/q_a \times 100 \tag{105}$$

where

$$\triangle q = q_c - q_b$$

It might be well to mention here that both Li and Gardner made no correction in their heat balances for heat losses in the column due to evaporation, q_e. Although the continuous-water phase heat balance is not effected by q_e, and is calculated by means of equation (97), the net rate of heat transfer to the discontinuous phase is definitely effected by q_e. However, Li and Gardner neglected this effect in their

calculations, and determined the net rate of heat transfer to the discontinuous phase by an equation of the form,

$$q_b^* = q_D - q_B \tag{106}$$

where

q_b^* = net rate of heat transfer to the discontinuous phase, uncorrected for heats of evaporation, Btu/hr.

Similar to equations (104) and (105) above, Li and Gardner defined an average measure of heat transfer between phases by an equation of the form,

$$q_a^* = (q_b^* + q_c)/2 \tag{107}$$

and the percent deviation from q_a^* by the expression,

$$\% \text{ deviation} = \triangle q^*/q_a^* \times 100 \tag{108}$$

where

$$\triangle q^* = q_c - q_b^* \tag{109}$$

As was previously mentioned in section 11.421, values of $\triangle q^*$, defined by equation (109) above, were determined from the results of this investigation for the development of a correlation for the prediction of heat losses from in column due to benzene evaporation.

For the sake of clarification, it might be well to mention here that Li used the symbol q for both q_c and q_b^* as defined above, and Gardner used the symbol q_c for both q_c and q_b^*. In addition, Li and Gardner both used the symbols q_a and $\triangle q$ for q_a^* and $\triangle q^*$ as defined above.

q_w was correct, a careful examination of his method of calculation for q_B revealed it to be in error, due to the fact that an average benzene solubility was used over the above temperature range rather than terminal solubilities.

Assuming benzene entering the column at 30°C saturated with water, heats of solution for water in benzene were calculated for the benzene leaving 95 percent saturated and at temperatures of 40, 50, 60, and 70°C. The data on solubility of water in benzene was taken from Pavia (33). For these respective outlet temperatures, the heats of solution were found to be 3, 7, 12, and 19 Btu/hr respectively. Using these above four values of the heats of solution, it was possible to satisfactorily estimate values of q_B to be used in the recalculation of Li and Gardner's data, and in the calculations of this investigation.

11.525 Heat Transferred to Benzene as it Passes Through the Feed Distributor, q^*. Values of heat transferred to the benzene stream in the feed nozzle are calculated by an equation similar to equation (112) above.

$$q^* = v_D \rho_D C_D (T_{D2} - T^*_{D1})(60)(1.8) \qquad (117)$$

All terms are as previously defined. In this particular case, values of density and specific heat are evaluated at a new average phase temperature, T^*_{Da}, defined as,

$$T^*_{Da} = (T_{D2} + T_{D2})/2 \qquad (118)$$

11.526 Heats of Pulsing, q_{PF}. Li (25) at first arbitrarily assumed that roughly 75 percent of the heat of pulsing was generated in the

continuous water phase, while the rest was assumed generated inside the benzene droplets. However, since his interpretation of the heat of pulsing data, q_{PB}, led to relatively small values of the heat of pulsing, it was convenient, and caused no appreciable error, for him to assign all the heat of pulsing to the continuous phase.

Similarly, in this investigation all the heat of pulsing, interpreted for a flow system, q_{PF}, was assigned to the continuous phase, as can be seen from Figure 13, and the heat balance around the column. However, an examination of Figure 9 shows that the applicable heat of pulsing for a flow system, q_{PF}, determined from a reinterpretation of Li's data, are just about nil for the range of $\overline{\Pi}a$ values used in this investigation. Hence, they were assumed to be zero.

11.527 Net Rate of Heat Transfer between Phases, q_b and q_c. Values of the net rate of heat transfer between the continuous and discontinuous phases, q_c and q_b, were calculated from equations (100) and (101) of section 11.51 respectively, with the percent deviation in heat balances being determined by use of equation (105). In addition, the net rate of heat transfer to the discontinuous phases, uncorrected for heats of evaporation, q_b^*, was calculated using equation (106), with the uncorrected percent deviation in heat balances being determined by use of equation (108). When the direction of heat transfer was reversed, the net rate of heat transfer from the discontinuous phase was determined using equation (111), and the net rate of heat transfer to the continuous phase calculated from equation (110). All other heat effect were determined as previously described.

11.528 Heats of Evaporation, q_e. Heats of evaporation were calculated from equation (97) in the calculations of this investigation, and in the recalculation of Li and Gardner's data.

11.6 Methods of Calculation

11.61 Method of Li and Gardner. In section 7.3, equations necessary for the calculation of variables defining heat transfer in liquid-liquid contactors were presented. It will be remembered, that under contitions where the temperature difference between the two phases is linear throughout the column, as a function of the net rate of heat transfer between phases, use of the ln-mean temperature driving force, as defined by equation (36), was justified. It will also be remembered that the terminal conditions of temperature differences, defined by equations (37) and (38), whould be those associated with the mechanisms involved in the transfer of heat between phases only in the defined column height, Z .

Li and Gardner, however, used in their calculations the actual measured terminal temperatures which were influenced by end-effects at both the top and bottom of the column, and were not associated only with the defined column height, Z. Thus, assuming use of the ln-mean temperature driving force to be valid, Li and Gardner calculated temperature driving forces by the relation,

$$\triangle T_{lm} = \frac{(T_{C1} - T_{D1}) - (T_{C2} - T_{D2})}{\ln(T_{C1} - T_{D1})/(T_{C2} - T_{D2})}$$

$$= \frac{(T_{C2} - T_{D2}) - (T_{C1} - T_{D1})}{\ln(T_{C2} - T_{D2})/(T_{C1} - T_{D1})} \qquad (119)$$

In addition, any calculations of heat transfer variables which involved the net rate of heat transfer between phases, values of q_a^* were used.

11.62 Revised Methods of Calculations. The method of calculation employed in this investigation, and in the recalculation of Li and Gardner's data, was essentially the same as that employed by Li and Gardner with one exception. Values of q_a, rather than q_a^*, were used in the calculation of heat transfer variables which involved the net rate of heat transfer between phases. Related to this method of calculation, percent deviations in the heat balances were, by necessity, determined using values of q_a and $\triangle q$, rather than values of q_a^* and $\triangle q^*$ as employed by Li and Gardner. Ln-mean temperature driving forces were again used in the calculations, and were determined as described in the previous section by means of equation (119).

11.63 Discussion of Revised Methods of Calculation. As was mentioned in Section 11.61, the terminal conditions of temperature differences used in the calculation of ln-mean temperature driving forces, should only be those associated with the mechanisms involved in the transfer of heat between phases in the defined column height, Z. However, in all the calculations, both in this investigation and in the calculations of Li and Gardner, actual measured terminal temperatures were used in the determination of ln-mean temperature differences. As was indicated in Section 11.61 these actual measured terminal temperatures are somewhat different from those associated with the defined column height Z, because of end-effects.

In Section 7.4, a brief discussion of end-effects in liquid-liquid contactors for mass transfer was given. Similar end-effects, however, were also noted in the heat transfer studies of this investigation. It is believed that these end-effects came from four major sources, heat transfer across the benzene-water interface at top of the column, heat transfer to or from the feed streams in the feed distributors, and heat generation within the pulse line to the column resulting from friction around the pulse pump packing gland.

It is obvious that a certain amount of heat is going to transfer across the benzene-water interface, regardless of the direction of heat transfer between phase. This is due to the fact that always some finite temperature driving force will always exist between phases at this location. Thus, since the benzene outlet thermopile is actually located in the benzene phase above the interface, its readings will reflect the net consequence of all these diverse effects. As a result, the benzene outlet temperatures indicated by this thermopile are different from the ones desired, associated only with the heat transfer in the defined column height, Z.

As mentioned in Section 9.32, past experience had shown that the inlet benzene temperature was definitely influenced by the outlet water temperature. This was due to heat transfer to or from benzene in the benzene feed nozzle. As described in Section 9.32, an attempt was made to reduce this heat transfer, in both the benzene and water feed distributors, by providing an air space around the nozzles. However, actual measurements of benzene feed temperature in the feed line, about one foot from the column, and in the benzene nozzle, made in this investigation,

indicated that heat transfer was still occurring in the distributor. In addition, results of this investigation also showed that the measured outlet water temperature was influenced by this heat transfer in the benzene nozzle. Under operating conditions of high V_D/V_C ratio (3.87 - 3.99), and relatively high temperature levels, it was found for heat transfer from the continuous to the discontinuous phase, that the measured outlet water temperature was actually lower than the measured benzene inlet temperature in the feed distributor. (See runs 193 and 196 of this investigation.) It was quite evident that the measured outlet temperatures of the continuous water phase were influenced by the heat transfer through the benzene inlet nozzle and vertical positioning of the thermopile. Thus, just as for the benzene case, the water outlet temperatures indicated by the water outlet thermopile were different from those associated only with heat transfer in the defined column height, Z.

A similar end-effect was noted at the top of the column when the direction of heat transfer was from the discontinuous benzene phase to the continuous water phase. At a low V_D/V_C ratio of 0.37, it was found that the actual measured benzene outlet temperature was lower than the measured water inlet temperature (see run 200 of this investigation). Again, this effect is attributed to heat transfer through the water inlet nozzle and the vertical positioning of the thermopile, and it definitely affected the measured benzene and water temperatures at the top of the column.

Although the exact nature of this heat transfer to or from the feed distributors is not clearly understood, it is believed that most of it

results from metal conduction as discussed in Section 9.32. However, no matter what the nature of mechanism of this heat transfer might be, it is clearly evident that it is present, and definitely affects the actual measured terminal temperatures. The important question is the magnitude of the errors thereby introduced.

An attempt was made to correct the measured outlet water temperature for the heat transferred to the benzene in this benzene feed distributor, q^*, for runs 193 and 196. Values of a corrected water outlet temperature, T^*_{C2}, were calculated by determining the change in the water outlet temperature, ΔT^*_C, resulting only from the transfer of heat, q^*, in the benzene nozzle. Values of ΔT^*_C were determined using the relation

$$\Delta T^*_C = \frac{q^*}{v_C \rho_C c_C (60)(1.8)} \tag{120}$$

where

$$\Delta T^*_C = T^*_{C2} - T_{C2} \tag{121}$$

T^*_{C2} = corrected water outlet temperature, °C.

All other terms are as previously defined. Since T_{C2} is known, equation (121) above may be rearranged to give T^*_{C2} as,

$$T^*_{C2} = \Delta T^*_C + T_{C2} \tag{122}$$

Values of T^*_{C2} were only determined for runs 195 and 194. Calculations would have been impossible were it not for the data from these two runs. This method of calculation was only used to determine an

approximate order of magnitude of the heat transfer variables, and results obtained really have little significance since none of the runs were treated by the above method.

It might have been possible to partially correct all of the other heat transfer results for end-effects in the bottom of the pulse column by the above procedure. However, this was not done due to the fact that uncorrected end-effects still would have existed at the top of the column. It was, therefore, concluded that at this time, calculated results should inherently include the total effect of the end-effects, rather than just a portion. It is believed that the presence of end-effects for heat transfer in liquid-liquid contactors should be the subject of a separate investigation.

As was mentioned above, another heat effect at the bottom of the column tending to influence water outlet temperatures was that of heat generation in the pulse line due to packing gland friction around the pulse pump. It was found at high pulsing rates, $\overline{\Pi}_D$ = 800 to 1200 ft/hr, that the outlet water temperature was raised due to this heat generation. However, because of the flow conditions used in the column, this heat generation did not effect any of the other column temperatures. This may be clearly seen from some of the data recorded during the course of a run in which this heat effect was observed, as shown in Table 9.

Table 9. Thermopile readings for run 143

$\overline{T}_D = 800 \qquad V_D/V_C = 2.85$

Thermopiles °C

Time	4:10 pm	4:25 pm	4:35 pm	4:45 pm	4:55 pm	5:05 pm
No. 1	45.68	45.51	45.51	45.51	45.51	45.59
No. 2	38.03	37.89	37.89	38.13	38.18	38.30
No. 3	31.88	31.47	31.47	31.47	31.47	31.47
No. 4	51.00	50.79	50.79	50.74	50.69	50.71

The thermopile locations are identified in Table 10.

Table 10. Identification of thermopiles

Thermopile No.	Stream Involved
No. 1	Benzene outlet, T_{D1}
No. 2	Water outlet, T_{C2}
No. 3	Benzene inlet, T_{D2}
No. 4	Water inlet, T_{C1}

An examination of Table 9 shows that all the column temperatures had essentially reached steady-state values of 4:35 pm, although the water outlet temperature continued to rise. This effect, however, could be and was controlled by carefully controlling the pressure on packing gland on the pulse pump. When a heat effect was observed, the packing gland was loosened.

12.0 EXPERIMENTAL PROGRAMS AND RESULTS

12.1 Summary of Heat Transfer Measurements

The number of heat transfer runs made in this investigation, and the number of heat transfer runs recalculated from the data of Li and Gardner total 117. In this total number of runs, V_D/V_C ratios were varied from 0.35 to almost 4.00, while $\overline{\Pi}_D$ values ranged from 50 to 1200 ft/hr. Values of the ln-mean temperature difference, $\triangle T_{lm}$, were varied from 1.24 to 13.72 ^{o}C.

In addition, several runs were made to determine the effect of temperature level upon the heat transfer performance of the column, as well as to determine the validity of using a ln-mean temperature difference in the heat transfer calculations. Runs were also made to determine the effect of the total flow rate, expressed as $(V_D + V_C)$, ft/hr, upon the performance of the pulse column.

In most of the above runs, the direction of heat transfer was from the continuous to the discontinuous phase. However, runs with heat being transferred from the discontinuous benzene phase to the continuous water phase were made in order to study the effects of reversed direction of heat transfer.

All heat transfer measurements, both experimental and calculated, for this investigation and for the heat transfer studies of Li and Gardner, are presented in Appendix Tables 1, 2, and 3 respectively. In addition, each table of the appendix has been subdivided into sections, designated by the following letters after the table number, with table designation such as 1A, 1B, etc.

Section Letter	Title of Section
A	Measured Flow Conditions
B	Calculated Flow Conditions
C	Measured Temperature Conditions
D	Calculated Temperature Conditions
E	Rates of Heat Transfer
F	Calculated Heat Transfer Responses

All data in Appendix Tables 1, 2, and 3 are arranged in order of increasing V_D/V_C ratio, or $\overline{\Pi}_D$ values, or difference between inlet stream and temperatures, $\triangle T_i$, where $\triangle T_i$ is defined as,

$$\triangle T_i = T_{C1} - T_{D2} \tag{123}$$

In addition, each section has been subsectioned into groups of runs in which one or more of the above variables are held constant, and are set apart with values of the constant variable or variables being indicated at the top of the group. Also, run numbers used by Gardner follow consecutively those of Li, and run numbers of this investigation follow consecutively those used by Gardner. Thus, there are no identical run number listed in Appendix Tables 1, 2, or 3.

It might be well to mention again at this point that part of Li and Gardner's data have been recalculated using the revised method of calculation described in Section 11.62.

12.2 Precision of Heat Balances

It is quite obvious that one measure of the reliability of any results obtained from heat transfer studies on the pulse column is that

of the agreement between heat balances, and the percent deviation from q_a, as described in Section 11.51. As was mentioned in Section 11.43, average absolute values of the percent deviations in the heat balances of 3.8, 12.1 and 8.2 percent were obtained for Li and Gardner, and in this investigation respectively, employing the revised method of calculation described in Section 11.62. In addition, when the sign of the percent deviation (plus or minus) was taken into account, net average percentage deviations of -1.8 + 8.6, and -0.4% were obtained for Li and Gardner, and in this investigation, respectively, employing the revised method of calculation.

From the above, it was concluded that the heat balances, and therefore the desired heat transfer measures of this investigation and those recalculated from Li's data, were reliable to well within 10%. In the following correlations, more "weight" was allocated to the results of this investigations than to the recalculated results of Gardner. However, it should be noted here that the result of Gardner are good considering the nature of the heat transfer problem involved, but not as consistent as those of Li and of this investigation.

12.3 Reproducibility of a Run

In order to determine the reproducibility of precision of the equipment, and to check the column performance from time to time with a run for which the results were known, a standard run was defined. The standard run was characterized by the following operating conditions,

$\overline{\Pi}_D$ = 150 ft/hr

V_D/V_C = 1.0

$T^*_{D2} \cong 31\ ^\circ C$

$T_{C1} \cong 51\ ^\circ C$

$\Delta T_i \cong 18.4\ ^\circ C$

Five such runs were made during the course of this investigation, and designated by run numbers 131, 132, 133, 141, and 168 of Table 11. Runs 131 through 133 were made at the very outset of this heat transfer study to determine the reproducibility of the apparatus. Run 141 was made at the completion of a series of runs in which the operating conditions were different than those for a standard run, and approximately one-fourth the way through all the runs of this investigation. This was done to detect any obvious mal-functioning of the apparatus since the results of this run could be readily compared to those obtained from runs 131 through 133. Similarly, run 168 was made under operating conditions defining a standard run, approximately one-half the way through all the runs of this study.

Results of the five standard runs are summarized below in Table 11.

Table 11. Summary of heat transfer results for standard runs

Run No.	Δq, Btu/hr	% Dev.	$H\Theta U_{oc}$	$H\Theta U_{od}$
131	- 4	- 1.4	0.732	0.309
132	+ 78	+ 24.6	0.860	0.400
133	+ 5	1.8	0.760	0.312
141	+ 14	4.9	0.875	0.359
168	+ 8	2.8	0.857	0.323
Averages	+ 20.2	6.5	0.817	0.341

An examination of Table 11 show that, on the average, results of the standard runs are reproducible within 10%, with this precision being assumed for the results of this investigation throughout the entire period of time.

12.4 Axial Temperature Probe

12.41 Introduction. As was previously mentioned in Section 9.33, stainless steel temperature probe was installed in the column in an attempt to obtain information on the behavior of temperature driving forces within the column. In particular, it was hoped that exploration of temperature profiles in the column would yield valuable information concerning the validity of the use of ln-mean temperature difference driving forces in the heat transfer calculations. It was also hoped that the investigation of temperature profiles in the column would reveal some information concerning temperature end-effects at each end of the column.

12.42 Technique Employed. As described in Section 9.475, the perforated plates in the column were so arranged that a selected group of holes, all of those approximately 1/4-inch from the plate edges, were in the same vertical line. The extension of this line to the bottom end plate located the entry port, in which was placed a "Knocentrick" Teflon-packed packing gland of an adjustable nature such that the temperature probe could be moved up or down in the column through the packing gland and the selected plate holes. Holes 3/4-inch in diameter were cut in the column insulation at each plate so that the terminal position of the

probe with respect to a plate could be visibly observed by temporary removal of hole-plugs.

12.421 Limitations. Because of the mechanical design of the column, and because of the position in which it was installed (bottom of the column close to the floor), it was impossible to move the temperature probe more than an inch or so above the top plate in the column. It was also impossible to move the temperature probe to a position below the bottom plate since the bottom-end of the probe would hit the floor. Also, if the measuring junction of the probe passed below the bottom plate in the column, it would spring into a position such that it would no longer be in line with the holes in the perforated plates. Thus, it would become impossible to pass the temperature probe back through the column without completely disassemblying the column.

12.422 Probe Positions in the Column. Temperature readings were taken at essentially three positions near each plate in the column by means of the temperature probe. These positions were approximately 1/8-inch above each plate, 1/8-inch below each plate, (except for the last plate at the bottom of the column), and at a position approximately half way between the plates. The plates in the column have been numbered one through eight consecutively, with the top plate in the column being designated as plate one. In addition, the three positions at which temperature was observed for each plate have been designated as positions A, B, and C, respectively, and are shown in Figure 14.

12.423 Flow Conditions Employed. Temperature measurements at the positions indicated above were only made for runs in which a high V_D/V_C ratio (approximately 3.0) was employed. In so planning, it was felt that

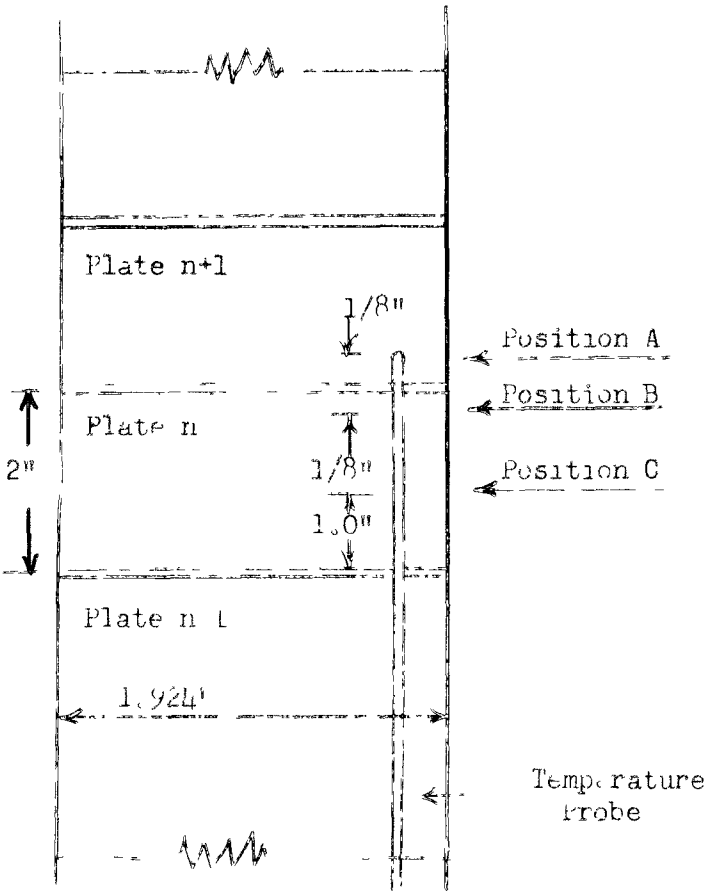

Figure 14. Positions of temperature-measurement probe with respect to plates.

the maximum amount of information concerning temperature profiles within the column could be obtained under these conditions, based on the two following reasons. First, for a given total flow rate through the column ($V_D + V_C$), high values of the V_D/V_C ratios gave the maximum amount of hold-up under a plate for a given rate of pulsing. Thus it was thought possible to get a more accurate reading of the discontinuous phase temperature as measured at Position B since the quantity of benzene in contact with the measuring junction of the probe was relatively large. Second, it was believed that the maximum amount of internal circulation within the continuous phase would occur between plates under operating

conditions of high V_D/V_C ratio. Thus, continuous phase temperature profiles, when determined at high V_D/V_C ratios, would tend to vary the most from the counter-current profiles in favor of a mixer-settler pattern. Thus, high V_D/V_C ratios would tend to test more severely the mathematical model employed.

12.43 Results.

12.431 Presentation of Results. Determination of temperature profiles within the column were made for runs 147, 145, 135, 142, 143, and 140 of this investigation, at $\overline{\Pi}_D$ values of 80, 150, 300, 600, 800, and 1200 ft/hr, respectively. An average benzene inlet temperature of approximately 31°C was employed with an average water inlet temperature of approximately 50°C. The V_D/V_C ratio was approximately 3.0 for all runs. Results obtained from measurements made with the temperature probe are presented in Table 12.

12.432 Interpretation of Measurements. It should be emphasized here that the readings obtained are time averages over a pulse cycle, and reflect the interaction of the true temperature fluctuations and the time lag of the probe. This point has been discussed previously in Section 10.232.

Temperature measurements made at position A were simply interpreted as a measure of the continuous phase temperature prior to contacting the discontinuous phase across the plate. Similarly, temperature measurements at position C were interpreted simply as a measure of the discontinuous phase temperature midway between the plates.

Interpretation of probe measurements at position B, however, vary depending upon the operating conditions employed in the column. Consider

Table 12. Temperature probe readings

Run No.	Probe Position	Probe Temperatures, °C Plate No. 1	2	3	4	5	6	7	8
147	A	45.65	44.55	42.85	40.95	39.30	37.65	36.35	34.65
	B	45.35	44.05	42.15	40.55	38.65	37.25	34.70	-
	C	44.55	42.85	40.95	39.30	37.80	36.45	34.70	-
145	A	45.65	43.45	41.70	40.35	38.45	36.85	35.60	34.25
	C	43.65	41.90	40.35	38.55	37.15	35.60	34.25	-
135	A	35.15	43.55	40.05	41.10	39.60	38.50	37.55	36.05
	C	43.70	42.55	41.20	39.80	39.00	37.90	36.30	-
142	A	44.55	43.55	42.35	41.05	39.50	38.25	37.15	36.15
	C	43.60	42.70	41.20	39.90	38.55	37.55	36.80	-
143	A	45.40	44.50	43.50	42.05	40.80	39.60	38.65	37.80
	C	44.95	43.95	42.65	41.15	40.30	39.15	38.00	-
140	A	44.35	43.65	42.85	41.90	40.95	39.90	38.90	37.90
	C	43.85	43.15	42.25	41.35	40.20	39.25	38.25	-

a situation in which the column is operating under some steady-state conditions. If the pulse pump were momentarily stopped, dispersed benzene would coalesce under each plate in the column, and measurements at position B would essentially indicate temperatures of the coalesced benzene. It should be noted, however, that such indicated temperatures would vary somewhat with respect to time, due to heat transfer across the benzene-water interface. Now assume that the pulse pump is started at a very low frequency. During the first part of the upward stroke,

the coalesced benzene beneath the plates would be redispersed and flow upwards towards the nest plate. During this period, temperatures indicated would increase due to contact of the probe with the hotter continuous phase. However, as soon as benzene again begins to coalesce beneath the plate, indicated temperature at position B would decrease, and remain essentially constant until the downward stroke of the pulse is begun. At this time, temperature indicated at position B would increase again due to hot continuous phase being pulled through the plates even though benzene is still coalesced beneath the plates. This behavior may be illustrated as shown in Figure 15.

From Figure 15, it can be seen that at very low pulsing rates measurements at position B could be timed to indicate temperatures of the coalesced benzene phase under the plate at the end of the up-stroke and at the beginning of the downstroke for a given pulse cycle. A benzene flow pattern similar to that indicated above actually has been observed in photographs taken by Gardner at $\overline{fI}_D$ = 150 ft/hr and a V_D/V_C ratio of 2.93. However, as the rate of pulsing increases, it is obvious that this period of time over which the coalesced discontinuous phase temperatures could be measured, θ, decreases as shown in Figure 16.

In addition, Figure 16 also indicated that at the higher rates of pulsing the time average temperature indicated at position B also increases, and therefore reads higher above the temperature of the benzene.

A temperature behavior pattern similar to that described above is clearly indicated in Figure 17. It will be noted that the continuous water phase temperature profiles, shown on Figure 17, have been displaced upward by 1.5, 2.0, 3.0, 3.0, and 4.5°C for $\overline{fI}_D$ values of 150, 300, 600,

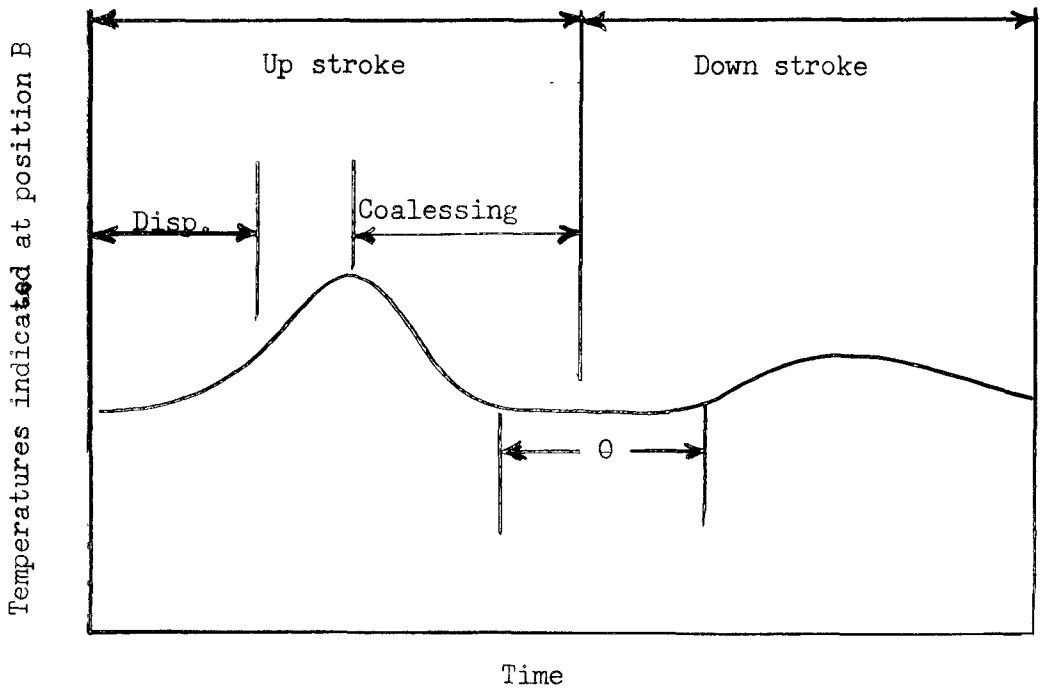

Figure 15. Assumed behavior of probe at position B

800, and 1200 ft/hr, respectively, for the sake of clarity. However, the curves for $\overline{\Pi}_D$ = 80 and $\overline{\Pi}_D$ = 150 ft/hr show definite regions of essentially constant temperature. For these two particular curves, it will be noted that from position C to A, the continuous phase temperature is essentially constant. Thus, it is reasonable to assume that the dispersed benzene phase has coalesced beneath the plates. Under such condition the, temperatures indicated at position B by the probe will be an approximate measure of the coalesced discontinuous phase temperatures beneath the plates. In addition, it will be noted that the average phase temperature increases as the rate of pulsing, $\overline{\Pi}_D$, also increases.

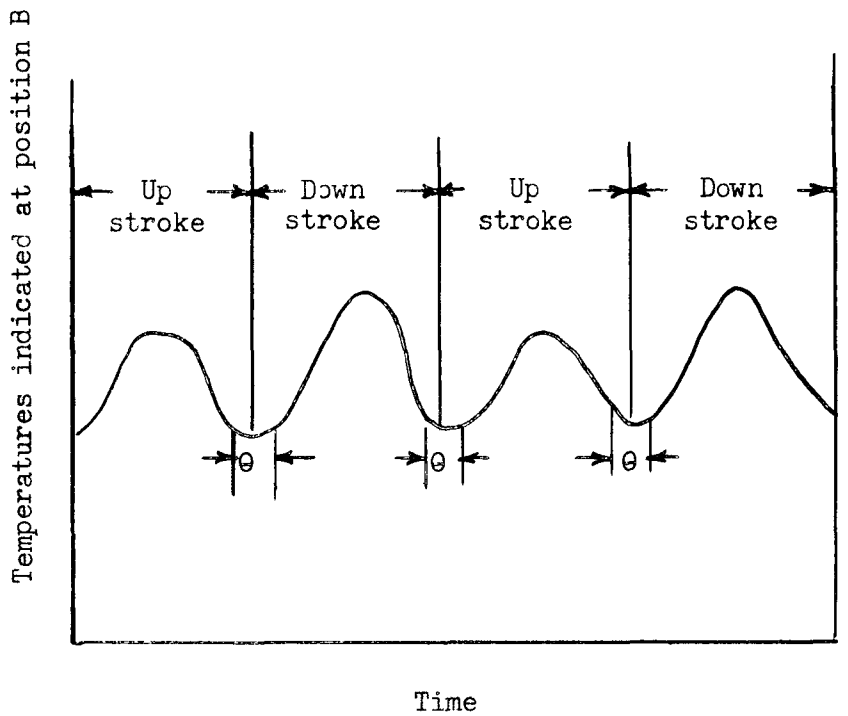

Figure 16. Assumed behavior of probe at position B

12.433 Interpretation of Profiles. Temperature profiles of the continuous water phase, consisting of only A and C position measurements, are shown in Figure 17 for all six $\overline{\Pi}_D$ values used in this investiagtion. As was mentioned above in Section 12.432, five of these profiles have been displaced by a finite number of degrees for the sake of clarity in determining overall behavior patterns.

It will be noted that temperatures between positions C and A have been represented by solid lines. This was due to the fact that temperatures in the region are interpreted as more nearly reading the time continuous phase temperature and hence having more meaning. In contrast, temperature variations between positions A and C are not known definitely,

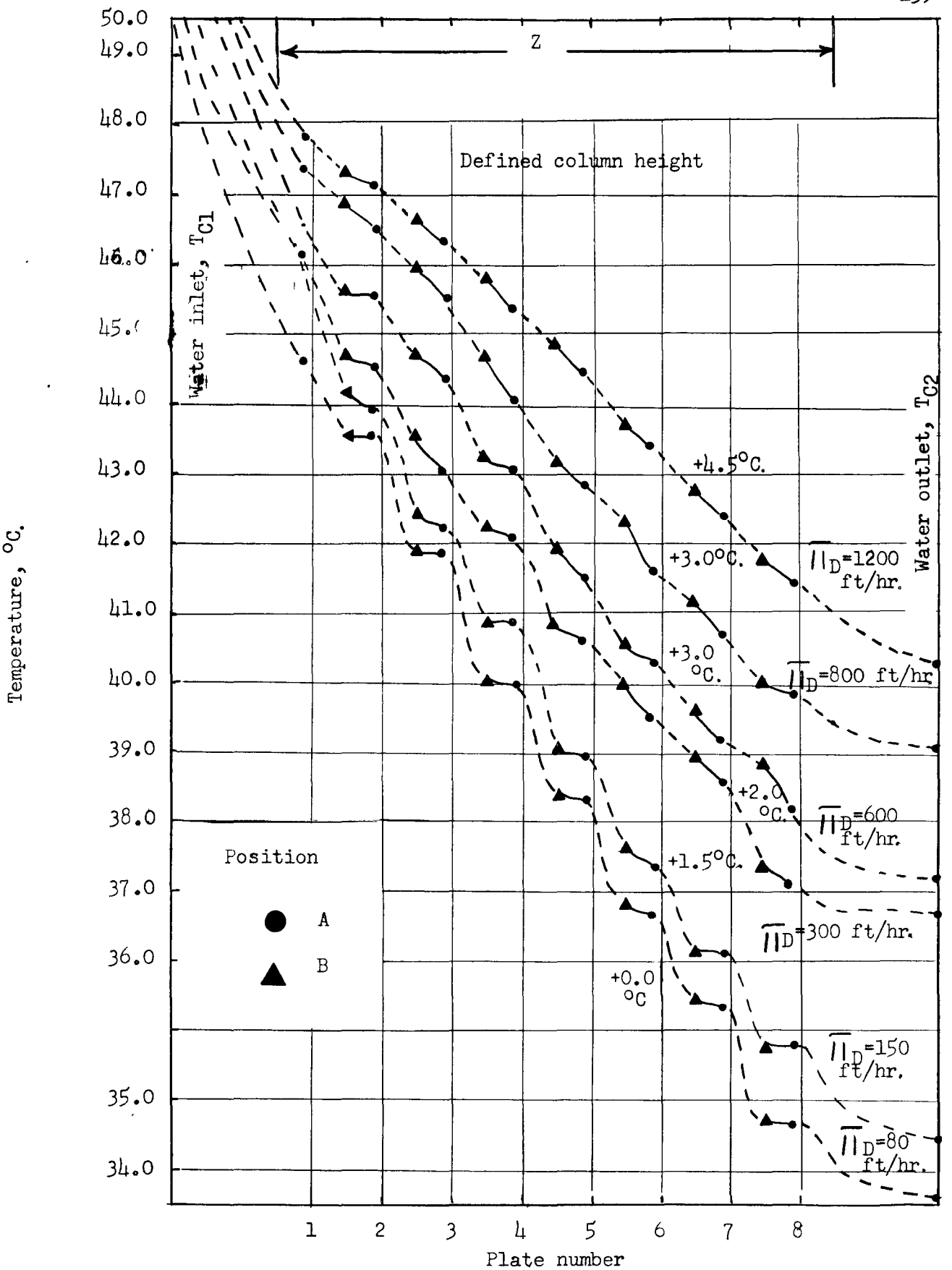

Figure 17. Temperature behavior patterns for continuous phase

and therefore have been estimated by the dotted lines. In both Figures 17 and 18, temperatures outside the defined column height, Z, have been estimated with dotted lines.

An examination of Figure 17 indicates that at low rates of pulsing, $\overline{\prod}_D$ = 150 ft/hr or below, most of the heat transfer between phases takes place from about position A to position C below or across the plates. This was indicated by the fact that the temperature profiles of the continuous phase are essentially constant from positions C to A below as previously discussed. Thus at the lower rates of pulsing, it was felt that the pulse column behaved as a mixer-settler, with the plates and spaces between plates acting as the mixing and settling regions respectively. This interpretation is supported completely by the photographs taken by Gardner at $\overline{\prod}_D$ = 150 ft/hr. However, as the rate of pulsing increase above $\overline{\prod}_D$ = 150 ft/hr, both phases become more mixed throughout the entire column, with results that the continuous phase temperature profiles become more and more linear as the rate of pulsing increases as shown in Figure 17.

As was mentioned above in Section 12.432, for $\overline{\prod}_D$ value of 150 ft/hr or less, it is reasonable to assume that measurements at position B are a reasonable approximation of the discontinuous phase temperature. Employing this deduction for the lowest rate of pulsing used in this investigation, $\overline{\prod}_D$ = 80 ft/hr, temperature profiles for the continuous and discontinuous phases were constructed are shown in Figure 18. The continuous phase profile was drawn similar to those shown in Figure 17. The discontinuous phase temperature profile, however, was represented by a dotted line completely since the entire profile had to be estimated

from temperature measurements at position B only. However, in estimating the benzene phase temperature profile, use was made of the fact that in the region where the water phase profile was essentially constant since there is relatively no heat transfer in this region.

From the continuous phase temperature profile and the estimated discontinuous phase profile, shown on Figure 18, it was now possible to determine a fair measure of the temperature difference between phases, $T_C - T_D$, at any point on the defined column height Z, as a function of either T_C or T_D. For this particular run, values of $T_C - T_D$ as a function of T_C were determined at positions approximately half way between positions C to A, or about one-quarter the distance of a plate spacing above each plate. This particular position was selected primarily for the reason that both phase temperature profiles are essentially constant in this region, and are thereby probably more reliable.

No doubt the estimated values of T_D from the discontinuous temperature profile, shown in Figure 18, are in error to some degree due to intermittent short contact of the temperature probe with the water phase as indicated in Section 12.432. However, the true temperature differences between phases should be proportional to the indicated measured temperature differences between phases. Thus, if a linear relationship between $(T_C - T_D)$ and T_C or T_D is obtained, only the slope of such a relationship will be altered by the above error.

12.434 Validity of ln-mean Temperature Difference. In Section 7.32, the usual conditions under which use of a ln-mean temperature difference driving force was valid were given. These stated conditions, however represent a special case of the necessary and sufficient

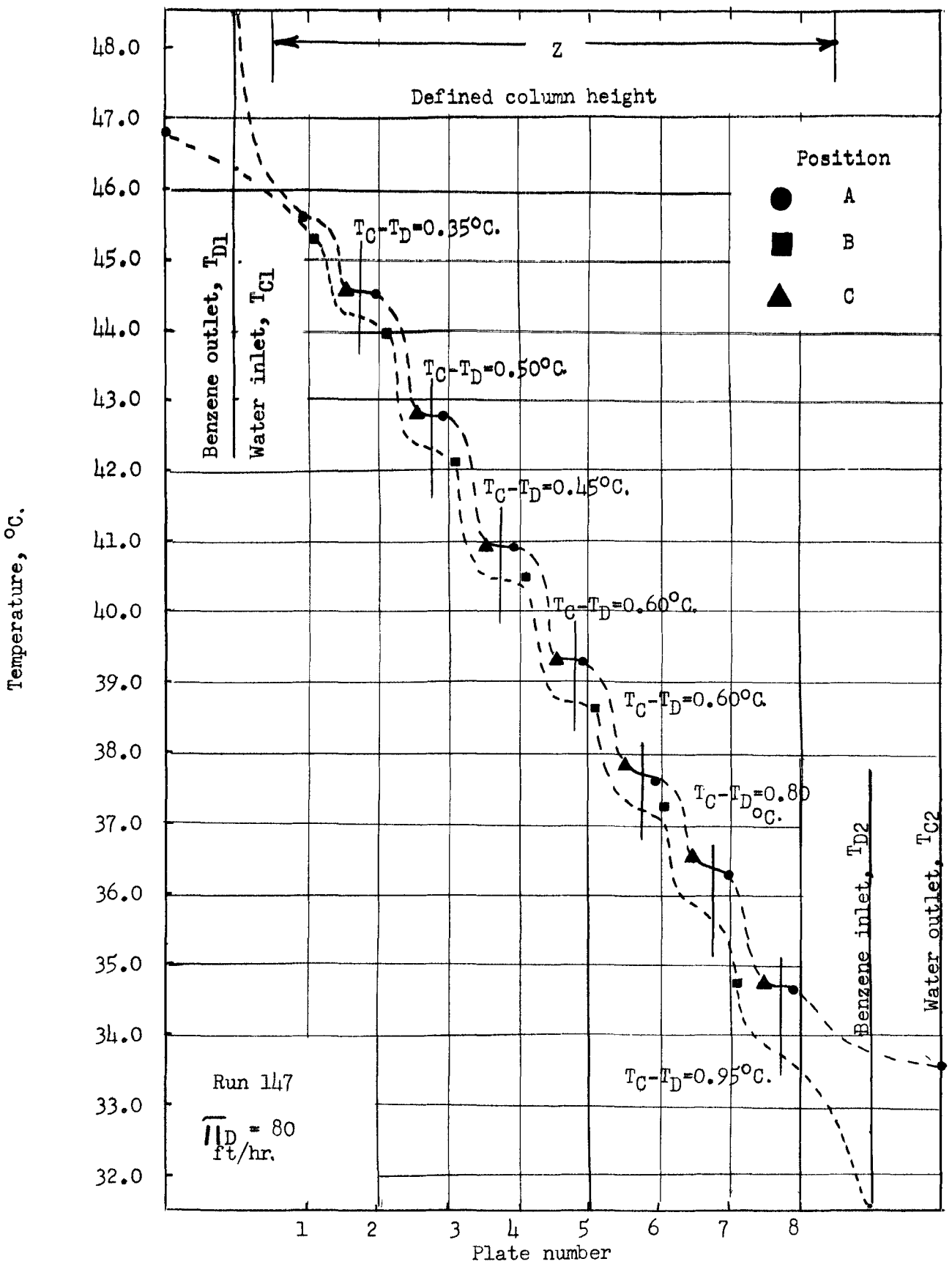

Figure 18. Temperature behavior patterns for continuous and discontinuous phase at low rate of pulsing.

conditions of steady-state operation, no heat effects other than heat transfer between phases, and $(T_C - T_D)$ being a linear function of T_C or T_D.

The first of these conditions is obviously met since all the temperature profiles shown in Figures 17 and 18 were determined under steady-state conditions as were all the other heat transfer runs. Although there were heat effects other than the net rate heat transfer between phases, q, these were relatively small in comparison. Thus, the second condition above was essentially met. As was mentioned in Sections 12.433, values of $(T_C - T_D)$ as a function of T_C were determined from Figure 18, and are shown in Figure 19. Value of $(T_C - T_D)$ as a function of T_C were presented rather than as a function of T_D since it was felt that values of T_C were more accurate than the estimated values of T_D for reasons discussed in Section 12.432.

An examination of Figure 19 shows that, within the defined column height, Z, the plot of T_C versus $T_C - T_D$ is essentially linear. Although Figure 18 was determined for the lowest rate of pulsing employed in this investigation, $\overline{U}_D$ = 80 ft/hr, a linear relation between $(T_C - T_D)$ and T_C would still be obtained at the higher rates of pulsing, since the conditions specified in Section 7.32 are still approximated, and Figure 17 indicates essentially a linear water phase temperature profile at the higher rates of pulsing.

Thus, it may be concluded that use of ln-mean temperature difference in heat transfer calculations is valid over the regions defined by the column height, Z, for all operating conditions employed in this investigation. However, in this study the terminal temperature conditions

were influenced by end-effects, and use of the measured temperatures in calculation of ln-mean temperature differences would result in some error, as described in Section 11.63.

12.435 End-effects. Shown on Figure 18 are the approximate positions of temperature measurements for the benzene and water inlet and outlet streams, expressed in terms of the number of plates above or below the top or bottom plates in the column. Approximate position of the measured water phase inlet and outlet temperatures are shown in a similar manner on Figure 17.

If there were no end-effects present at either end of the column, temperatures of both streams should remain essentially constant once they have passed through the region of defined column height, Z. An examination of Figures 17 and 18 shows this to be essentially true at the bottom of the column, where estimated temperature profiles indicate only relatively small decreases in the continuous phase temperature and increases in the discontinuous phase temperature outside the column height, Z. Though perhaps small, end-effects are definitely present at the bottom of the column, with Figure 17 indicating an increase in bottom end-effects as the rate of pulsing, $\overline{\eta}_D$, increases.

Figures 17 and 18 indicate much larger heat transfer end-effects at the top of the column in the continuous phase stream, as compared to the bottom of the column. Figure 18 also indicates approximately the same order of magnitude of end-effects in the discontinuous phase at either end of the column. However, such behavior would be expected in this situation because of the high V_D/V_C ratio, approximately 3 employed in run 147.

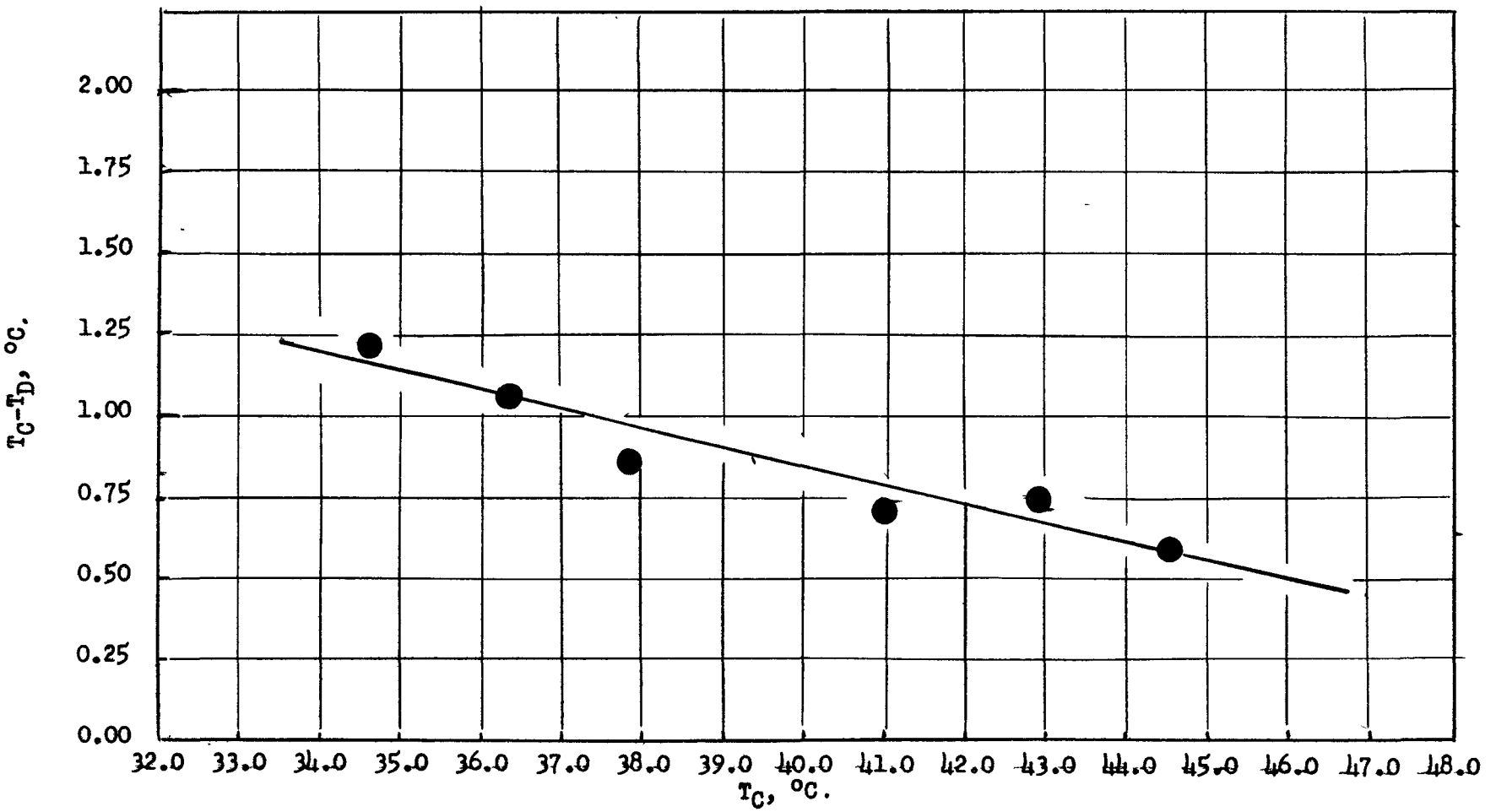

Figure 19. Temperature difference between phases as a function of the continuous phase temperature

Larger end-effects in the continuous phase would be expected at the top of the column, as compared to the bottom, because of the transfer of heat across the benzene-water interface, and benzene evaporation at the top of the column, as described in Section 11.63. For the flow conditions employed in this investigation, temperature differences between phases at the top and bottom of the column are approximately the same. Thus, the rate of heat transfer across the feed stream inlet nozzles should be approximately the same at each end of the column. However, since heat transfer in the benzene distributor is the major source of end-effects at the bottom of the column, and since Figure 18 indicates this effect to be relatively small, such an effect is therefore assumed to be relatively small in the water phase distributor at the top of the column. Thus, the major souces of end-effects in the top of the column have been attributed to heat transfer across the benzene-water interface, and to benzene evaporation as mentioned above.

12.5 Correlations of Major Heat Transfer Responses.

12.51 Effect of V_D/V_C Ratio and Rate of Pulsing, $\overline{f}_D$, upon Heat Transfer Responses.

12.511 Introduction. As previously mentioned in Section 7.122, Pike, et al (35), in studying the flooding characteristics of the pulse column used in this investigation, found the major controlling variables to be a rate of pulsing $\overline{f}$, and the ratio of superficial velocity, V_D/V_C. At that time it was felt that these variables would also be important in describing other responses of the pulse column, such as rates of heat and mass transfer, and pressure drop.

Although two different rates of pulsing have been defined in Section 7.122, $\overline{\Pi}_D$ and $\overline{\Pi}_C$, past experience has shown, both in the mass transfer studies of Pike, et al (36), and the heat transfer studies of Li (25), that the data correlated very well as a function of $\overline{\Pi}_D$. For this reason, $\overline{\Pi}_D$ was used rather than $\overline{\Pi}_C$, although numerically, Figure 3 indicates very little difference between the two, other than that of sign, for the values of FA and flow conditions employed. Values of $\overline{\Pi}_D$ were originally chosen by Pike, et al (36), for the reason that the rates of pulsing described by $\overline{\Pi}_D$ were in the direction of flow of the dispersed benzene phase.

12.512 Effect on $H\Theta U_{OC}$ and $H\Theta U_{OD}$. To determine the effect of the V_D/V_C ratio and $\overline{\Pi}_D$ upon $H\Theta U_{OC}$ and $H\Theta U_{OD}$, three series of runs were made at average V_D/V_C ratios of 0.38, 1.00, and 3.00. In all of these runs the total flow rate through the column, expressed as $(V_D + V_C)$, was held constant at approximately 40 ft/hr. In addition, the benzene inlet temperature for all of these runs was approximately 32°C. However, each series of these runs consisted of sets of runs made at different values of ΔT_i, defined by equation (123) in Section 12.1. In addition values of $\overline{\Pi}_D$ were varied from 150 to 1200 ft/hr in each set.

Appropriate runs of Li were also used in the correlation for operating conditions similar to those employed in the three series of runs. None of Gardner's data was due to the fact that he only employed one value of ($\overline{\Pi}_D$ = 150 ft/hr). However, for corresponding operating conditions, an examination of Tables 13, 14, and 15 indicate that his results agree very well with those of Li and of this investigation at $\overline{\Pi}_D$ = 150 ft/hr.

Results of the three series of runs, expressed in the terms of $H\Theta U_{OC}$ and $H\Theta U_{OD}$, are shown in Figures 20 and 21 for values $H\Theta U_{OC}$ and $H\Theta U_{OD}$ respectively. An examination of Figures 20 and 21 clearly indicate that both $H\Theta U_{OC}$ and $H\Theta U_{OD}$ are correlated by equations of the form,

$$H\Theta U_{OC} = b_1 \left(\overline{\Pi}_D\right)^{m_1} \tag{124}$$

and

$$H\Theta U_{OD} = b_2 \left(\overline{\Pi}_D\right)^{m_2} \tag{125}$$

Figure 20 and 21 definately show that b_1, b_2, m_1, and m_2 are variable coefficients and functions of the V_D/V_C ratio.

The relationship of m_1 and m_2 as a function of V_D/V_C were determined by plotting the actual measured slopes, m, of Figures 20 and 21 against the V_D/V_C ratio as shown on Figure 22. An examination of Figure 22 shows that both m_1 and m_2 are well correlated by the expression,

$$m_1 = m_2 = b_3 \left(V_D/V_C\right)^{m_3} \tag{126}$$

where

$$b_3 = 0.117$$

$$m_3 = 0.762$$

Similarly, the functional dependence of b_1 and b_2 upon the V_D/V_C ratio was determined by plotting the actual measured intercepts, b, of Figures 20 and 21 against V_D/V_C as shown in Figure 23. An examination of Figure 23 also shows that b_1 and b_2 are correlated by the expressions,

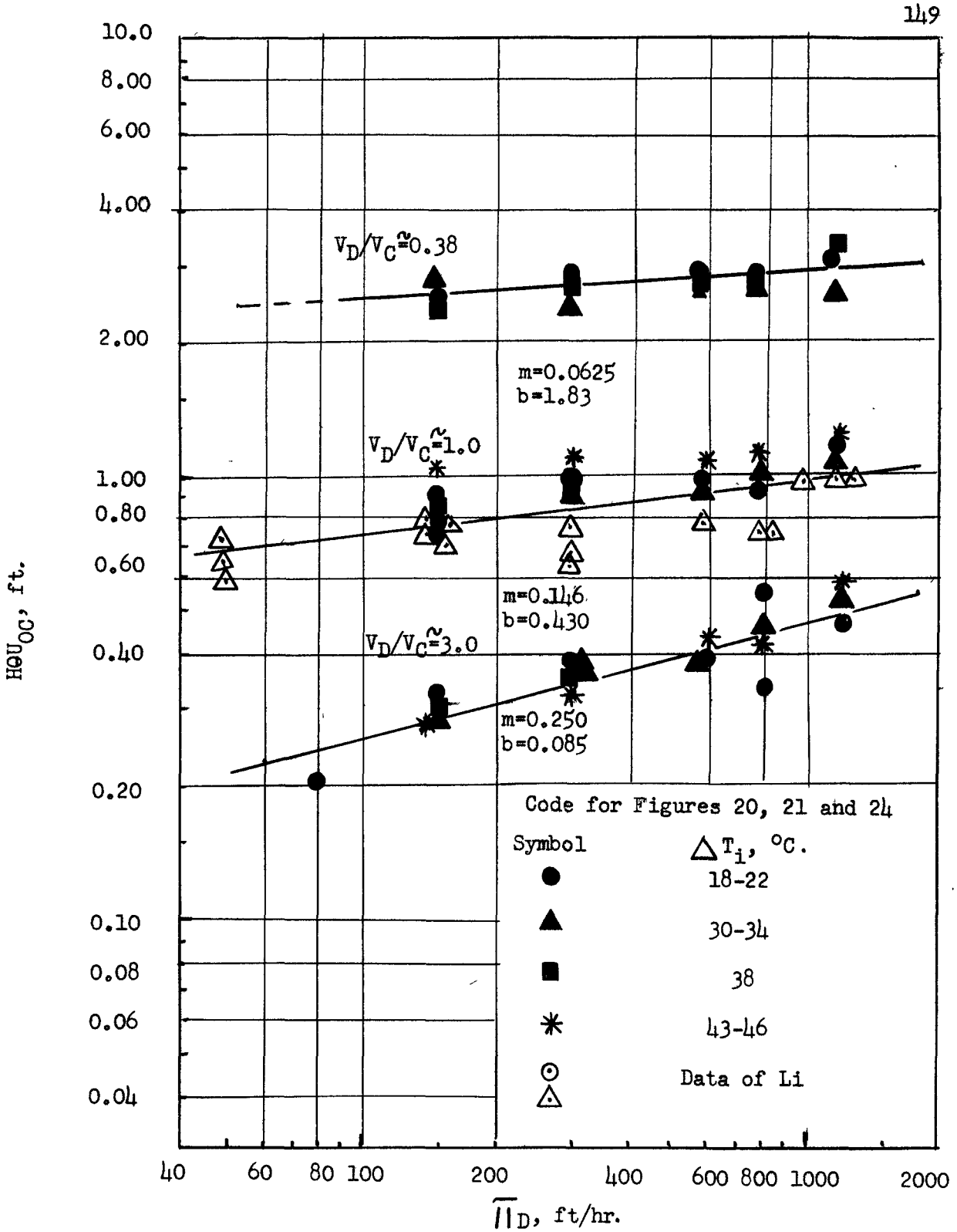

Figure 20. Effect of rate of pulsing upon height of continuous phase overall heat transfer unit

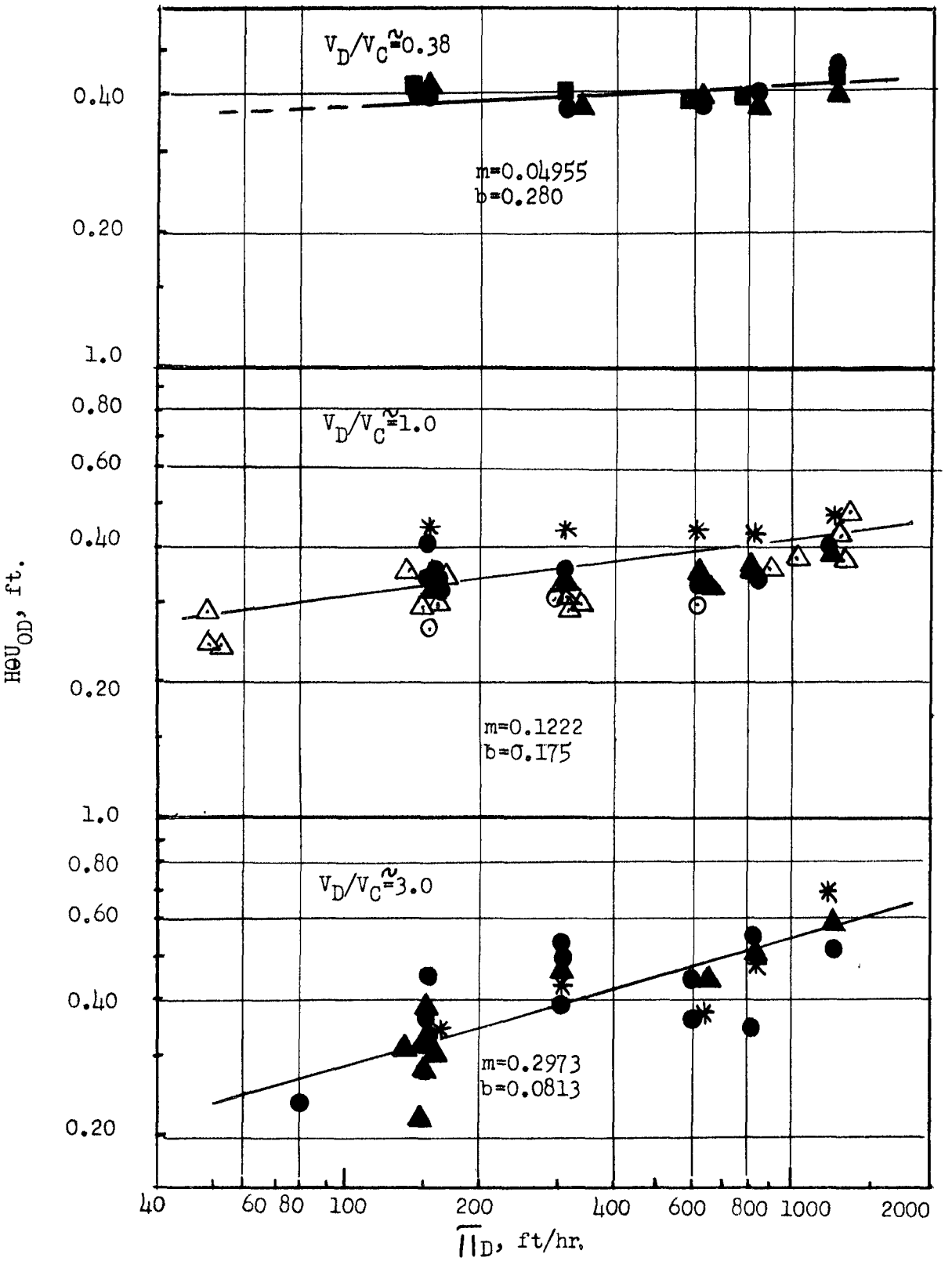

Figure 21. Effect of rate of pulsing upon height of discontinuous phase overall heat transfer unit

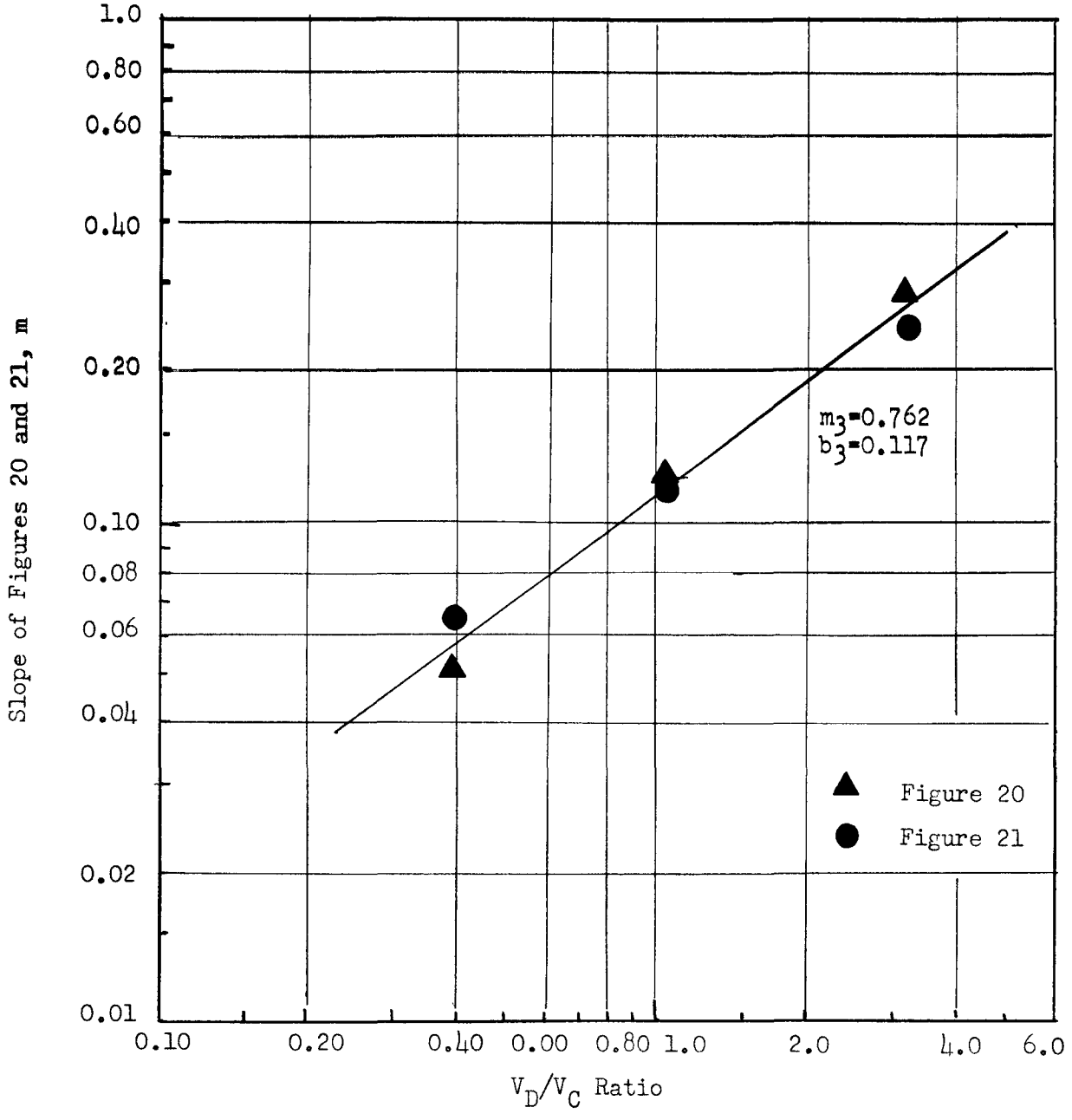

Figure 22. Effect of superficial velocity ratio upon height of overall heat transfer units

$$b_1 = b_4 \, (V_D/V_C)^{m_4} \tag{127}$$

and

$$b_2 = b_5 \, (V_D/V_C)^{m_5} \tag{128}$$

where

$b_4 = 0.42$

$b_5 = 0.165$

$m_4 = -1.580$

and

$m_5 = -0.580$

When independently determined, these exponents were -1.576 and -0.581. Since later reasoning induced that these exponents should differ by exactly 1.00, a slight adjustment was made as indicated.

At this stage, equations (124) and (125) above for correlating $H\Theta U_{OC}$ and $H\Theta U_{OD}$ became the following:

$$H\Theta U_{OC} = 0.42(V_D/V_C)^{-1.58} \overline{(\Pi_D)}^{0.117(V_D/V_C)^{0.762}} \tag{129}$$

and

$$H\Theta U_{OD} = 0.165(V_D/V_C)^{-0.58} \overline{(\Pi_D)}^{0.117(V_D/V_C)^{0.762}} \tag{130}$$

12.513 Effect on Ua. By using values of Ua obtained from the same runs employed in determining the effect of $\overline{\Pi}_D$ and V_D/V_C on $H\Theta U_{OC}$ and $H\Theta U_{OD}$, the effects of these variables upon Ua were determined by

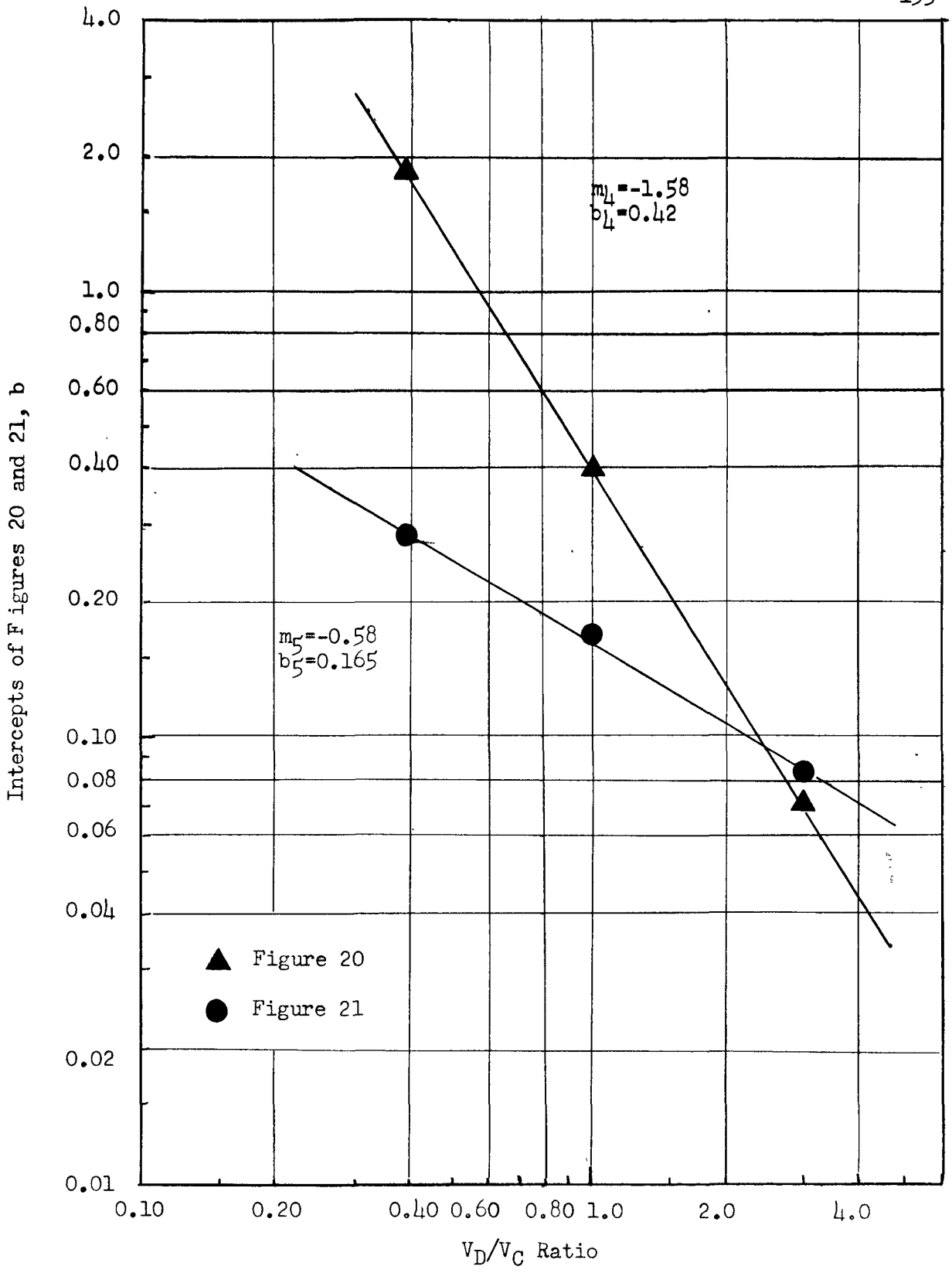

Figure 23. Effect of superficial velocity ratio upon height of overall heat transfer units

plotting Ua against $\overline{\Pi}_D$ as shown in Figure 24. An examination of Figure 24 clearly shows that Ua may also be correlated by an equation of the form,

$$Ua = b_6 \left(\overline{\Pi}_D\right)^{m_6} \tag{131}$$

Again it is quite evident that both the coefficient b_6, and the exponent m_6, are also functions of the V_D/V_C ratio. The relationship between m_6 and V_D/V_C was determined by plotting the actual measured slopes, m, of Figure 24 against V_D/V_C as shown in Figure 25. An examination of Figure 25 indicates that m_6 may be well correlated as a function of V_D/V_C by the relation,

$$m_6 = b_7 - \log \left(V_D/V_C\right)^{m_7} \tag{132}$$

where

$b_7 = -0.039$

$m_7 = 0.423$

Similarly, the relation between b_6 and the V_D/V_C ratio may be determined by plotting the actual measured intercepts, b, of Figure 24 against V_D/V_C as shown in Figure 26. An examination of Figure 26 shows that b_6 may be correlated as a function of V_D/V_C by the familar relation,

$$b_6 = b_8 \left(V_D/V_C\right)^{m_8} \tag{133}$$

where

$b_8 = 1660$

and

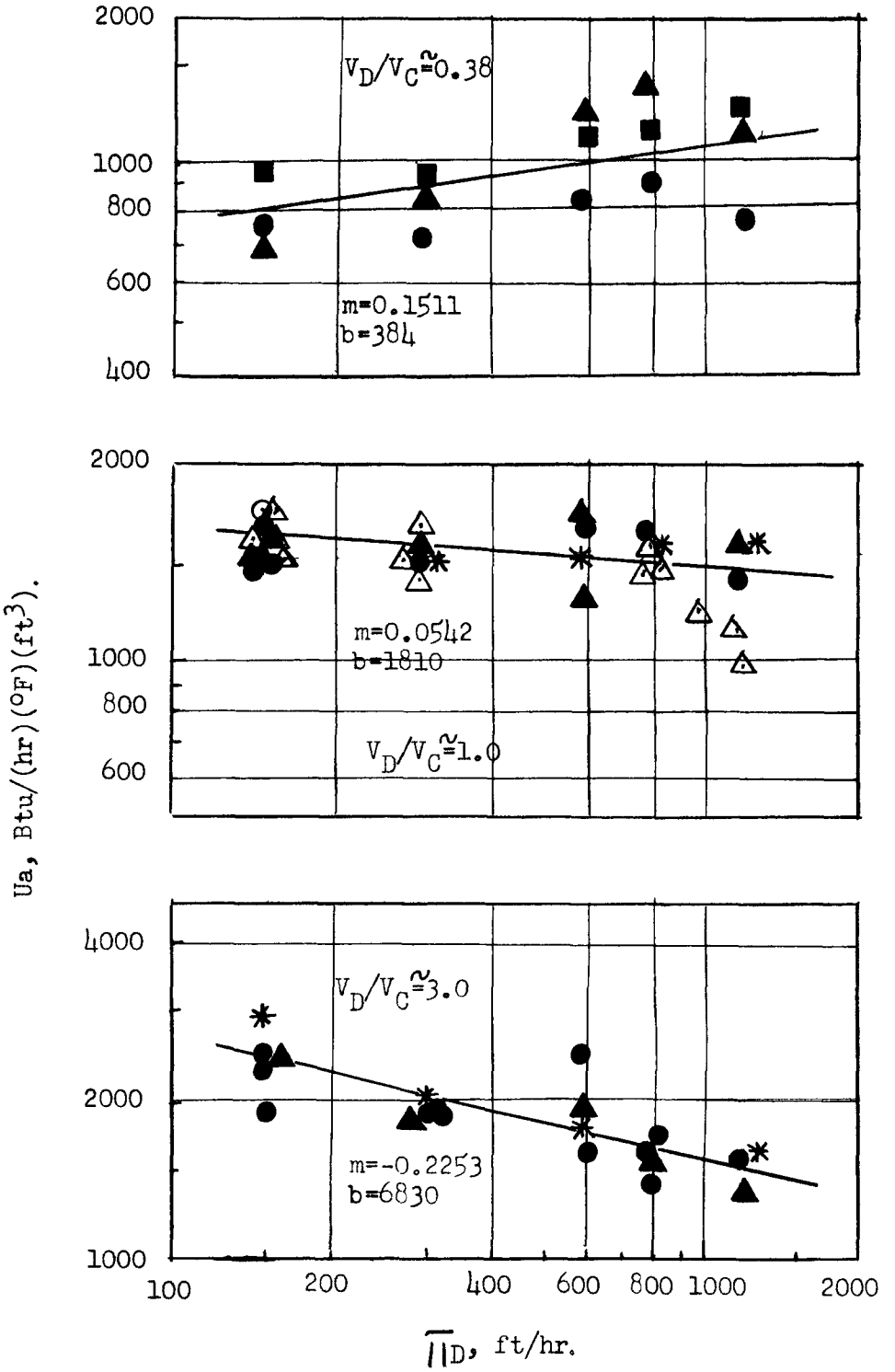

Figure 24. Effect of rate of pulsing upon overall volumetric heat transfer coefficient

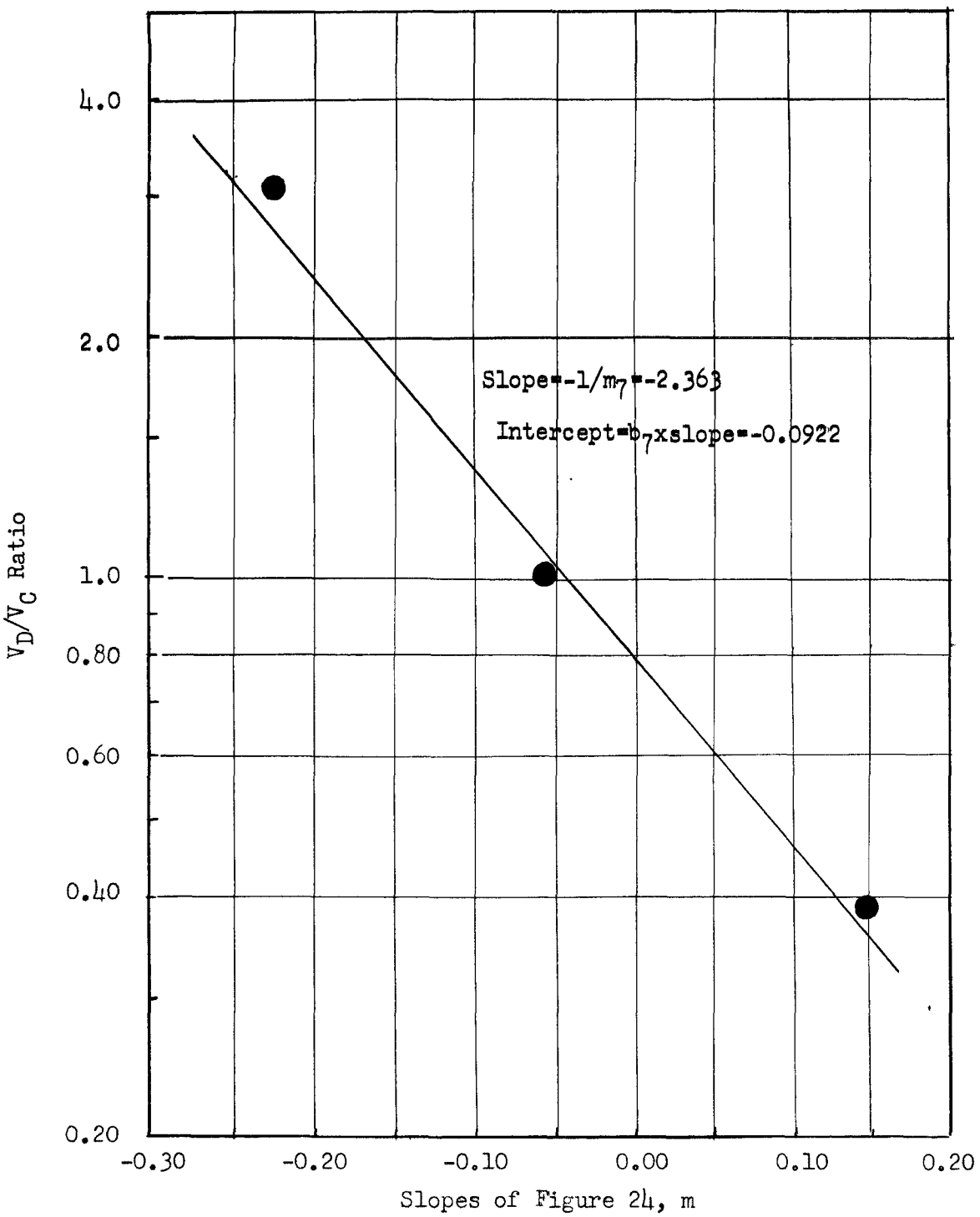

Figure 25. Effect of superficial velocity ratio upon overall volumetric heat transfer coefficient

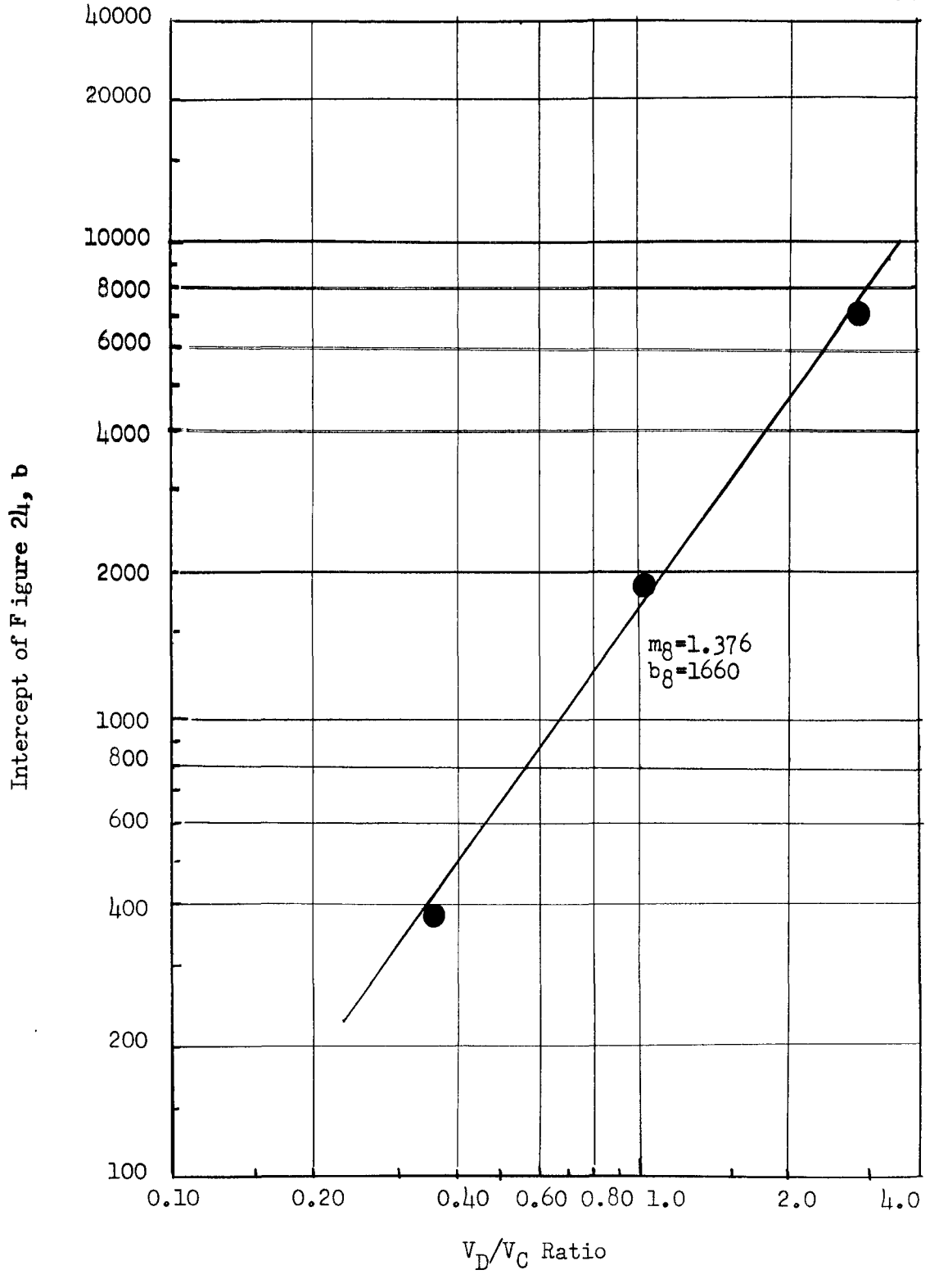

Figure 26. Effect of superficial velocity ratio upon overall volumetric heat transfer coefficient

$m_8 = 1.376$

Hence equation (131) above for correlating Ua as a function of $\overline{\Pi}_D$ and V_D/V_C now becomes:

$$Ua = 1660\ (V_D/V_C)^{1.376}\ (\overline{\Pi}_D)^{-0.039-\mathrm{Log}(V_D/V_C)^{0.423}} \qquad (134)$$

12.514 Discussion of Correlations. Figures 20 and 21 and 24 show a slight, but definite effect of $\triangle T_i$, and therefore $\triangle T_{lm}$, upon $H\Theta U_{OC}$, $H\Theta U_{OD}$ and Ua respectively. However, these Figures indicated that this effect of is quite uniformly distributed over the range of $\overline{\Pi}_D$, values employed in this investigation, i.e., the $\triangle T_{lm}$ influence is not more pronounced at one value of $\overline{\Pi}_D$ than at another. It was therefore felt that this effect would only shift the vertical positions of the curves shown in Figures 20, 21, and 24, and not change the values of their slopes. Thus it was concluded that effect of $\triangle T_{lm}$ upon $H\Theta U_{OC}$, $H\Theta U_{OD}$, and Ua would only appear in the coefficients b_4, b_5, and b_8 of equations (129), (130), and (134) respectively. The effect of $\triangle T_{lm}$ upon these coefficients is quantitatively determined below in Section 12.52.

12.52 Effect of Ln-Mean Temperature Difference, $\triangle T_{lm}$, upon Heat Transfer Responses.

12.521 Introduction. As was mentioned above, Figures 20, 21, and 24 imply a slight dependence of $H\Theta U_{OC}$, $H\Theta U_{OD}$, and Ua upon the ln-mean temperature difference $\triangle T_{lm}$. This agrees with the findings of Gardner (13). It was also concluded that this effect would appear in the coefficients b_4, b_5, and b_8. Thus the effect of $\triangle T_{lm}$ upon $H\Theta U_{OC}$, $H\Theta U_{OD}$,

and Ua, could simply be determined by obtaining the relation between $\triangle T_{lm}$, and the coefficients b_4, b_5, and b_8.

12.522 Effect on $H\Theta U_{OC}$ and $H\Theta U_{OD}$. Equations (129) and (130) above may be rearranged to give b_4 and b_5 expressed as,

$$b_4 = \frac{H\Theta U_{OC}}{(V_D/V_C)^{-1.58} (/|_D) - 0.117(V_D/V_C)^{0.762}} \tag{135}$$

and

$$b_5 = \frac{H\Theta U_{OD}}{(V_D/V_C)^{-0.58} (/|_D) - 0.117(V_D/V_C)^{0.762}} \tag{136}$$

By using the results obtained from the three series of runs described in Section 12.511, the effect of $\triangle T_{lm}$ upon $H\Theta U_{OC}$ and $H\Theta U_{OD}$ was determined by plotting values of b_4 and b_5, calculated from equations (135) and (136) above, against $\triangle T_{lm}$ as shown in Figure 27. In addition a few appropriate runs of Gardner were employed to obtain values of b_4 and b_5 at low values of $\triangle T_{lm}$.

An examination of Figure 27 indicates that b_4 and b_5 may be correlated as a function of $\triangle T_{lm}$ by the expressions,

$$b_4 = b_9 (\triangle T_{lm})^{m_9} \tag{137}$$

and

$$b_5 = b_{10} (\triangle T_{lm})^{m_{10}} \tag{138}$$

where by setting the slopes equal,

$m_9 = m_{10} = 0.133$

and

$b_9 = 0.34$

$b_{10} = 0.13$

Thus, $H\Theta U_{OC}$ and $H\Theta U_{OD}$ may now be correlated by the relation,

$$H\Theta U_{OC} = 0.34(V_D/V_C)^{-1.58}(\overline{/\!/}_D)^{0.117(V_D/V_C)^{0.762}}(\triangle T_{lm})^{0.133} \quad (139)$$

and

$$H\Theta U_{OD} = 0.13(V_D/V_C)^{-0.58}(\overline{/\!/}_D)^{0.117(V_D/V_C)^{0.762}}(\triangle T_{lm})^{0.133} \quad (140)$$

12.523 Effect on Ua. Equation (134) above may also be rearranged to express b_8 as follows:

$$b_8 = \frac{Ua}{(V_D/V_C)^{1.376}(\overline{/\!/}_D)^{-0.039-\mathrm{Log}(V_D/V_C)^{0.423}}} \quad (141)$$

By again employing the results obtained from the same runs that were used in the correlations of Section 12.521, the effect of $\triangle T_{lm}$ on Ua may be determined by plotting values of b_8, calculated from equation (141), against $\triangle T_{lm}$ as shown in Figure 28. An examination of Figure 28 indicates that b_8 may be correlated as a function of $\triangle T_{lm}$ by the expression,

$$b_8 = b_{11}(\triangle T_{lm})^{m_{11}} \quad (142)$$

where

b_{11} 2260

$m_{11} = -0.133$

The choice of m_{11} was slightly arbitrary in its relationship with m_9 and m_{10}. Hence, Ua may now be correlated by the relation,

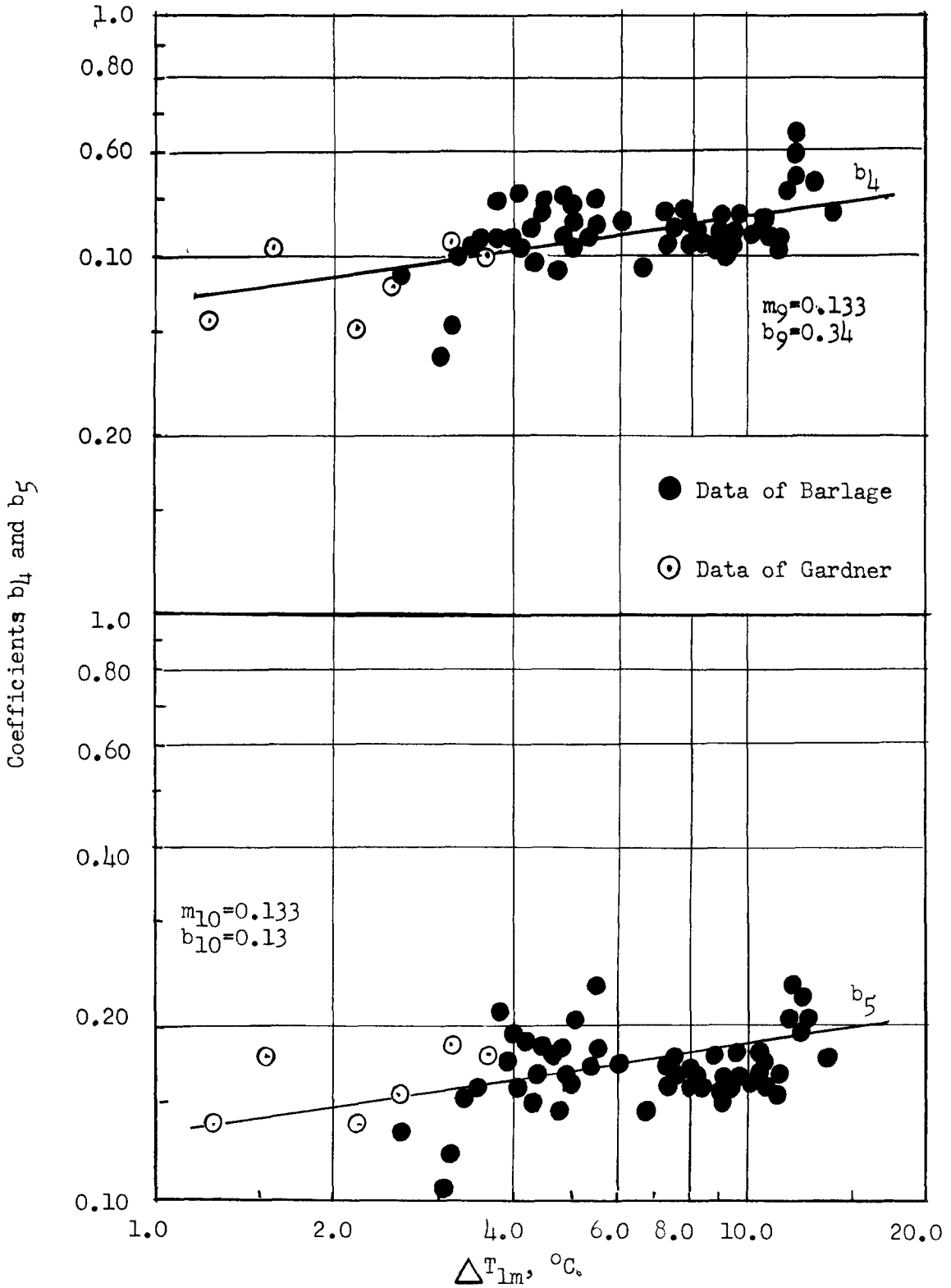

Figure 27. Effect of ln-mean temperature difference upon height of overall heat transfer units

$$Ua = 2260(V_D/V_C)^{1.376} (1/D)^{-0.039-\mathrm{Log}(V_D/V_C)^{0.423}} (\Delta T_{lm})^{-0.133} \quad (143)$$

12.53 Effect of Total Flow Rate, $V_D + V_C$, Upon Heat Transfer Responses.

12.531 Introduction. Up until this point, all of the preceding correlations have been determined from experimental results obtained under operating conditions at essentially constant $(V_D + V_C)$. Such runs include all of the three series of the investigation mentioned in Section 12.512, all runs of Li, and portion of Gardner runs which were made at V_D/V_C ratio of approximately unity. For all of these runs, $(V_D + V_C)$ was about 40 ft/hr. Now it is generally known that spray columns, for instance, increased in contact efficiency as flow rate conditions approached flooding. This is understandable, since hold-up and interfacial area increase as flooding is approached. By analogy, one might assume that pulse column HTU values would decrease as the sum of the flow rates $(V_D + V_C)$ increases, at constant V_D/V_C ratio. In fact, however, it has been observed both by Griffith, Jasny and Tupper (16) and by Thornton (49,50), that for pulse column mass transfer, the HTU values increase with $(V_D + V_C)$, and hence the net rate of mass transfer decreases. The situation invites an exploration of the effect of $(V_D + V_C)$ on heat transfer in pulse column.

Employing a proceedure similar to that used in Section 12.52, the effect of $(V_D + V_C)$ upon HOU_{OC}, HOU_{OD}, and Ua was determined by obtaining the relation between $(V_D + V_C)$ and the coefficients, b_9, b_{10}, and b_{11} of equations (139), (140), and (143) respectively.

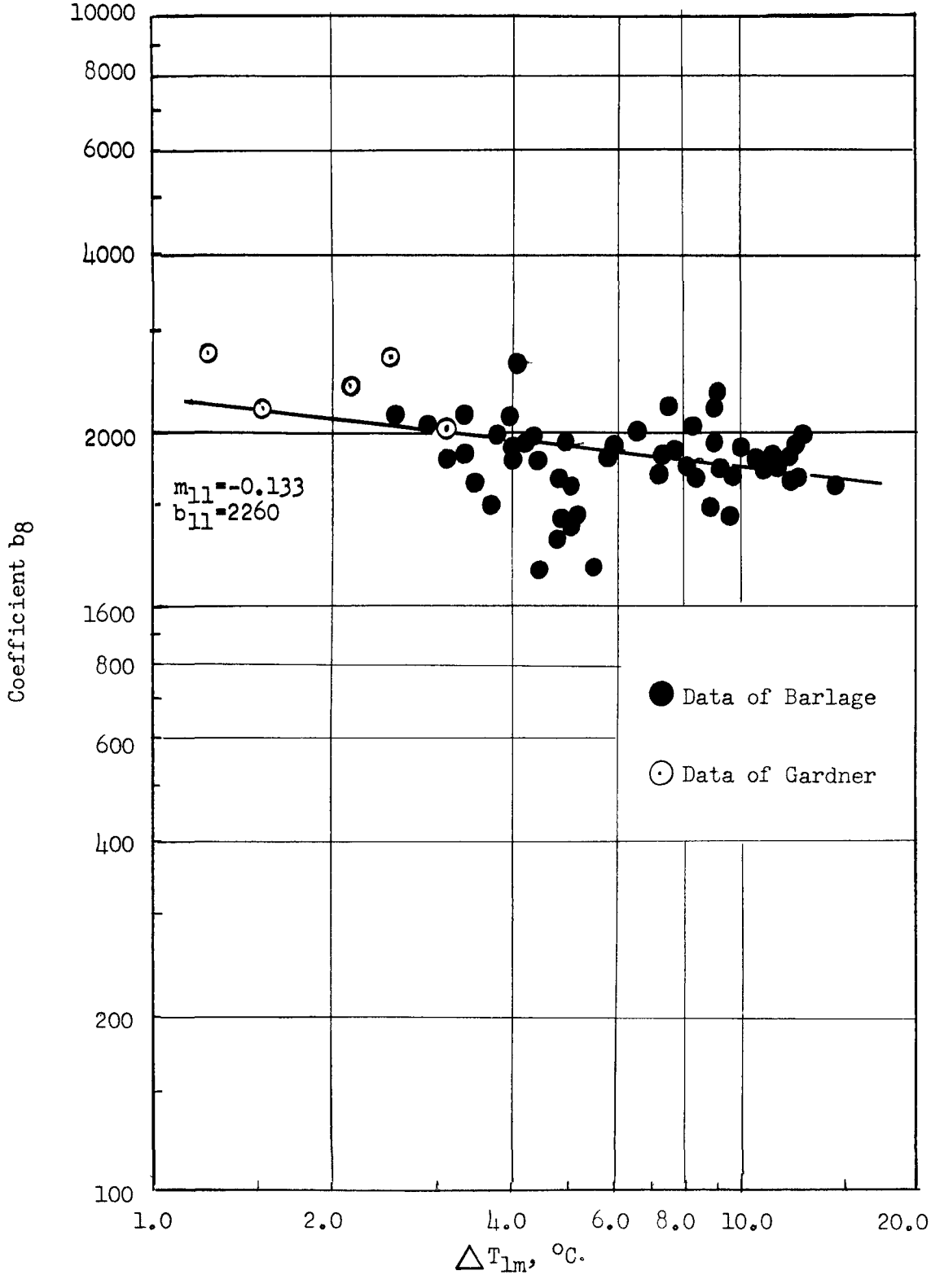

Figure 28. Effect of ln-mean temperature difference upon overall volumetric heat transfer coefficient

12.532 Effect on $H\Theta U_{OC}$ and $H\Theta U_{OD}$. Special runs 197, 198, 199 of this investigation, with $(V_D + V_C)$ of 26.0, 39.9, and 90.7 ft/hr respectively, were made specifically to measure the effect of $(V_D + V_C)$ upon $H\Theta U_{OC}$, $H\Theta U_{OD}$, and Ua. Some other runs from the series of runs in which V_D/V_C was approximately 0.38 and $\triangle T_i$ approximately 18°C, were also usable and employed. In addition, all results of Gardner for a V_D/V_C ratio greater than unity were included to provide values of $(V_D + V_C)$ greater than 40 ft/hr.

Equations (139) and (140) above may be rearranged to express b_9 and b_{10} as

$$b_9 = \frac{H\Theta U_{OC}}{(V_D/V_C)^{-1.58} (\overline{H}_D)^{0.117(V_D/V_C)^{0.762}} (\triangle T_{lm})^{0.133}} \qquad (144)$$

and

$$b_{10} = \frac{H\Theta U_{OD}}{(V_D/V_C)^{-0.58} (\overline{H}_D)^{0.117(V_D/V_C)^{0.762}} (\triangle T_{lm})^{0.133}} \qquad (145)$$

The functional dependence of b_9 and b_{10} upon $(V_D + V_C)$ was determined by plotting values of b_9 and b_{10}, calculated from the above equations, against $(V_D + V_C)$ as shown in Figure 29. An examination of Figure 29 shows that b_9 and b_{10} may be correlated with $V_D + V_C$ by the relations,

$$b_9 = b_{12} (V_D + V_C)^{m_{12}} \qquad (146)$$

and

$$b_{10} = b_{13} (V_D + V_C)^{m_{13}} \qquad (147)$$

Where by setting the slopes equal, as they apparently are,

$$m_{12} = m_{13} = -0.262$$

and

$$b_2 = 1.00$$

$$b_{13} = 0.36$$

Thus $H\Theta U_{OC}$ and $H\Theta U_{OD}$ may now be correlated by the expressions,

$$H\Theta U_{OC} = 1.00(V_D/V_C)^{-1.58}(V_D + V_C)^{-0.262}\overline{(/\!/_D)}^{0.117}(V_D/V_C)^{0.762} \times (\triangle T_{lm})^{0.133} \qquad (148)$$

and

$$H\Theta U_{OD} = 0.36\,(V_D/V_C)^{-0.58}(V_D/V_C)^{-0.262}\overline{(/\!/_D)}^{0.117}(V_D/V_C)^{0.762} \times (\triangle T_{lm})^{0.133} \qquad (149)$$

12.533 Effect on Ua. Equation (143) above may also be rearranged to express b_{11} as:

$$b_{11} = \frac{Ua}{(V_D/V_C)^{1.376}\overline{(/\!/_D)}^{-0.039-\mathrm{Log}(V_D/V_C)^{0.423}}(\triangle T_{lm})^{-0.133}} \qquad (150)$$

By again using the results of the runs mentioned above, the relation between b_{11} and $(V_D + V_C)$ was determined by plotting values of b_{11}, calculated by equation (150), against $(V_D + V_C)$ as shown in Figure 30. An examination of Figure 30 indicates that b_{11} may be correlated by the

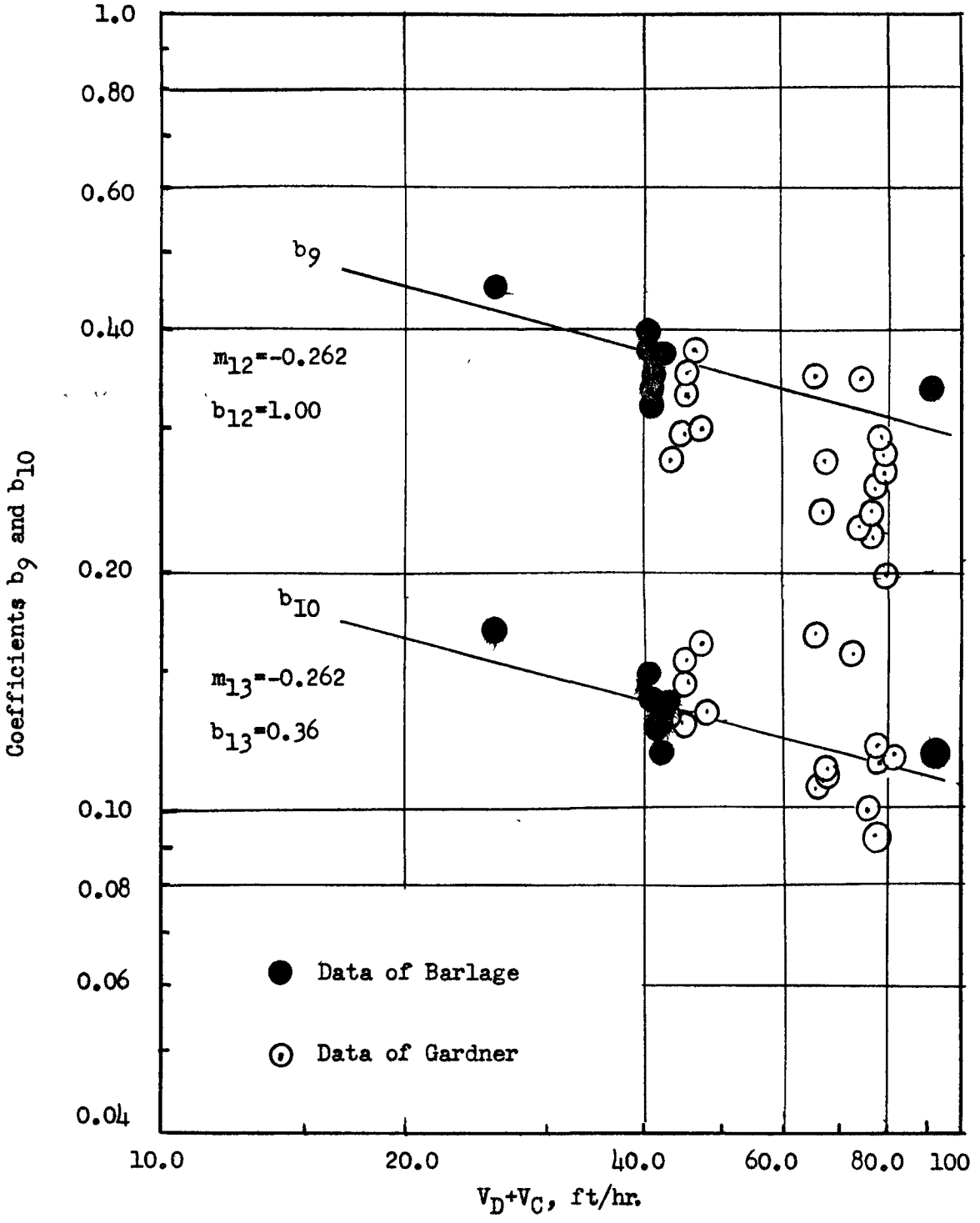

Figure 29. Effect of total volumetric flow rate upon height of overall transfer units

expression,

$$b_{11} = b_{14} (V_D + V_C)^{m_{14}} \tag{151}$$

where

$$b_{14} = 8.9$$

$$m_{14} = 1.376$$

It should be noted here that the measured slop was actually 1.42. However, it was adjusted slightly in order that m_{14} would arbitrarily agree with m_8 of Section 12.513.

Thus Ua may now be correlated by the relation,

$$Ua = (V_D/V_C)^{1.376} (V_D + V_C)^{1.376} (\overline{\Pi}_D)^{-0.039-\text{Log}(V_D/V_C)^{0.423}} (\triangle T_{lm})^{-0.133} \tag{152}$$

12.534 Discussion of Correlations. An examination of Figure 29 and 30 shows perhaps more random scatter for Gardner's data in comparison to the data of this investigation. Therefore, somewhat more "weight" was allocated to the data of this investigation than to those of Gardner in drawing the lines in Figures 29 and 30.

12.54 Effect of Temperature Level upon Heat Transfer Responses.

12.541 Introduction. Gardner (13), in study the effect of $\triangle T_{lm}$ on the heat transfer responses of the column, actually had his results clouded somewhat due to the effect of temperature level. This resulted from the fact that for a given set operating conditions, $\overline{\Pi}_D$ and V_D/V_C

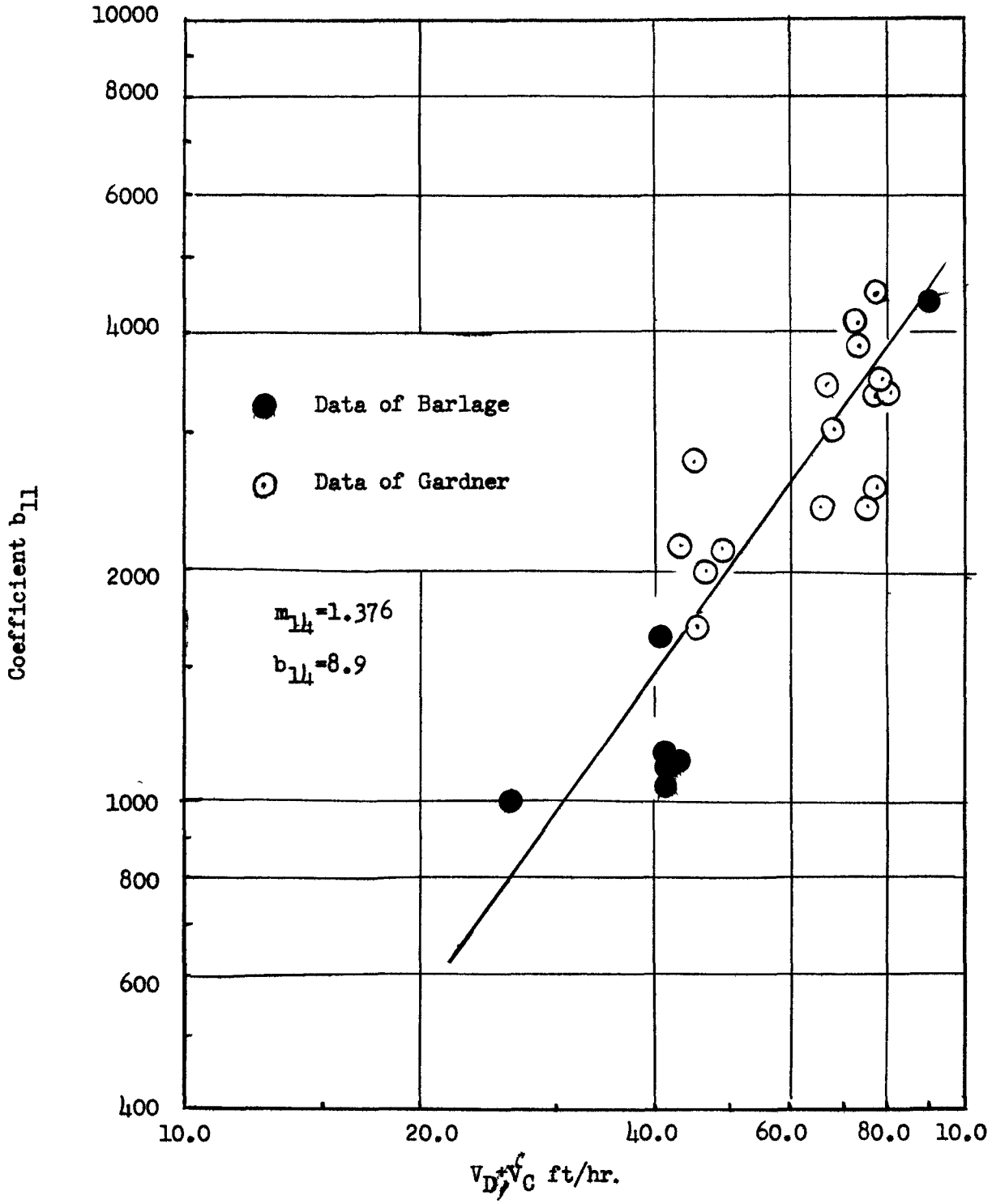

Figure 30. Effect of total volumetric flow rate upon overall volumetric heat transfer coefficient

in particular, values of ΔT_{lm} could only be varied by changing the water inlet temperature, T_{C1}, since the benzene inlet temperature was essentially set constant at room temperature. Thus, the temperature level of the runs changed for different values of ΔT_{lm}, resulting in changes in the physical properties of each phase from run to run.

In this investigation, it was decided provionsally that a suitable measuring temperature level would be that of kinematic viscosity, defined as

$$\nu = \frac{\mu}{\rho} \tag{153}$$

where

ν = kinematic viscosity, centipoises/gm/cm.^{3}

ρ = density, gms/cm^3

μ = viscosity, centipoises

Kinematic viscosity was selected as a measure of temperature level for two main reasons. First, Thornton (50) in studying the effect of pulse wave form and plate geometry on the mass transfer performance and throughput of pulse column, used the kinematic viscosity of the continuous phase in all of his mass transfer and flooding correlations. Second, it was felt that natural convection within the benzene drops played an important role in the heat transfer performance of the column. Under such conditions for geometrically similar systems, inertia, viscous, and buoyant forces became important, and are incorporated in the Grashof number, defined as,

$$\text{Grashof number} = Gr = \frac{L^3 \rho^2 g_c \beta \Delta T}{\mu^2} \tag{154}$$

where

L = some characteristic length of system

ρ = fluid density

g_c = dimensional constant

β = coefficient of volumetric expansion of fluid

ΔT = temperature difference within system

μ = viscosity of system

Equation (154) may be rearranged as

$$Gr = \frac{L^3 g_c \beta \Delta T}{\mu^2 / \rho^2} = \frac{L^3 g_c \beta \Delta T}{\nu^2} \tag{155}$$

Thus, it can be seen that kinematic viscosity becomes an important factor in systems involving natural convection.

Actually, it has been found that heat transfer by natural convection is partially described by the product of the Grasof and the Prandtl numbers raised to some power, n, or

$$(Gr)(Pr)^n = (L^3 g_c \beta \Delta T / \nu^2)(C_p \mu / k)^n \tag{156}$$

It might appear that in this case the μ term of the Prandtl number might cancel out one of the viscosity terms of the Grashof number. This is hardly so, however, because the Prandtl number itself is substantially constant over the ranges of temperature involved.

In most natural convection cases, n = 1/4. Therefore, for a given system of substantially constant geometry, it can be said that

$$Gr = k' (\Delta T/\nu^2)^n \qquad (157)$$

where

n = 0.25.

12.542 Effect on $H\Theta U_{OC}$ and $H\Theta U_{OD}$. Special runs 188 through 196 of this investigation were divided into three groups of three runs each, with each group run at a different temperature level. In all of these runs, ΔT_i was controlled to approximately 10°C so that the physical properties of the benzene phase would only be averaged over a 10°C interval at the maximum. Average benzene temperatures for the three temperature levels employed were approximately 34, 49, and 61°C. Although nine runs were involved in studying the effect of temperature level, results of runs 193 and 196 were decided to be not reliable for reasons given in Section 11.63.

The effect of ν on $H\Theta U_{OC}$, $H\Theta U_{OD}$ and Ua was determined by obtaining the effect of ν on the coefficients b_{12}, b_{13}, and b_{14} of equation (148), (149), and (152), respectively.

Equations (148) and (149) above may be rearranged to express b_{12} and b_{13} as,

$$b_{12} = \frac{H\Theta U_{OC}}{(V_D/V_C)^{-1.58} (V_D + V_C)^{-0.262} (\overline{\Pi}_D)^{0.117} (V_D/V_C)^{0.762} (\Delta T_{lm})^{0.133}} \qquad (158)$$

and

$$b_{13} = \frac{H\Theta U_{OD}}{(V_D/V_C)^{-0.58}\,(V_D + V_C)^{-0.262}\,(\overline{\mu}_D)^{0.117}\,(V_D/V_C)^{0.762}\,(\Delta T_{lm})^{0.133}} \quad (159)$$

Using these results of the runs mentioned above, the relation between b_{12} and b_{13} was determined by plotting vlaues of b_{12} and b_{13}, calculated from equations (158) and (159), against ν_D (and also ν_C) as shown in Figure 31, where

ν_D = kinematic viscosity of discontinuous phase, centipoises/gm/cm^3.

ν_C = kinematic viscosity of continuous phase, centipoises/gm/cm^3.

An examination of Figure 31 indicates that b_{12} and b_{13} may be correlated with either ν_D or ν_C by the expression

$$b_{12} = b_{15}\,(\nu)^{m_{15}} \quad (160)$$

and

$$b_{13} = b_{16}\,(\nu)^{m_{16}} \quad (161)$$

where

$b_{15} = 1.0$

$b_{16} = 0.38$

and for reasons presented later in the discussion of these correlations, m_{15} and m_{16} are set equal at the value

$$m_{15} = m_{16} = -0.266$$

Hence, $H\Theta U_{OC}$ and $H\Theta U_{OD}$ may now be correlated by the expression

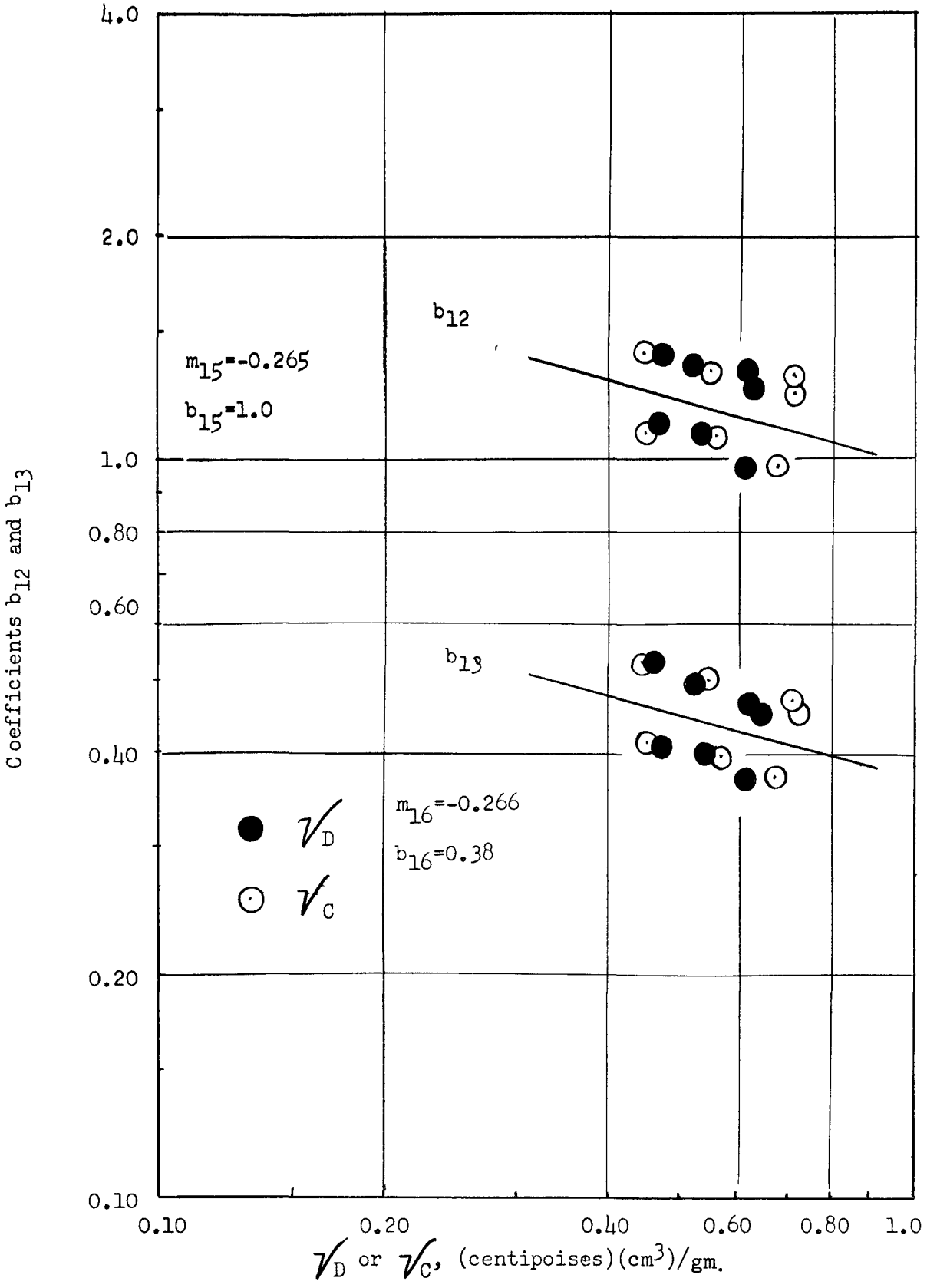

Figure 31. Effect of kinematic viscosity upon height of overall heat transfer coefficients

$$H\Theta U_{OC} = 1.0(V_D/V_C)^{-1.58}(V_D + V_C)^{-0.262}(\mu_D)^{0.117(V_D/V_C)^{0.762}} x$$

$$(\Delta T_{lm})^{0.133}(\nu_D)^{-0.266} \qquad (162)$$

Here ν_D is arbitrarily chosen over ν_C on the basis that it is implied by a presumed Grashof number.

and

$$H\Theta U_{OD} = 0.38(V_D/V_C)^{-0.58}(V_D + V_C)^{-0.262}(\mu_D)^{0.117(V_D/V_C)^{0.762}} x$$

$$(\Delta T_{lm})^{0.133}(\nu_D)^{-0.266} \qquad (163)$$

An examination of equations (162) and (163) indicate that the terms, $(\Delta T_{lm})^{0.133}$ and $(\nu_D)^{-0.266}$, may be combined into a single term $(\Delta T_{lm}/\nu_D{}^2)^{0.133}$. Thus, equations (162) and (163) may now be put into the final form,

$$H\Theta U_{OC} = 1.0(V_D/V_C)^{-1.58}(V_D + V_C)^{-0.262}(\mu_D)^{0.117(V_D/V_C)^{0.762}} x$$

$$(\Delta T_{lm}/\nu_D{}^2)^{0.133} \qquad (164)$$

and

$$H\Theta U_{OD} = 0.38(V_D/V_C)^{-0.58}(V_D + V_C)^{-0.262}(\mu_D)^{0.117(V_D/V_C)^{0.762}} x$$

$$(\Delta T_{lm}/\nu_D{}^2)^{0.133} \qquad (165)$$

12.543 Effect on Ua. If the same relation between ΔT_{lm} and $\nu_D{}^2$ exists with Ua as existed with $H\Theta U_{OC}$ and $H\Theta U_{OD}$, then a plot of log b_8,

defined by equation (141), versus log $(\Delta T_{lm}/\gamma_D^2)$ should yield a straight line with slop, m_{17}, equal to -0.133, similar to that obtained for ΔT_m versus b_8, shown in Figure 28. Such a proposed plot is shown in Figure 32, and very definitely indicates a slope, m_{17}, about equal to that of Figure 28, or -0.133.

Thus, it is now possible to relate the effect of temperature level upon Ua by the term $(\Delta T_{lm}/\gamma_D^2)^{-0.133}$, and represent the final correlation of Ua by the expression

$$Ua = 8.9(V_D/V_C)^{1.376}(V_D + V_C)^{1.376}(\overline{\mu}_D)^{-0.039-Log(V_D/V_C)^{0.423}} \times (\Delta T_{lm}/\gamma_D^2)^{-0.133} \qquad (166)$$

12.544 Discussion of Correlations. Equation (157) indicates that if natural convection does participate as a mechanism of heat transfer, the exponent of γ_D should be negative and twice that of ΔT_{lm}.

Since it has already been determined that the exponents of ΔT_{lm} in the correlations of $H\Theta U_{OC}$ and $H\Theta U_{OD}$ were both 0.133, then the exponent has been applied to the correlations of Figure 31, (corresponding to $m_{15} = m_{16} = -0.266$) with reasonable success, thus strongly indicating the presence of natural convection.

Thus, it was possible to show the existence of the term $(\Delta T_{lm}/\gamma_D^2)^{0.133}$ in the correlation for both $H\Theta U_{OC}$ and $H\Theta U_{OD}$, and Figure 32 indicates also corresponding term in the correlation of Ua in the form $(\Delta T_{lm}/\gamma_D^2)^{-0.133}$.

12.55 <u>The Effect of Reversing the Direction of Heat Transfer on Heat Transfer Responses.</u>

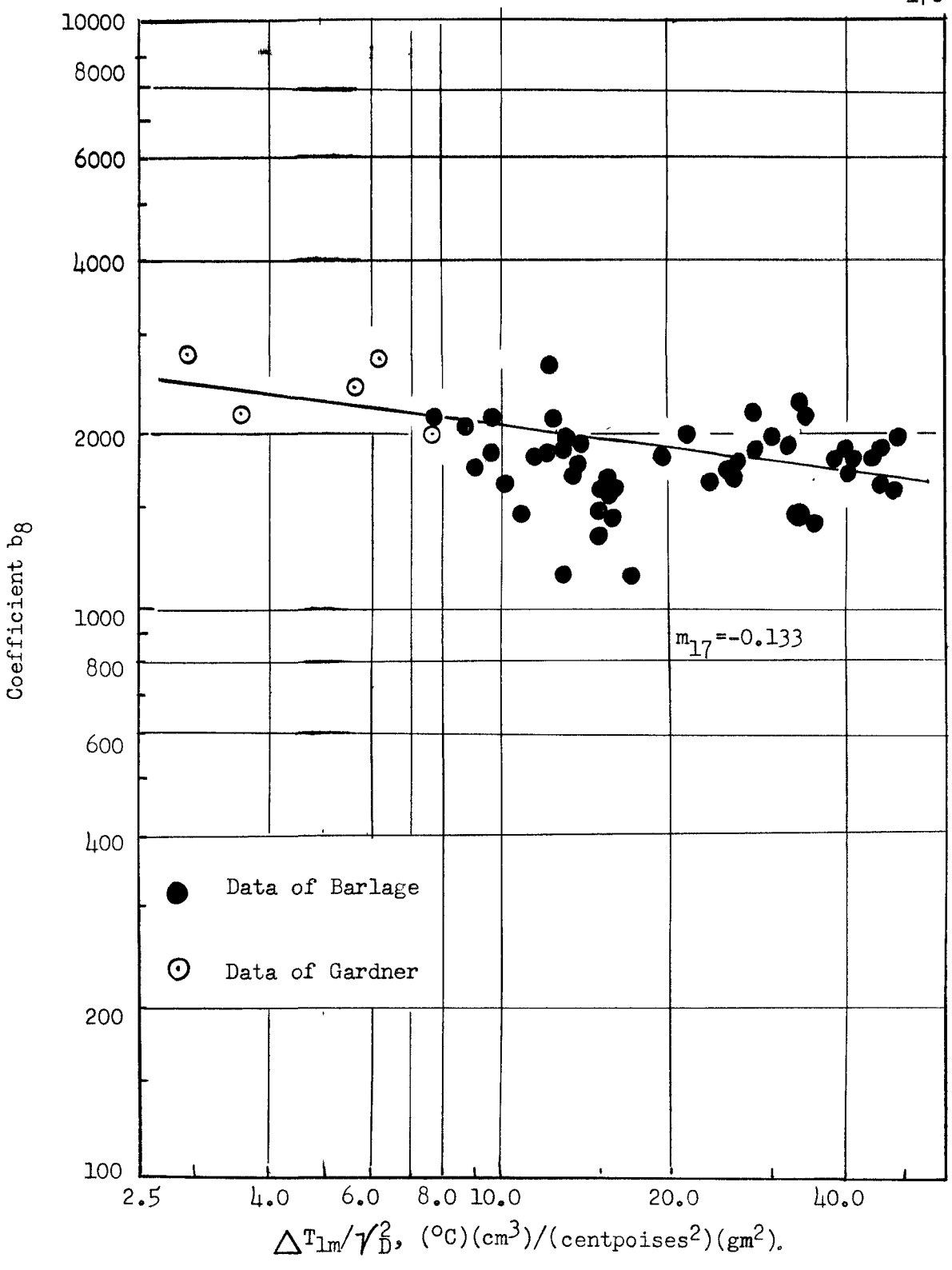

Figure 32. Effect of kinematic viscosity upon overall volumetric heat transfer coefficients

12.551 Introduction. Up until this point, all the results presented were for heat transfer from the continuous to the discontinuous phase. Such a direction of heat transfer was employed by both Li and Gardner in all of their runs, and was also employed in all the runs of this investigation thus far mentioned. However, in an attempt to obtain more information the mechanisms of heat transfer to and from droplets, a few runs of this investigation were made with heat being transferred from the discontinuous to continuous phase.

12.552 Effect on $H\Theta U_{OC}$ and $H\Theta U_{OD}$. Runs 200 through 206 of this investigation were made with the direction of heat transfer being reversed from that previously used. All runs were made employing an inlet benzene temperature of approximately 50°C, with an inlet water temperature of about 32°C. In addition, all runs were made at a total flow rate, $(V_D + V_C)$, or approximately 40 ft/hr.

Runs 200, 201, and 202 were all made at a $\overline{\Pi}_D$ value of 300 ft/hr at V_D/V_C ratios of 0.37, 3.16 and 0.92 respectively. The remaining runs were all made at a V_D/V_C ratio of approximately unity, with values of $\overline{\Pi}_D$ varying from 150 to 1200 ft/hr.

The effect of reversing the direction of heat transfer upon $H\Theta U_{OC}$ and $H\Theta U_{OD}$ is clearly shown in Figure 33 as related to $\overline{\Pi}_D$. For contrast, points are shown on Figure 33, for values of $H\Theta U_{OC}$ and $H\Theta U_{OD}$, calculated from the correlation represented by equations (164) and (165) for the identical run conditions of V_D/V_C ratio, $\overline{\Pi}_D$, $(V_D + V_C)$, and $(\Delta T_{lm}/\gamma_D^2)^{0.133}$ (reversed in sign), employed in the reversed runs. This was done so that a comparison of results for the two directions of

heat transfer might be obtained under identical operating conditions. The indicated lines are purposely made parallel.

12.553 Effect on Ua. Employing results of the runs mentioned above, the effect of reversing the direction of heat transfer upon Ua is shown in Figure 34, as related to $\overline{\Pi}_D$. In addition, values of Ua, calculated from equation (166) are also shown on Figure 34, so that a comparison of results for the two directions of heat transfer might be made for identical operating conditions. The indicated lines are purposely made parallel, although a steeper slope might be employed for the upper points.

12.554 Effect on Exponents of $(\Delta T_{lm}/V_D^2)$. Figures 33 and 34 strongly suggest the correlations developed for relating $H\Theta U_{OC}$ and $H\Theta U_{OD}$ and Ua to the operating variables, V_D/V_C, $(V_D + V_C)$, and $\overline{\Pi}_D$ might also be applicable to the reversed heat transfer situation. This is due to the fact that the slopes of lines representing $H\Theta U_{OC}$, $H\Theta U_{OD}$ and Ua as a function $\overline{\Pi}_D$ are essentially the same for the two directions of heat transfer.

If the assumptions are made that the correlations of equations (129), (130), and (134) apply equally as well to the two directions of heat transfer, then the effect of heat transfer reversal upon the exponents of $(\Delta T_{lm}/V_D^2)$, as relates to $H\Theta U_{OC}$ and $H\Theta U_{OD}$ may be obtained by plotting values of b_{18} and b_{19} against $(\Delta T_{lm}/V_D^2)$ as shown on Figure 35. The two coefficients b_{18} and b_{19}, which are essentially the same as b_4 and b_5, defined for heat transfer to the discontinuous phase, are defined, thus.

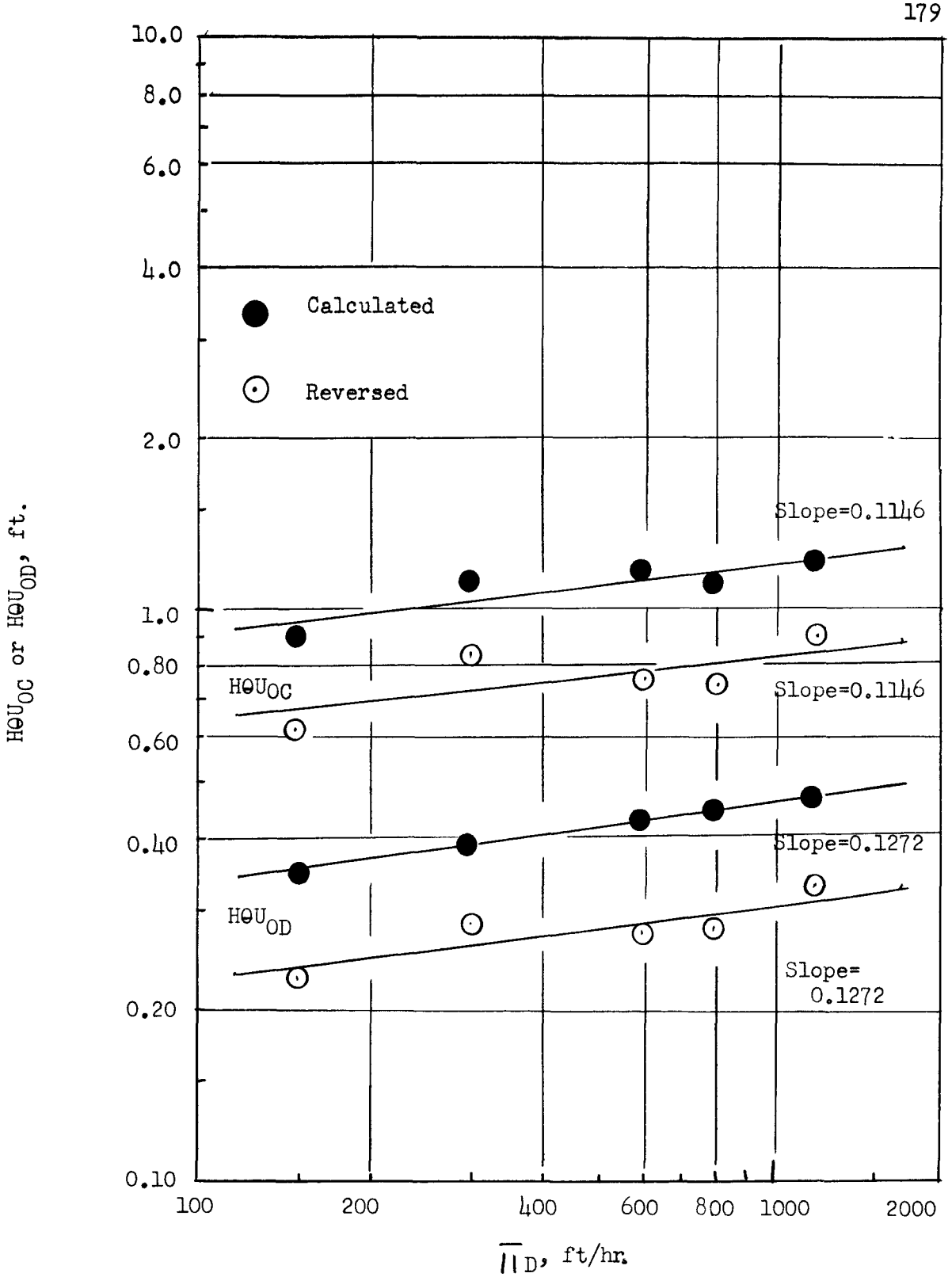

Figure 33. Effect of reversed direction of heat transfer upon height of overall heat transfer units

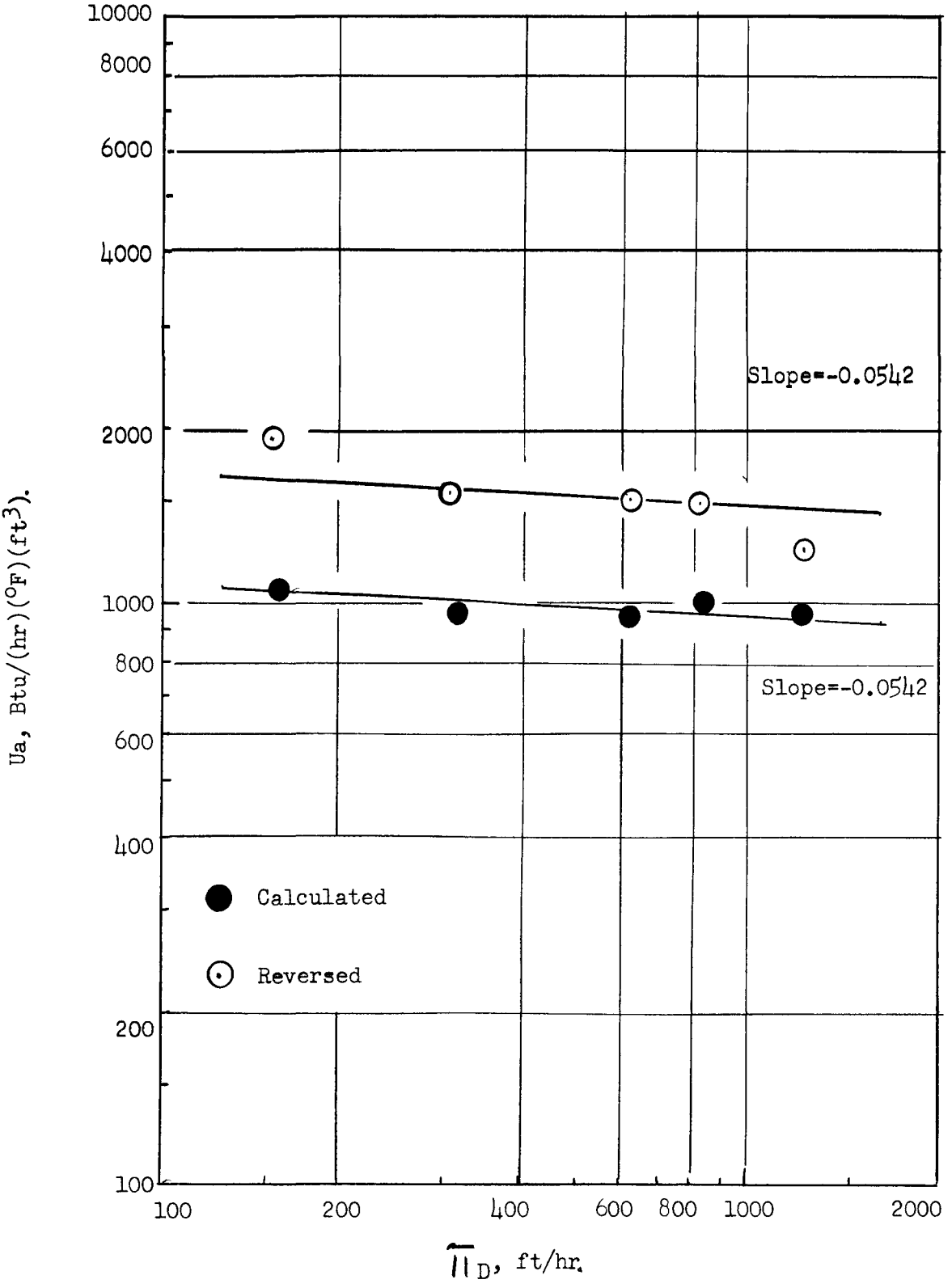

Figure 34. Effect of reversed direction of heat transfer upon overall volumetric heat transfer coefficient

$$b_{18} = \frac{H\Theta U_{OC}}{(V_D/V_C)^{-1.58}\,(V_D + V_C)^{-0.262}\,(\overline{\mu}_D)^{0.117(V_D/V_C)^{0.423}}} \qquad (167)$$

and

$$b_{19} = \frac{H\Theta U_{OD}}{(V_D/V_C)^{-0.58}\,(V_D + V_C)^{-0.262}\,(\overline{\mu}_D)^{0.117(V_D/V_C)^{0.423}}} \qquad (168)$$

An examination of Figure 35 shows the slopes, m, for the two lines are poorly defined because of the small range of $(\Delta T_{lm}/\gamma_D^2)$. Nonetheless, it is obvious that the slope involved is greater than the 0.133 found for the original direction of heat transfer. The slope was taken to be 1.30, by averaging the magnitudes of independent slope values for this figure and the later figure, Figure 36.

Similarly, the effect of heat transfer reversal upon the exponent of $(\Delta T_{lm}/\gamma_D^2)$ as related to Ua, was appraized by plotting values of b_{20} against $(\Delta T_{lm}/\gamma_D^2)$ as shown in Figure 36. Again b_{20} is similar to b_8 defined for heat transfer from the continuous to discontinuous phase as is defined as

$$b_{20} = \frac{Ua}{(V_D/V_C)^{1.376}\,(V_D + V_C)^{1.376}\,(\overline{\mu}_D)^{-0.039-\mathrm{Log}(V_D/V_C)^{0.423}}} \qquad (169)$$

An examination of Figure 36 shows a line drawn through the results with a slope of -1.30 is entirely reasonable.

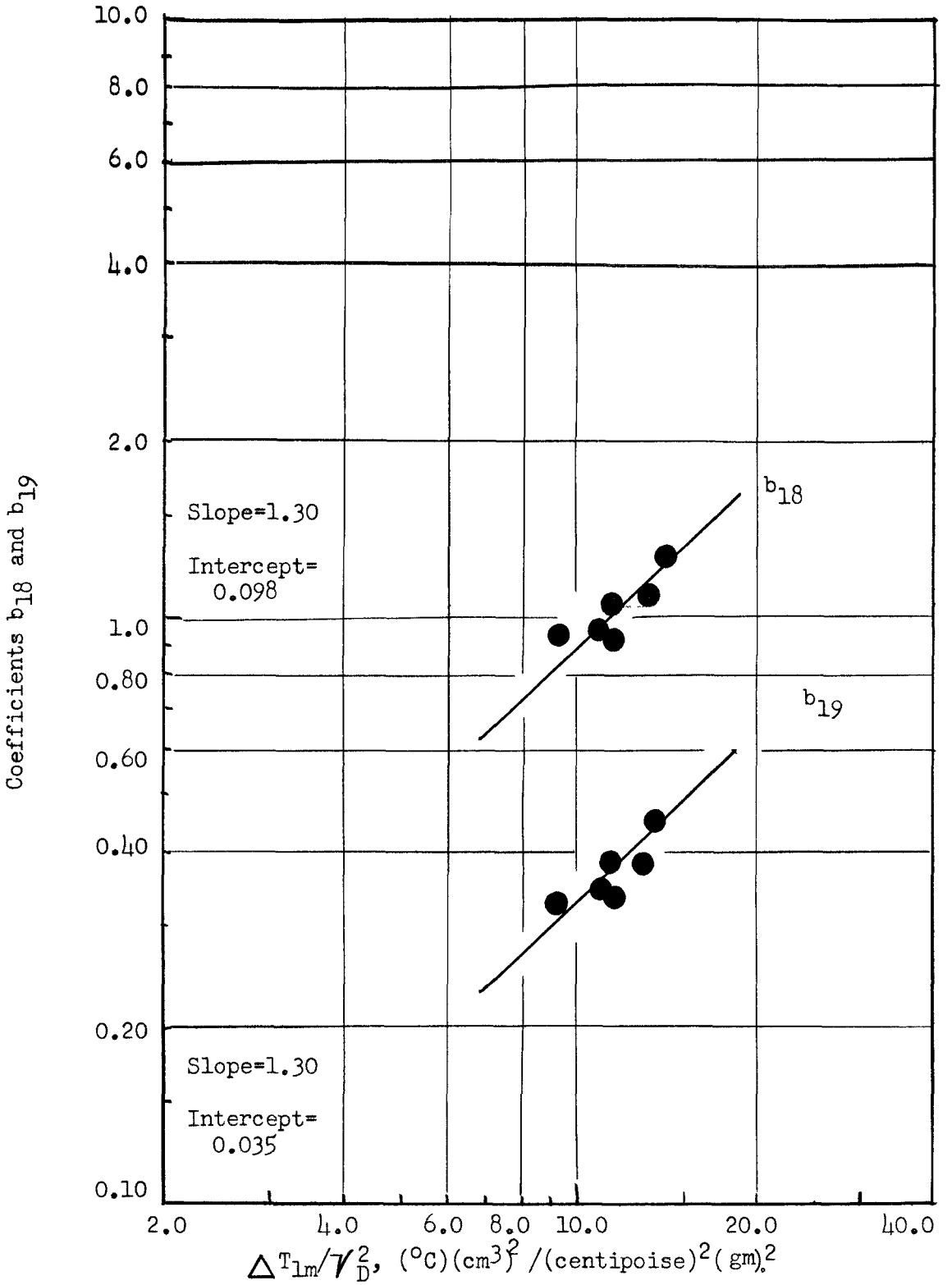

Figure 35. Effect of kinematic viscosity upon height of overall heat transfer units for reversed direction of heat transfer

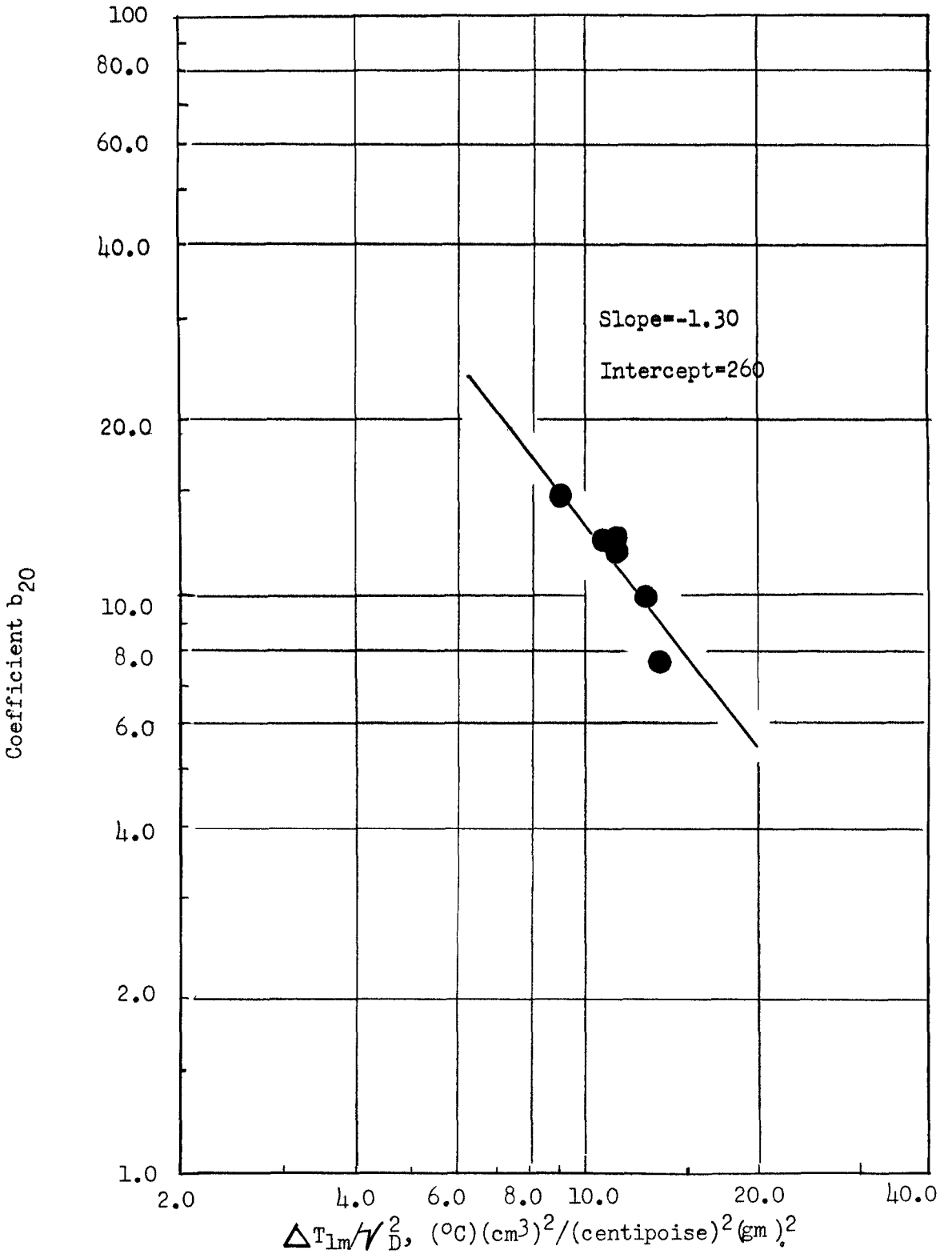

Figure 36. Effect of kinematic viscosity upon overall volumetric heat transfer coefficient for reversed direction of heat transfer

13.0 DISCUSSION AND CONCLUSIONS

13.1 Behavior Patterns

13.11 Discussions of Overall Results. In Section 11.2, a detailed analysis of all the behavior patterns considered to be important factors in the heat transfer performance of the pulse column is given. It is now felt that all major heat effects within the column have been quantitatively evaluated, particularly heat losses due to evaporation, as accounted for by equation (97). The fact that all important heat effects are now properly accounted for is supported by the fact that average absolute percent deviations in the heat balances are consistantly less than 10-percent. In addition, it has also been shown that the heat transfer responses obtained are reliable and are reproducible with a precision within 10-percent due to the accuracy with which the heat transfer measurement may now be made.

13.12 Limitations. As discussed in Section 11.63, one source of error still remaining in the heat transfer calculations is that due to end-effects within the column. Since no satisfactory method for correcting this error has been formulated, it should be remembered that all of the preceeding correlations have this inherent error in them.

It is felt, however, that in the future some means should be employed to correct for or eliminate this source of error. Probably the easiest method would be to relocate the thermopiles in the column in such a way that the temperatures indicated by them would only be the terminal temperatures at each end of the defined column height, Z. This would be a relatively simple matter at the bottom of the column since

it would only entail moving thermopile #2 (water outlet) further into the column until it was essentially level with thermopile #3, (benzene inlet). In this manner, essentially all end-effects at the bottom of the column might be eliminated from the temperature measurements. Relocation of the thermopiles at the top of the column, however, would not be quite as simple due to the benzene-water interface. It is felt, though, that some suitable positioning of these thermopiles could be made so as to substantially reduce the top end-effects inherent the temperature measurements.

13.2 Experimental Program and Results.

13.21 Temperature Probe Results. An examination of Figure 19 of Section 12.434 definately indicates that use of a ln-mean temperature difference is valid over the region defined by the column height Z, or within the region of perforated plates. However, as mentioned in Section 11.63, temperatures used in the calculation of values of $\triangle T_{lm}$ are somewhat in error due to end-effect within the column, as indicated by Figures 17 and 18 of Section 12.433.

It is interesting to compare the temperature probe results of this investigation with those obtained on spray towers.

Pierce, et al (34), using the system mercury dispersed in water, found from their temperature profile data that a plot of $(T_D - T_C)$ versus T_C was not linear, and therefore use of a logarithmic temperature difference was not justified. This behavior was attributed to recirculation of the continuous phase within the column, particularly at the

interface-end of the column, where 80-percent of the total temperature rise of the continuous phase occurred.

Garwin and Smith (15) calculated rigorous values of U from temperature profile data of the continuous phase, and compared these with those calculated using a ln-mean temperature difference. They found that the ratio of the rigorously to logarithmically calculated values of U increased as hold-up within the column increased. They encountered discrepancies up to about twenty percent. Again, this behavior was attributed to recirculation of the continuous phase at high flow rates of the discontinuous phase.

No doubt the difference between temperature profile obtained in pulse columns and in spray columns results from the presence of perforated plate in the pulse column. It is felt that these plates, spaced relatively close together, prevent large circulation patterns in the continuous phase from developing, as found in spray columns, although such patterns on a smaller scale do exist between the individual plates. Li (25) found evidence to support this from the fact that when the column was statically filled with water, temperature readings at either end of the columns never agreed no matter how much time was allowed for equilibrium. This behavior was attributed to the fact that the plates within the column tend to block natural convection from one end to the other thus accounting for the difference in temperatures.

13.3 Correlation of Major Heat Transfer Responses.

13.31 Discussions of Final Correlations. The final correlations for the three major heat transfer responses, $H\Theta U_{OC}$, $H\Theta U_{OD}$, and Ua are as follows:

$$H\Theta U_{OC} = 1.0(V_D/V_C)^{-1.58}(V_D + V_C)^{-0.262}(\mu_D)^{0.117(V_D/V_C)^{0.762}} x$$

$$(\Delta T_{lm}/\gamma_D^2)^{0.133} \qquad (164)$$

$$H\Theta U_{OD} = 0.38(V_D/V_C)^{-0.58}(V_D + V_C)^{-0.262}(\mu_D)^{0.117(V_D/V_C)^{0.762}} x$$

$$(\Delta T_{lm}/\gamma_D^2)^{0.133} \qquad (165)$$

and

$$Ua = 8.9(V_D/V_C)^{1.376}(V_D + V_C)^{1.376}(\mu_D)^{-0.039-\mathrm{Log}(V_D/V_C)^{0.423}} x$$

$$(\Delta T/\gamma_D^2)^{-0.133} \qquad (166)$$

Since the exponents of the (V_D/V_C) and $(V_D + V_C)$ terms are the same in equation (166) above, the two terms may be combined into a simpler form,

$$Ua = 8.9\ V_D\left[(V_D/V_C + 1)\right]^{1.376}(\mu_D)^{-0.039-\mathrm{Log}(V_D/V_C)^{0.423}} x$$

$$(\Delta T_{lm}/\gamma_D^2)^{-0.133} \qquad (170)$$

It should be noted again that the above correlations are without correction for end-effects. As was previously mentioned, such end-effects influence the measured terminal temperature used in the calculation of ΔT_{lm}, and other heat transfer responses. However, since end-effects

Hence equation (174) above may be written,

$$\frac{H\Theta U_{OD}}{H\Theta U_{OC}} = 0.37(V_D/V_C) \tag{175}$$

Now if equation (165) above is divided by equation (164), then we have that

$$\frac{H\Theta U_{OD}}{H\Theta U_{OC}} = \frac{(0.38)}{(1.00)} \frac{(V_D/V_C)^{-0.58}}{(V_D/V_C)^{-1.58}} = 0.38\ (V_D/V_C) \tag{176}$$

Thus a comparison of equations (175) and (176) indicates a large degree of internal consistancy within the correlations as compared with the theoretical correlations.

13.32 Comparison of $(V_D + V_C)$ Effect for Mass and Heat Transfer. It generally is known that spray columns increase in contact efficiency as flow rate conditions approach flooding. This is understandable since hold up and interfacial area increase as flooding is approached. However, just the opposite has been found to occur in pulse columns. It has been observed by both Griffith, et al (16), and Thornton (49), (50), that for pulse columns in mass transfer response, values of HTU increased with increased $(V_D + V_C)$, and hence the net rate of mass transfer decreased. Thornton (49), (50), expressing $(V_D + V_C)$ in terms of percent flooding, reported values of HTU_{OC} that increased linearly with $\left[(V_D + V_C)/C_F\right]^{0.118}$ for perforated plates, and with $\left[(V_D + V_C)/C_F\right]^{0.303}$ for special expanded-mesh plates, all at a V_D/V_C ratio of unity, where

C_F = flooding capacity of column, ft/hr.

then

$$H\theta U_{OC} \frac{V_D \rho_D C_D}{V_C \rho_C C_C} = H\theta U_C \frac{V_D \rho_D V_D}{V_C \rho_C C_C} + H\theta U_D \tag{171}$$

Now equating $H\theta U_D$ from equations (49) and (171),

$$H\theta U_{OD} - H\theta U_C \frac{V_D \rho_D C_D}{V_C \rho_C C_C} = H\theta U_{OC} \frac{V_D \rho_D C_D}{V_C \rho_C C_C}$$

$$-H\theta U_C \frac{V_D \rho_D C_D}{V_C \rho_C C_C} \tag{172}$$

or

$$H\theta U_{OD} = H\theta U_{OC} (V_D/V_C) \frac{\rho_D C_D}{\rho_C C_C} \tag{173}$$

and

$$H\theta U_{OD}/H\theta U_{OC} = \frac{\rho_D C_D}{\rho_C C_C} (V_D/V_C) \tag{174}$$

Over the range of temperature employed in this investigation, the $\rho_D C_D/\rho_C C_C$ term is essentially constant due to the fact that ρ_C and C_C for water are practically constant, and ρ_D and C_D for benzene decrease and increase respectively with temperature at approximately the same rate. It has been found that over the range of temperatures employed in this investigation,

$$\frac{\rho_D C_D}{\rho_C C_C} = 0.37$$

are usually expressed in terms of a column length, it is felt that this effect would only change the above correlations by some constant.

An examination of the above correlations shows that all of the variables employed are those which are readily available or easily measured in comparison to some theoretical correlations that have been developed. Thornton (50) and Logsdail and Thornton (30), in studying the performance and through-put of pulse columns in mass transfer responses, developed theoretical equations which were extremely complex, and involved terms such as fractional hold-up which can only be evaluated by additional experimentation.

Thus it is felt that the above correlations, represented by equations (164), (165), and (170), adequately describe heat transfer responses for the pulse column and system used in this investigation, and are relatively simple to use.

A large degree of internal consistancy in the above correlations for $H\Theta U_{OC}$ and $H\Theta U_{OD}$ may be demonstrated by rearranging equations (49) and (50) of Section 7.0 as follows:

$$H\Theta U_{OC} = H\Theta U_{C} + H\Theta U_{D} \frac{V_C \rho_C C_C}{V_D \rho_D C_D} \qquad (50)$$

$$H\Theta U_{OD} = H\Theta U_{D} + H\Theta U_{C} \frac{V_D \rho_D C_D}{V_C \rho_C C_C} \qquad (49)$$

Dividing equation (50) through by $\frac{V_C \rho_C C_C}{V_D \rho_D C_D}$,

The heat transfer response of the pulse column has been found to be just the opposite of that for mass transfer as far as its relation with $(V_D + V_C)$ is concerned. Equations (164) and (165) above indicate that values of $H\Theta U_{OC}$ or $H\Theta U_{OD}$ decrease with increased $(V_D + V_C)$, as a function of $(V_D + V_C)^{-0.262}$, indicating an increased net rate of heat transfer between phases. Similar behavior patterns, however, have been noted for heat transfer in spray columns. Rosenthal (40) found that values of Ua increases with increasing values of V_D and V_C. Garwin and Smith (16) found that values of U decreases with increased $(V_D + V_C)$, although values of Ua were found to increase with $(V_D + V_C)$, as the others had found.

Thus the above results indicate a marked difference between the mass and heat transfer responses of a pulse column, as a function of the total flow rate, $(V_D + V_C)$. This must reflect a basic difference in some aspects of the total mechanisms, and tends to refute the analysis currently assumed to relate heat transfer and mass transfer.

13.33 Interpretation of $(\Delta T_{lm}/\mathcal{V}_D^2)$ Term.

13.331 Heat Transfer from the Continuous to Discontinuous Phase. In the series of runs in which $\mathcal{V}_D$ was tested as a possible variable for heat transfer from the continuous to discontinuous phase, final correlations indicated that $H\Theta U_{OC}$ and $H\Theta U_{OD}$ varied as a function of $\mathcal{V}_D^{-0.266}$. It should be noted that for this particular series of runs, values of ΔT_i were held constant at approximately 10°C, and only the temperature levels of the runs were varied for a given set of operating conditions. Thus by controlling both the inlet benzene and water temperatures such that ΔT_i = 10°C for all runs, the average phase

temperature could be set at any desired values within limits, although the change in temperature of either phase would be less than 10°C. In addition, values of ΔT_{lm} were essentially constant for all runs in this series. Thus it was concluded that the ν_D (or ν_C) effect, shown in Figure 31, are not to any appreciable exrent enfluenced by changes in ΔT_{lm}, and therefore represent a true kinematic viscosity effect, (or at least a physical-property effect).

In addition, the maximum possible range of temperature levels were employed in determining the effect of ν_D on $H\Theta U_{OC}$ and $H\Theta U_{OD}$, from essentially room temperature to the boiling point of a benzene-water azeotrope. An extension of this range would have necessitated additional modification of the equipment such that the inlet temperatures of the water and benzene could be reduced to below room temperature.

In summary, because of the range of temperature levels and experimental proceedure employed in determining the exponents of ν_D (or ν_C), as shown in Figure 31, it is felt that combining ΔT_{lm} and ν_D into the term $(\Delta T_{lm}/\nu_D^2)^{0.133}$ is an indication that natural convection does participate as a mechanism of heat transfer since the above term may be considered as part of a Grashof number, or perhaps Grashof-Prandtl combination. In addition, the fact that the exponent of this term is less than 0.25, the exponent applied to the Grashof number for most pure natural convection heat transfer situations, is actually further indication that natural convection is present within the drop. This may deduced as follows: An examination of the circulation patterns within rising drop, shown in Figure 5, would indicate that when heat is transferred from the continuous phase to the drop, heating of the outer

layers of the drop would cause those regions of the drop to become less dense as compared to the inside. Thus there would be a tendency for pure natural convection patterns to be set up within the drop which would tend to buck those patterns resulting from viscous forces between the two liquids, shown in Figure 5. In effect the tendency for natural circulation would be partially restrained. Thus it is reasonable to expect that the exponent on a Grashof number would be less for this situation than for pure natural convection, even though the above picture is greatly simplified in comparison to the complex mechanisms that actually exist within the drops.

13.332 Heat Transfer from the Discontinuous to Continuous Phase. Figure 35 shows the effect of $(\Delta T_{lm}/\gamma_D^2)$ on $H\Theta U_{OC}$ and $H\Theta U_{OD}$ for the reversed heat transfer situation, or for heat transfer from the discontinuous to continuous phase. It should be noted here that the $(\Delta T_{lm}/\gamma_D^2)$ term in this case is actually established only in regard to the ΔT_{lm} term, since the values of γ_D were practically the same for all runs used in the correlations of Figure 35. It is felt that the results shown in Figure 35, although limited, are a reasonable approximation for the exponents on $(\Delta T_{lm}/\gamma_D^2)$ for the reversed situation. Since it is logical to assume that natural convection also plays an important part in the reversed heat transfer, γ_D was included by analogy in the correlation of Figure 36 as if part of a Grashof number, or as $(\Delta T_{lm}/\gamma_D^2)$.

An examination of Figure 35 indicates that the exponent of the term $(\Delta T_{lm}/\gamma_D^2)$ is about 1.30. The value is not firmly established. Again such an exponent is reasonable in the light of prior reasoning since heat transfer from the drops to the continuous phase tends to cool the

outer layers of the drops, in comparison to the inside, and set up natural convection patterns which enhanced those shown in Figure 5 for the drag effect. Thus one would expect the exponent on the $(\Delta T_{lm}/\gamma_D^2)$ term to be greater than that for pure natural convection alone, that is, greater than 0.25.

13.34 Approximate Correlations for the Reversed Direction of Heat Transfer. As mentioned in Section 12.554, Figures 33 and 34 indicate that the correlations developed for relating $H\Theta U_{OC}$, $H\Theta U_{OD}$ and Ua to the operating variable V_D/V_C, $(V_D + V_C)$, and $\overline{\Pi}_D$, might well be applicable to the reversed heat transfer situation. If this assumption is made, then the coefficients for correlation of $H\Theta U_{OC}$, $H\Theta U_{OD}$, and Ua may be obtained in part from Figures 35 and 36, as well as the exponents of the $(\Delta T_{lm}/\gamma_D^2)$ terms. Thus, correlations for the reversed direction of heat transfer situation have been inferred to be:

$$H\Theta U_{OC} = 0.098(V_D/V_C)^{-1.58}(V_D + V_C)^{-0.262}(\overline{\Pi}_D)^{0.117(V_D/V_C)^{0.762}} \times (\Delta T_{lm}/\gamma_D^2)^{1.30} \quad (177)$$

$$H\Theta U_{OD} = 0.035(V_D/V_C)^{-0.58}(V_D + V_C)^{-0.262}(\overline{\Pi}_D)^{0.117(V_D/V_C)^{0.762}} \times (\Delta T_{lm}/\gamma_D^2)^{1.30} \quad (178)$$

and

$$Ua = 260\ V_D(V_D/V_C + 1)^{1.376}\ (1/D)^{-0.039-\mathrm{Log}(V_D/V_C)^{0.423}}\ x$$

$$(\Delta T_{lm}/\gamma_D^2)^{-1.30} \qquad (179)$$

13.35 Possible Dimensionless Form. All terms in the above correlations for HTU_{OC} and HTU_{OD} are dimensional with the exception of the V_D/V_C ratio. However, it is felt that the present terms are actually components of dimensionless groups.

Thornton (50) and Yoshida and Koyanagi (57) formulate dimensionless groups out of HTU values for mass transfer with the term

$$\frac{HTU}{\mu^2/\rho^2 g_c} = \frac{HTU}{\nu^2/g_c} \qquad (180)$$

These results might be considered to be a new type of a Nusselt number.

However, it is also possible to put values of HTU into dimensionless form as a part of a conventional Nusselt number, defined as

$$Nu = hD/k \qquad (181)$$

Since k/h may be considered as a film thickness in heat transfer, x, the Nusselt number may be considered as the ratio of a characteristic dimension, D, to a film thickness x, which in turn may be measured by some single characteristic tending to define drop size. Thus we might contrive a dimensionless number like this,

$$HTU/D_P \text{ or } H\Theta U/D_P \tag{182}$$

where

D_P = some characteristic dimension such as drop size, plate hole diameter, etc. ft.

Li and Newton (26) have employed the FA produced for a pulse column to calculate phase velocity through the perforated plates to use in a Reynolds number. Since it has already been shown that values of $\overline{\Pi}_D$ and FA are intimately related, it is, therefore, conceivable that the $\overline{\Pi}_D$ term could be part of a Reynolds number. One possible form of such as Reynolds number might be

$$\overline{\Pi}_D \rho D_P/\mu \tag{183}$$

As already indicated, it is felt that the $(\Delta T_{lm}/V_D^2)$ term is part of a Grashof number, for natural convection. However, it should be noted that when a Grashof number is correlated with a Nusselt number, a Prandtl number is also involved to the same power as the Grashof number as indicated by equation (156). Since the Prandtl number shows very little change in magnitude over the temperature ranges employed, there was no point in employing one here.

It is felt that the $(V_D + V_C)$ or $V_D\left[(V_D/V_C) + 1\right]$ term of the above correlations may be put into dimensionless form as part of a percent-of-flooding term, defined as

$$\% \text{ Flooding} = (V_D + V_C)/C_F \tag{184}$$

where

C_F = flooding capacity of column, ft/hr.

This has been done by several workers, notably Thornton (50). Thus we may finally include a Prandtl number separate from the natural convection effect, and infer that

$$f(H\Theta U/D_P) = \left[(Re),(Gr,Pr),(V_D/V_C),(\% \text{ Flooding}),(Pr)\right] \quad (185)$$

It would take measurements on a number of different systems, and on different column characteristics to test the extension of the present correlations to the form assumed above, or one similar to it is principle.

13.36 Analogy between Heat and Mass Transfer. A manner of comparing heat and mass transfer results was presented in detail by Li. That treatment is considered a suitable start on an adequate manner of comparing the heat transfer results, as presently correlated, with mass transfer results. His comparison was based on the conventional Colburn analogy between heat and mass transfer.

This aspect was not pursued here because it has since developed that the mass transfer results available to Li on this same benzene-water system, have been found by Pike (37) to be in error as a result of an error in measurement of the solubility of water in benzene. Although this faulty solubility data have now been corrected, the mass transfer data have not as yet been revised. Therefore, any reasonable test of the analogy between heat and mass transfer for this case is a problem for the future.

14.0 NOMENCLATURE

14.1 English Letters

a = Constant

a' = Constant

a = Interfacial heat transfer area for heat transfer between phases, ft^2/ft^3.

A = Pulse amplitude, in.

A = Superficial cross-sectional area of contractor, ft^2.

b = Constant

b' = Constant

c = Constant

c' = Constant

C_C = Heat capacity of continuous phase, Btu/(lb)(^oF).

C_D = Heat capacity of discontinuous phase, Btu/(lb)(^oF).

C_F = Flooding capacity of column, ft/hr.

D = Pipe or tube diameter, ft.

D_P = Characteristic dimension such as drop size, plate hole diameter, etc., ft.

D_v = Diffusion coefficient, ft^2/hr.

E_B = Heat equivalent of batch of liquid and of solids in immediate contact with liquid, Btu/^oF.

E_H = Eddy diffusivity of heat transfer.

E_i = Heat equivalent for flow system of infinitesimal increment of flow, Btu/^oF.

E_M = Eddy diffusivity of momentum transfer.

f = Fanning friction factor, dimensionless

F = Pulse frequency, in/min.

$F\Theta$ = Dimensionless product

g_c = Constant, 32.17 (lb-mass)(ft)/(lb-force)(sec)^2.

Gr = Grashof number = $L^3\rho^2 g_c \beta \Delta T/\mu^2$, dimensionless

h = Heat transfer coefficient at pipe wall in contact with flowing fluid, Btu/(hr)(ft^2)($^\circ$F).

HTU_C = Height of a continuous phase mass transfer unit, ft.

HTU_D = Height of a discontinuous phase mass transfer unit, ft.

HTU_{OC} = Height of an overall continuous phase mass transfer unit, ft.

HTU_{OD} = Height of an overall discontinuous phase mass transfer unit, ft.

$H\Theta U_C$ = Height of a continuous phase heat transfer unit, ft.

$H\Theta U_D$ = Height of a discontinuous phase heat transfer unit, ft.

$H\Theta U_{OC}$ = Height of an overall continuous phase heat transfer unit, ft.

$H\Theta U_{OD}$ = Height of an overall discontinuous phase heat transfer unit, ft.

j_H = j-factor for heat transfer, dimensionless

j_M = j-factor for mass transfer, dimensionless

k = Constant

k = Thermal conductivity, Btu/(hr)(ft^2)($^\circ$F/ft).

k_c = Mass transfer coefficient, lb moles/(hr)(ft^2)(lb mole/ft^3).

K = Constant

L = Length of pipe or tube, ft.

m = Constant

m = Slope of equilibrium curve averaged over the continuous film

M_C = Molecular mass of continuous phase

M_D = Molecular mass of discontinuous phase

n = Constant

N = Rate of diffusion of diffusing component, lb moles/(ft^2)(hr).

N_C = Number of continuous phase mass transfer units

N_D = Number of discontinuous phase mass transfer units

N_{OC} = Number of overall continuous phase mass transfer units

N_{OD} = Number of overall discontinuous phase mass transfer units

$\bar{N}_C$ = Number of continuous phase heat transfer units

$\bar{N}_D$ = Number of discontinuous phase heat transfer units

$\bar{N}_{OC}$ = Number of overall continuous phase heat transfer units

$\bar{N}_{OD}$ = Number of overall discontinuous phase heat transfer units

Nu = Nusselt number = hD/k, dimensionless

p = Constant

ΔP = Pressure drop across 22 plates, in. of fluid flowing

$\sum P$ = Summation of benzene and water vapor pressures, evaluated at the benzene outlet temperature, mm Hg.

Pr = Prandtl number = $\mu C/k$, dimensionless

q = net rate of heat transfer between continuous and discontinuous phase, Btu/hr.

q_a = Average net rate of heat transfer between phases, Btu/hr.

q_b = Net rate of heat transfer to the discontinuous phase, Btu/hr.

q_B = Heat of solution of water in benzene resulting from mass transfer of water into the benzene, Btu/hr.

q_c = Net rate of heat transfer to the discontinuous phase because of temperature difference, Btu/hr.

q_C = Net sensible heat effect in continuous phase, Btu/hr.

q_D = Net sensible heat effect in discontinuous phase, Btu/hr.

q_e = Heat of evaporation losses from the column, Btu/hr.

q_L = Steady-state heat losses from the column, Btu/hr.

q_{PB} = Heat of pulsing for batch system in 8-plate column, Btu/hr.

q_{PF} = Heat of pulsing for flowing system in 8-plate column, Btu/hr.

q_w = Heat of solution of benzene in water, Btu/hr.

$\triangle q$ = Deviation in heat balances, Btu/hr.

q^* = Heat transferred to benzene as it passes through the distributor, Btu/hr.

q_b^* = Net rate of heat transferred to the discontinuous phase, uncorrected for heat of evaporation, Btu/hr.

$\triangle q^*$ = Deviation in heat balances, uncorrected for heat of evaporation, Btu/hr.

Q_F = Total amount of heat generated in fluid passing through the column due to heat of pulsing, Btu.

Re = Reynolds number = $D\rho U/\mu$, dimensionless

S = Area under pulse curve, in.

S = Superficial cross-sectional area of column, ft^2.

Sc = Schmidt group = $\mu/\rho D_v$, dimensionless

Sh = Sherwood number = $k_c D/D_v$ dimensionless

St = Stanton number = $h/C\rho U$, dimensionless

T_C = Bulk temperature of continuous phase, °C.

T_D = Bulk temperature of discontinuous phase, °C.

T_i = Interfacial temperature between discontinuous and continuous phases, °C.

T_R = Room temperature, °C.

T_{C1} = Actual measured inlet temperature of continuous phase, °C.

T_{C2} = Actual measured outlet temperature of continuous phase, °C.

T_{D1} = Actual measured outlet temperature of discontinuous phase, °C.

T_{D2} = Actual measured inlet temperature of discontinuous phase, °C.

T_{C2}^* = Corrected water outlet temperature, °C.

T_{D2}^* = Actual measured benzene temperature in feed line, °C.

ΔT_C = Temperature change in continuous phase, °C.

ΔT_D = Temperature change in discontinuous phase, °C.

ΔT_i = Difference between inlet stream temperatures, °C.

ΔT_L = Average column temperature minus room temperature, °C.

ΔT_{lm} = Ln-mean temperature difference, °C.

ΔT_P = Increase in fluid temperature due to heat of pulsing, °C.

U = Instantaneous fluid velocity, in/min.

U = Overall heat transfer coefficient for heat transfer between phases, Btu/(hr)(°F)(ft^2).

Ua = Overall volumetric heat transfer coefficient for heat transfer between phases, Btu/(hr)(°F)(ft^3).

v = Volumetric flow rate, ft^3/min.

V_C = Superficial velocity of continuous phase, ft/hr.

V_D = Superficial velocity of discontinuous phase, ft/hr.

V_T = Total contactor volume, ft^3.

X_C = Mole fraction of solute in bulk of continuous phase

X_D = Mole fraction of solute in bulk of discontinuous phase

X_{Ci} = Mole fraction of solute in continuous phase at interface between phases.

X_{Di} = Mole fraction of solute in discontinuous phase at interface between phases.

X_C^* = Mole fraction of solute in bulk of continuous phase which would be in equilibrium with X_D

X_D^* = Mole fraction of solute in bulk of discontinuous phase which would be in equilibrium with X_C

Z = Defined column height, ft.

14.2 Greek Letters

$\alpha = E_M \rho / \varepsilon$

β = Coefficient of volumetric expansion

ε = Eddy viscosity, (lb-force)(hr)/ft^2.

ν_C = Kinematic viscosity of continuous phase, centipoises/(gm)/(cm^3).

ν_D = Kinematic viscosity of discontinuous phase, centipoises/(gm)/(cm^3).

θ = Pulse time, min.

$\Delta\theta$ = Resident time of fluid element in column, hr.

$\overline{u}_a$ = Average flow rate, or the volume of liquid pulsed past a plate during a stroke, divided by the product of the column cross-sectional area and actual time of flow in that direction, ft/hr.

$\overline{u}_C$ = Average flow rate of total material past the plates in the in the direction of the continuous phase flow, averaged over the actual time of flow in that direction, ft/hr.

$\overline{u}_D$ = Defined the same as $\overline{u}_C$, only for a direction the same as that of the discontinuous phase, ft/hr.

π' = 3.1416

ρ_C = Density of continuous phase, lb/ft^3.

ρ_D = Density of discontinuous phase, lb/ft^3.

τ = Shear stress, lb-force/ft^2.

μ = Viscosity, (lb-force)(hr)/ft^2.

14.3 Commerical Trade Names

"Ameripol" A series of synthetic rubbers of the butadiene-styrene type, manufactured by the Goodrich-Gulf Chemicals, Inc., Cleveland 15, Ohio.

"Constametric" A dual-piston pump designed to combine the two sinu soidal discharge slow patterns into a single pattern a constant flow rate. Manufactured by the Milton Roy Company, 1300 East Mermaid Lane, Philadelphia 18, Penna.

"Chromalox" Metal-clad electric heating units manufactured by the Edwin L. Wiegand Company, 7500 Thomas Blvd., Pittsburgh 8, Penna.

"Del" A series of protective coatings manufactured by the David E. Long Corp., 220 East 42nd Street, New York 17, N. Y.

"Double-Tough" A line of surface-hardened "Pyrex" pipe and fittings manufactured by the Corning Glass Works, Corning, N. Y.

"Fisher" Trade name attached to items sold by the Fisher Scientific Company, 7722 Woodbury Drive, Silver Springs, Maryland

"Glyptal" Trade-mark for a group of alkyd-type synthetic resins and plasticizers, manufactured by the General Electric Company, 1 River Road, Schenectady 5, N. Y.

"Helipot" A precision helically-wound, liniar potentiometer manufactured by the Helipot Division of Beckman Instrument, Inc., Fullerton, California.

"Isotemp" Trade name assigned to a precision line of waterbaths, by the Fisher Scientific Company, 7722 Woodbury Drive, Silver Springs, Maryland.

"Kel-F" Poly (trifluorochloroethylene) plastic manufactured by the M. W. Kellogg Company, Chemical Manufacturing Division, Jersey City 3, N. J.

"Koncentrik" A line of "Teflon" seated tubing fittings manufactured by the Special Screw Products Company, 100 Northfield Road, Bedford, Ohio.

"Lightnin" Pilot-plant sized mixers manufactured by the Mixing Equipment Company, Inc., Rochester 11, N. Y.

"Microset" Small relay-switches manufactured by Micro-Switch, a Division of Minneapolis-Honeywell Regulator Company, Freeport, Illinois.

"Mylar" Poly (ethylene terephthalate) resin manufactured by E. I. du Pont de Nemours and Co., Inc., Circleville, Ohio.

"Protecto-Flex" Molded and protected fiber-glas insulation, fitting to pipe. Miracle Adhesives Corporation, 214 East 53rd Street, New York 22, N. Y.

"Pyrex" Borosilicate glass No. 7740 of the Corning Glass Works, Corning, N. Y.

"Rotameter" A variable-area orifice meter. Originally the trademark of a particular line of meters by the Fischer and Porter Company, Hatboro, Pennsylvania.

"Simplex" A single-piston line of piston pumps manufactured by the Milton Roy Company, Philadelphia 18, Pennsylvania.

"Stabl Vis" A type of float and rotameter, characterized by a minimum influence of viscosity, manufactured by the Fischer and Porter Company, Hatboro, Pennsylvania.

"Teflon" Poly (tetrafluoroethylene), E. I. du Pont de Nemours and Company, Wilmington, Delaware.

"Thymotrol" A non-mechanical converter of AC to DC current, General Electric Company, Fort Wayne, Indiana.

"Styrofoam" Trademark of a foamed polystyrene plastic, made by the Dow Chemical Company, Midland, Michigan.

"Utralite" Glass-fiber blanket insulation, Gustin-Bacon Manufacturing Co., 252 West 10th Street, Kansas City, Missouri.

"Variac" A line of variable auto-transformers made by the General Radio Company, Cambridge 39, Massachusetts.

"Westcoat Clear" A hot-melt protective strippable coating made by the Western Coating Company, Elyria, Ohio

15.0 LIST OF REFERENCES

1. Allen, H. D., W. D. Kline and others. 1947. Continuous hydrolysis of fats. Chem. Eng. Prog. 43:459-466

2. Barbouteau, I. 1956. Echange de chaleur par contact direct. Rev. inst. franc. petrole et Ann. combustibles liquids. 11:358-388.

3. Calderbank, P. H., and I. J. O. Korchinski. 1956. Circulation in liquid drops. Chem. Eng. Sci. 6:65-78.

4. Chilton, T. H., and A. P. Colburn. 1934. Mass transfer (absorption) coefficients. Ind. Eng. Chem. 26:1183-1187.

5. Chilton, T. H. and A. P. Colburn. 1935. Distillation and absorption in packed columns. Ind. Eng. Chem. 27:255-260.

6. Cohen, R. M., and G. H. Beyer. 1953. Performance of a pulse extraction column. Chem. Eng. Prog. 49:279-286.

7. Colburn, A. P. 1930. Relation between mass transfer (absorption) and fluid friction. Ind. Eng. Chem. 22:967-970.

8. Conkie, W. R., and P. Savic. 1953. Calculation of the influence of internal circulation in a liquid drop on heat transfer and drag. Report MT 23. National Research Council, Canada. Ottawa.

9. Danckwerts, P. V. 1951. Significance of liquid-film coefficients in gas absorption. Ind. Eng. Chem. 43:1460-1467.

10. Danckwerts, P. V. 1955. Gas absorption accompanied by chemical reaction. A. I. Ch. E. Journal 1:456-462.

11. Elzinga, E. R., and J. T. Banchero. 1958. Film coefficients for heat transfer to liquid drops. Preprint 3, presented at the Second National Heat Transfer Conference, A. I. Ch. E.-A. S. M. E. Preprinted by the American Institute of Chemical Engineers, New York.

12. Farmer, W. S. 1949. Controlling variables in liquid-liquid extraction from single drops. ORNL Report 635, U. S. Atomic Energy Commission, Oak Ridge National Laboratories, Oak Ridge, Tennessee.

13. Gardner, R. P. 1958. Agitated liquid-liquid heat transfer. Unpublished M. S. Thesis. North Carolina State College, Raleigh.

14. Garner, F. H., and A. H. P. Skelland. 1955. Some factors affecting droplet behavior in liquid-liquid systems. Chem. Eng. Sci. 4:149-157.

15. Garwin, L., and B. D. Smith. 1953. Liquid-liquid spray-tower operation in heat transfer. Chem Eng. Prog. 49:591-602.

16. Griffith, W. L., G. R. Jasney, and H. T. Tupper. 1952. The extraction of cobalt from nickel in a pulse column. Chemistry Report No. K-972. Massachusetts Institute of Technology, Cambridge.

17. Grover, S. S., and J. G. Knudsen. 1955. Heat transfer between immescible liquids. Chem. Eng. Prog. Symposium Series, Heat Transfer 51, No. 17. 71-78.

18. Hadamard, J. 1911. Slow steady-state motion of a viscous liquid sphere in a viscous liquid. Compt. rend., 152:1735-1738.

19. Handlos, A. E., and T. Baron. 1957. Mass and heat transfer from drops in liquid-liquid extraction. A. I. Ch. E. Journal 3:127-136.

20. Heertjes, P. M., and others. 1954. Mass transfer between isobutanol and water in a spray column. Chem. Eng. Sci. 3:122.

21. Higbie, R. 1935. The rate of absorption of a pure gas into a still liquid during short periods of exposure. Trans. Am. Inst. Chem. Eng. 31:365-388.

22. Johnson, A. I., and others. 1957. Spray-extraction-tower studies. A. I. Ch. E. Jounal 3:101-110.

23. Kronig, R., and J. C. Brink. 1950. On the theory of extraction from falling droplets(I). Appl. Sci. Res. A2:142.

24. Kronig, R., and B. Van der Veen, and P. Ijzerman. 1951. On the theory of extraction from falling droplets(II). Appl. Sci. Res. A3:103.

25. Li, S. C. 1957. Heat transfer in a pulse column. Unpublished M. S. Thesis. North Carolina State College, Raleigh.

26. Li, W. H., and W. M. Newton. 1957. Liquid-liquid extraction in a pulsed perforated-plate column. A. I. Ch. E. Journal. 3:56-62.

27. Licht, W., and J. Conway. 1950. Mechanism of solute transfer in spray towers. Ind. Eng. Chem. 42:1151-1157.

28. Linton, M., and K. L. Sutherland. 1957. Second International Congress of Surface Activity. Vol. I, 494, Butterworths Scientific Publications, London.

29. Logsdail, D. H., and J. D. Thornton. 1957. The effect of column diameter upon the performance and throughput of pulsed plate columns. Trans. Inst. Chem. Eng. 35:331-342.

30. McAdams, W. H., J. B. Pohlenz, and R. C. St. John. 1949. Transfer of heat and mass between air and water in a packed tower. Chem. Eng. Prog. 45:241-252.

31. McDowell, R. V., and J. E. Myers. 1956. Mechanism of heat transfer to liquid drops. A. I. Ch. E. Journal. 2:384-388.

32. Mottel, W. J. 1955. Mixer settler development- Use of a shrouded paddle. DP-130. E. I. du Pont de Nemours and Company. Explosives Department - Atomic Energy Division, Technical Division, Savannah River Laboratory.

33. Pavia, R. A. 1958. The solubility of water in benzene. Unpublished M. S. Thesis. North Carolina State College, Raleigh.

34. Pierce, R. D., and others. 1959. Heat transfer and fluid dynamics in mercury-water spray columns. A. I. Ch. E. Journal. 5:257-262.

35. Pike, F. P., and E. E. Erickson. 1955. The development of a theory of pulse column flooding behavior. Progress Report No. 10, U. S. Atomic Energy Commission Contract No. AT-(40-1)-1320. Department of Engineering Research, North Carolina State College, Raleigh.

36. Pike, F. P., and E. E. Erickson. 1957. The performance of contactors for liquid-liquid extraction. Progress Report No. 17, U. S. Atomic Energy Commission Contract No. AT-(40-1)-1320. Department of Engineering Research, North Carolina State College, Raleigh.

37. Pike, F. P. 1957-1958. Personal Communications.

38. Prandtl, L. 1910. Z. Physik. 11:1072, and 1928, 29:487.

39. Reynolds, O. 1874. Proc. Manchester Lit. Phil. Soc. 8: Reprinted in Scientific Papers of Osborn Reynolds, Vol. II, Cambridge University Press, New York, 1901.

40. Rosenthal, H. 1949. Studies in the performance of a spray tower in liquid-liquid extraction. Unpublished M. S. Thesis. New York University, New York.

41. Ruckenstein, E. 1958. Turbulent exchange of heat or mass with a boundry. Chem. Eng. Sci. 7:265-268.

42. Schwindt, W., and B. Stuke. 1957. Second International Congress of Surface Activity. Vol. I, 482. Butterworths Scientific Publications, London.

43. Sege, G., and F. W. Woodfield. 1954. Pulse column variables. Chem. Eng. Prog. 50:396-402.

44. Sherwood, T. K., J. E. Evans, and J. V. A. Longcor. 1939. Extraction in spray and packed columns. Trans. A. I. Ch. E. 35:597-622.

45. Sherwood, T. K., and R. L. Pigford. 1952. Absorption and Extraction. McGraw-Hill Book Co., Inc. New York.

46. Spells, K. E. 1952. A study of circulation patterns within liquid drops moving through a liquid. Proc. Phy. Soc. (London). B65:541-546.

47. Surosky, A. E., and B. F. Dodge. 1950. Effect of diffusivity on gas-film absorption coefficients in packed towers. Ind. Eng. Chem. 42:1112.

48. Taylor, G. I. 1916. Brit. Advisory Comm. Aeronaut., Repts. and Mem. 272:423.

49. Thornton, J. D. 1954. Recent developments in pulsed-column techniques. Chem. Eng. Prog. Symposium Series. No. 13, Part III. 39-52.

50. Thornton, J. D. 1957. The effect of pulse wave-form and plate geometry on the performance and throughput of a pulsed column. Trans. Inst. Chem. Eng. 35:316-330.

51. Toor, H. L., and J. M. Marchello. 1958. Film-penetration model for mass and heat transfer. A. I. Ch. E. Journal. 4:97-101.

52. Treybal, R. E. 1951. Liquid Extraction. McGraw-Hill Book Co., Inc. New York.

53. Von Karman, Th. 1939. The analogy between fluid friction and heat transfer. Trans. Am. Soc. Mech. Eng. 61:705-710.

54. West, F. B., and others. 1952. Addition agents and interfacial barriers in liquid-liquid extraction. Ind. Eng. Chem. 44:625-631.

55. Whitman, W. G. 1923. The two film theory of gas absorption. Chem. & Met. Eng. 29:146-148.

56. Wiegandt, H. F., and R. L. Von Berg. 1954. Key to better extraction. Chem. Eng. 61:183-188.

57. Yoshida, F., and T. Koyanagi. 1958. Liquid phase mass transfer rates and effective interfacial area in packed absorption columns. Ind. Eng. Chem. 50:365-374.

Appendix Table 1A. Data of Barlage - Measured flow conditions

$V_D/V_C \cong 0.38$

$V_D + V_C \cong 40$ ft/hr

Run Number	Benzene: Vol. flow rate v_D ft^3/min.	Benzene: Sup. velocity V_D ft^3/hr-ft.^{2}	Water: Vol. flow rate v_C ft^3/min.	Water: Sup. velocity V_C ft^3/hr-ft.^{2}
		$\Delta T_i \cong 18.4°C.$		
173	0.00398	12.4	0.00942	29.3
174	0.00339	10.6	0.00958	29.8
175	0.00346	10.8	0.00950	29.6
176	0.00377	11.7	0.00937	29.2
177	0.00376	11.7	0.00944	29.4
		$\Delta T_i \cong 34.0°C.$		
178	0.00368	11.5	0.00943	29.4
179	0.00367	11.4	0.00921	28.7
180	0.00455	14.2	0.01025	31.9
181	0.00446	13.9	0.01242	38.7
182	0.00427	13.3	0.01014	31.6
		$\Delta T_i \cong 38.0°C.$		
183	0.00430	13.4	0.00991	30.9
184	0.00395	12.3	0.01011	31.5
185	0.00368	11.5	0.00955	29.7
186	0.00363	11.3	0.00969	30.2
187	0.00362	11.3	0.01002	31.2

Appendix Table 1A (continued)

$V_D/V_C \cong 1.0$

$V_D + V_C \cong 40$ ft/hr.

Run Number	Benzene: Vol. flow rate V_D ft^3/min.	Benzene: Sup. velocity V_D ft^3/hr-ft^2	Water: Vol. flow rate V_C ft^3/min.	Water: Sup. velocity V_C ft/hr-ft^2
		$\Delta T_i \cong 18.3$°C.		
168	0.00648	20.2	0.00636	19.8
169	0.00625	19.5	0.00639	19.9
170	0.00618	19.3	0.00645	20.1
171	0.00645	20.1	0.00635	19.8
172	0.00615	19.2	0.00645	20.1
		$\Delta T_i \cong 34.0$°C.		
158	0.00648	20.2	0.00605	18.8
159	0.00588	18.3	0.00626	19.5
160	0.00645	20.1	0.00581	18.1
161	0.00565	17.6	0.00603	18.8
162	0.00647	20.2	0.00625	19.5
		$\Delta T_i \cong 43.4$°C.		
163	0.00664	20.7	0.00610	19.0
164	0.00639	19.9	0.00618	19.3
165	0.00611	19.0	0.00585	18.2
166	0.00638	19.8	0.00606	18.9
167	0.00634	19.7	0.00625	19.5
		Standard Runs $\Delta T_i \cong 18.4$°C.		
131	0.00644	20.1	0.00644	20.1
132	0.00589	18.3	0.00643	20.0
133	0.00642	20.0	0.00644	20.1
141	0.00594	18.5	0.00627	19.5
168	0.00648	20.2	0.00636	19.8

Appendix Table 1A (continued)

$V_D/V_C \cong 3.0$

$V_D + V_C \cong 40$ ft/hr.

Run Number	Benzene: Vol. flow rate v_D ft^3/min.	Benzene: Sup. velocity V_D ft^3/hr-ft^2	Water: Vol. flow rate v_C ft^3/min.	Water: Sup. velocity V_C ft^3/hr-ft^2
		$\Delta T_i \cong 18.5^oC.$		
147	0.01056	32.9	0.00356	11.1
139	0.01137	35.4	0.00366	11.4
145	0.01126	35.1	0.00354	11.0
146	0.01070	33.3	0.00360	11.2
135	0.01147	35.7	0.00383	11.9
138	0.01129	35.2	0.00366	11.4
144	0.01091	34.0	0.00343	10.7
136	0.01140	35.5	0.00379	11.8
142	0.01130	35.2	0.00380	11.8
137	0.01132	35.3	0.00381	11.9
143	0.01078	33.6	0.00379	11.8
140	0.01066	33.2	0.00374	11.6
		$\Delta T_i \cong 31.0^oC.$		
153	0.01195	37.2	0.00378	11.8
154	0.01124	35.2	0.00364	11.3
155	0.01111	34.6	0.00363	11.3
156	0.01045	32.6	0.00342	10.6
157	0.01024	31.9	0.00338	10.5
		$\Delta T_i \cong 44.0^oC.$		
148	0.01109	34.5	0.00342	10.6
149	0.01170	36.4	0.00343	10.7
150	0.01050	32.7	0.00352	11.0
151	0.01030	32.1	0.00342	10.6
152	0.01044	32.5	0.00344	10.7

Appendix Table 1A (continued)

Special Runs

Run Number	Benzene		Water	
	Vol. flow rate v_D $ft^3/min.$	Sup. velocity V_D $ft^3/hr\text{-}ft^2$	Vol. flow rate v_C $ft^3/min.$	Sup. velocity V_C $ft^3/hr\text{-}ft^2$
188	0.00661	20.6	0.00650	20.2
189	0.00976	30.4	0.00362	11.3
190	0.01260	39.2	0.00341	10.6
191	0.00662	20.6	0.00657	20.5
192	0.00992	30.9	0.00352	10.9
193	0.01285	40.0	0.00332	10.3
194	0.00632	19.7	0.00623	19.4
195	0.01011	31.5	0.00374	11.6
196	0.01276	39.7	0.00320	10.0
197	0.00413	12.8	0.00425	13.2
198	0.00640	19.9	0.00643	20.0
199	0.01433	44.6	0.01479	46.1

Reversed Direction of Heat Transfer Runs

200	0.00361	11.2	0.00964	30.0
202	0.00606	19.0	0.00655	20.4
203	0.00626	19.5	0.00622	19.4
204	0.00625	19.5	0.00631	19.6
205	0.00653	20.3	0.00625	19.5
206	0.00638	19.9	0.00628	19.6
201	0.01116	34.8	0.00353	11.0

Appendix Table 1B. Data of Barlage - Calculated flow conditions

$V_D/V_C \cong 0.38$

$V_D + V_C \cong 40$ ft/hr.

Run Number	Total Sup. Velocity $V_D + V_C$ ft³/hr-ft²	Diff. in Sup. Velocity $V_D - V_C$ ft³/hr-ft²	Pulse Pump Frequency F cpm.	Pulse Pump Amplitude A in.	FA Product FA in/min.	Average Phase Velocities ft/hr. $\bar{V}_D$	$\bar{V}_C$	Ratio V_D/V_C
			$\Delta T_i \cong 18.4°C$					
173	41.7	- 16.9	30.6	0.50	15.3	154	155	0.42
174	40.4	- 19.2	58.6	0.50	29.3	300	290	0.35
175	40.4	- 18.8	57.4	1.00	57.4	600	560	0.36
176	40.2	- 16.8	77.9	1.00	77.9	800	760	0.40
177	41.1	- 17.7	77.5	1.50	116	1200	1100	0.40
			$\Delta T_i \cong 34.0°C.$					
178	40.9	- 17.9	30.4	0.50	15.2	154	155	0.39
179	40.1	- 17.3	59.6	0.50	29.8	300	290	0.40
180	46.1	- 17.7	58.5	1.00	58.5	600	560	0.44
181	52.6	- 24.8	77.4	1.00	77.4	800	760	0.36
182	44.9	- 18.3	76.0	1.50	114	1200	1100	0.42
			$\Delta T_i \cong 38.0°C.$					
183	44.3	- 17.5	30.6	0.50	15.3	154	155	0.43
184	43.8	- 19.2	58.4	0.50	29.2	300	290	0.39
185	41.2	- 18.2	57.6	1.00	57.6	600	560	0.38
186	41.5	- 18.9	75.0	1.00	75.0	800	760	0.38
187	42.5	- 19.9	75.5	1.50	113	1200	1100	0.36

Appendix Table 1B (continued)

$V_D/V_C \cong 1.0$

$V_D + V_C \cong 40$ ft/hr.

Run Number	Total Sup. Velocity $V_D + V_C$ ft³/hr-ft²	Diff. in Sup. Velocity $V_D - V_C$ ft³/hr-ft²	Pulse Pump Frequency F cpm.	Pulse Pump Amplitude A in.	FA Product FA in/min.	Average Phase Velocities ft/hr. $\bar{u}_D$	$\bar{u}_C$	Ratio V_D/V_C
			$\Delta T_i \cong 18.3°C.$					
168	40.0	0.4	28.6	0.50	14.3	150	134	1.02
169	39.4	- 0.4	57.3	0.50	28.7	300	270	0.98
170	39.4	- 0.8	57.3	1.00	57.3	600	545	0.96
171	39.9	0.3	76.6	1.00	76.6	800	730	1.02
172	39.3	- 0.9	76.6	1.50	115	1200	1100	0.96
			$\Delta T_i \cong 34.0°C.$					
158	39.0	0.4	28.6	0.50	14.3	150	134	1.07
159	37.8	- 1.2	57.4	0.50	28.7	300	270	0.94
160	38.2	2.0	57.2	1.00	57.2	600	545	1.11
161	36.4	- 1.2	76.6	1.00	76.6	800	730	0.94
162	39.7	0.7	76.6	1.50	115	1200	1100	1.04
			$\Delta T_i \cong 43.4°C.$					
163	39.7	1.7	28.6	0.50	14.3	150	134	1.09
164	39.2	0.6	57.2	0.50	28.6	300	270	1.04
165	37.2	0.8	57.2	1.00	57.2	600	545	1.04
166	38.7	0.9	76.6	1.00	76.6	800	730	1.05
167	39.2	0.2	77.4	1.50	116	1200	1100	1.01
			Standard Runs					
			$\Delta T_i \cong 18.4°C.$					
131	40.2	0.0	29.1	0.50	14.5	152	137	1.00
132	38.3	- 0.7	28.8	0.50	14.4	151	136	0.92
133	40.1	- 0.1	29.0	0.50	14.5	152	137	1.00
141	38.0	- 1.0	29.0	0.50	14.5	152	137	0.95
168	40.0	0.4	28.6	0.50	14.3	150	134	1.02

Appendix Table 1B (continued)

$V_D/V_C \cong 3.0$

$V_D + V_C \cong 40$ ft/hr.

Run Number	Total Sup. Velocity $V_D + V_C$ $ft^3/hr\text{-}ft^2$	Diff. in Sup. Velocity $V_D - V_C$ $ft^3/hr\text{-}ft^2$	Pulse Pump Frequency F cpm.	Pulse Pump Amplitude A in.	FA Product FA in/min.	Average Phase Velocities ft/hr. $\bar{u}_D$	$\bar{u}_C$	Ratio V_D/V_C
			$\Delta T_i \cong 18.5°C.$					
147	44.0	21.8	26.9	0.25	6.7	79	54	2.97
139	46.8	24.0	27.3	0.50	13.7	150	120	3.10
145	46.1	24.1	27.2	0.50	13.6	150	120	3.18
146	44.5	22.1	26.7	0.50	13.4	148	118	2.98
135	47.6	23.8	56.2	0.50	28.1	295	255	3.00
138	46.6	23.8	56.2	0.50	28.1	295	255	3.08
144	44.7	23.3	56.4	0.50	28.2	295	255	3.18
136	47.3	23.7	57.3	1.00	57.3	600	540	3.01
142	47.0	23.4	57.0	1.00	57.0	600	540	2.97
137	47.2	23.4	76.7	1.00	76.7	800	730	2.98
143	45.4	21.8	76.0	1.00	76.0	800	730	2.85
140	44.8	21.6	76.0	1.50	114	1200	1100	2.85
			$\Delta T_i \cong 31.0°C.$					
153	49.0	25.4	26.8	0.50	13.4	148	118	3.16
154	46.3	23.7	56.3	0.50	28.1	295	255	3.09
155	45.9	23.3	57.5	1.00	57.5	600	540	3.06
156	43.2	22.0	76.5	1.00	76.5	800	730	3.06
157	42.4	21.4	76.6	1.50	115	1200	1100	3.03
			$\Delta T_i \cong 44.0°C.$					
148	45.1	23.9	26.6	0.50	13.3	145	117	3.24
149	47.1	25.7	56.0	0.50	28.0	300	255	3.41
150	43.7	21.7	57.0	1.00	57.0	600	540	2.99
151	42.7	21.5	76.5	1.00	76.5	800	730	3.00
152	43.2	21.8	76.2	1.50	114	1200	1100	3.04

Appendix Table 1B (continued)

Special Runs

Run Number	Total Sup. Velocity $V_D + V_C$, $ft^3/hr\text{-}ft^2$	Diff. in Sup. Velocity $V_D - V_C$, $ft^3/hr\text{-}ft^2$	Pulse Pump Frequency F cpm.	Pulse Pump Amplitude A in.	FA Product FA in/min.	Average Phase Velocities ft/hr $\overline{u}_D$	$\overline{u}_C$	Ratio V_D/V_C
188	40.8	0.4	57.4	0.50	28.7	300	270	1.02
189	41.7	19.1	56.0	0.50	28.0	300	255	2.70
190	49.8	28.6	55.6	0.50	27.8	300	250	3.69
191	41.1	0.1	57.6	0.50	28.8	300	270	1.01
192	41.8	20.0	56.1	0.50	28.0	300	255	2.82
193	50.3	29.7	55.6	0.50	27.8	300	250	3.87
194	39.1	0.3	57.4	0.50	28.7	300	270	1.01
195	43.1	19.9	56.0	0.50	28.0	300	255	2.70
196	49.7	29.7	55.4	0.50	27.7	300	250	3.99
197	26.0	- 0.4	57.4	0.50	28.7	300	270	0.97
198	39.9	- 0.1	57.3	0.50	28.7	300	270	1.00
199	90.7	- 1.5	57.4	0.50	28.7	300	270	0.97
			Reversed Direction of Heat Transfer Runs					
200	41.2	-18.8	58.5	0.50	29.3	300	290	0.37
202	39.4	- 1.4	57.6	0.50	28.8	300	270	0.92
203	39.4	0.1	28.7	0.50	14.3	150	136	0.01
204	39.1	- 0.1	57.5	1.00	57.5	600	545	0.99
205	39.8	0.8	76.5	1.00	76.5	800	730	1.04
206	39.5	0.3	77.5	1.50	116	1200	1100	1.02
201	45.8	23.8	56.4	0.50	28.2	300	255	3.16

Appendix Table 1C. Data of Barlage - Measured temperature conditions

$V_D/V_C \cong 0.38$

$V_D + V_C \cong 40$ ft/hr.

Run Number	Benzene Temperatures (°C) T^*_{D2} (in)	T_{D2} (in)	T_{D1} (out)	Water Temperatures (°C) T_{C1} (in)	T_{C2} (out)
		$\Delta T_i \cong 18.4$°C.			
173	32.10	33.61	51.01	52.01	48.71
174	31.95	33.71	51.28	52.03	48.99
175	31.95	33.81	51.07	52.03	47.96
176	32.25	34.31	50.79	51.94	47.55
177	32.10	33.97	50.45	51.91	48.04
		$\Delta T_i \cong 34.0$°C.			
178	32.10	34.78	66.97	68.76	62.99
179	31.95	34.71	67.30	68.76	62.72
180	31.80	34.30	66.93	68.83	59.60
181	31.85	34.33	66.97	68.83	60.00
182	31.90	34.71	66.62	68.83	60.45
		$\Delta T_i \cong 38.0$°C.			
183	32.10	34.71	73.03	73.09	64.98
184	32.05	34.78	71.12	73.21	65.40
185	32.10	35.22	70.90	73.11	63.17
186	32.10	35.45	70.92	73.18	63.77
187	32.10	35.59	71.18	74.30	63.44

Appendix Table 1C (continued)

$V_D/V_C \cong 1.0$

$V_D + V_C \cong 40$ ft/hr;

Run Number	Benzene Temperatures (°C) T^*_{D2} (in)	T_{D2} (in)	T_{D1} (out)	Water Temperatures (°C) T_{C1} (in)	T_{C2} (out)
		$\Delta T_i \cong 18.3$°C.			
168	32.20	33.09	50.59	51.58	44.20
169	32.20	33.18	50.70	51.63	44.29
170	32.20	33.27	50.45	51.58	43.25
171	32.20	33.29	50.27	51.58	43.34
172	32.10	33.68	49.75	51.58	44.00
		$\Delta T_i \cong 34.0$°C.			
158	32.45	33.74	65.98	67.88	53.70
159	32.50	34.00	66.28	68.04	54.99
160	32.50	33.90	65.82	68.07	51.76
161	32.45	34.05	65.32	67.95	52.63
162	32.45	33.98	64.17	67.62	52.38
		$\Delta T_i \cong 43.4$°C.			
163	32.60	34.20	72.42	77.60	56.66
164	32.25	33.95	72.40	77.35	57.89
165	32.20	33.97	71.69	77.20	55.72
166	32.20	33.90	71.59	77.35	55.80
167	32.20	33.99	71.08	77.40	55.90
		Standard Runs $\Delta T_i \cong 18.4$°C.			
131	31.30	32.95	50.80	51.70	44.14
132	30.80	30.88	49.23	51.13	42.62
133	33.45	34.10	50.88	51.71	44.82
141	32.90	33.90	52.52	53.84	46.22
168	32.20	33.09	50.59	51.58	44.20

Appendix Table 1C (continued)

$V_D/V_C \cong 3.0$

$V_D + V_C \cong 40$ ft/hr.

Run Number	Benzene Temperatures (°C) T^*_{D2} (in)	T_{D2} (in)	T_{D1} (out)	Water Temperatures (°C) T_{C1} (in)	T_{C2} (out)
		$\Delta T_i \cong 18.5$°C.			
147	31.20	31.50	47.18	50.49	33.55
139	32.70	33.30	45.38	51.22	35.72
145	31.10	31.40	45.70	50.33	33.82
146	31.15	31.51	46.18	50.12	34.32
135	24.60	32.72	45.22	49.33	35.68
138	32.70	33.32	44.90	50.89	35.80
144	31.00	31.47	44.80	50.22	35.22
136	32.75	33.05	45.25	49.72	35.18
142	30.90	31.37	44.82	50.00	34.88
137	32.20	33.05	45.40	49.66	35.06
143	30.90	31.45	45.51	50.69	37.02
140	31.45	32.28	45.43	50.83	36.54
		$\Delta T_i \cong 31.0$°C.			
153	32.10	32.61	56.22	65.55	36.28
154	32.10	32.62	54.98	65.61	37.49
155	32.10	32.61	53.88	63.19	37.22
156	32.05	32.61	54.20	64.89	38.35
157	32.00	32.66	52.31	62.62	38.98
		$\Delta T_i \cong 44.0$°C.			
148	32.30	32.80	63.58	75.30	37.02
149	32.30	32.80	62.95	78.65	37.60
150	32.40	33.02	65.54	80.10	40.82
151	32.40	33.03	64.45	79.80	41.03
152	32.70	33.43	62.79	80.04	44.17

Appendix Table 1C (continued)

Special Runs

Run Number	Benzene Temperatures (°C) T^*_{D2} (in)	T_{D2} (in)	T_{D1} (out)	Water Temperatures (°C) T_{C1} (in)	T_{C2} (out)
188	30.30	30.88	40.36	40.79	36.83
189	30.35	30.65	37.75	40.25	33.06
190	30.40	30.59	36.54	40.23	32.02
191	43.95	45.58	54.17	55.10	50.85
192	44.35	45.77	50.99	53.30	46.64
193	44.60	45.90	49.84	52.99	47.66**
194	55.90	58.18	67.20	68.77	63.67
195	57.10	58.90	64.30	67.16	59.58
196	57.70	59.21	62.50	65.63	60.76**
197	32.90	33.80	42.35	43.20	38.86
198	33.30	33.99	43.39	43.98	39.80
199	33.60	34.10	44.22	44.42	40.92

Reversed Direction of Heat Transfer Runs

200	49.20	48.23	32.41	32.56	34.84
202	50.30	50.27	33.05	32.51	38.62
203	50.30	50.29	32.77	32.51	38.86
204	50.25	50.16	32.95	32.51	38.11
205	50.20	50.06	33.06	32.57	38.11
206	50.60	49.99	33.43	32.61	38.15
201	51.10	51.45	37.79	32.50	46.21

**Corrected water outlet temperatures.

Appendix Table 1D. Data of Barlage

Calculated temperature conditions

$V_D/V_C \cong 0.38$

$V_D + V_C \cong 40$ ft/hr.

Run Number	Temperature Differences					Room Temperature	Average Phase Temperatures, °C.	
	$T_{C1}-T_{D1}$	$T_{C2}-T_{D2}$	ΔT_{lm}	ΔT_{lm}	$T_{C1}-T_{D2}$	T_r	Benzene	Water
	ΔT_1	ΔT_2			ΔT_i			
	°C.	°C.	°C.	°F.	°C.	°C.	T_{Da}	T_{Ca}
				$\Delta T_i \cong 18.4$°C.				
173	0.89	15.10	5.01	9.02	18.40	30.2	42.4	50.4
174	0.75	15.28	4.85	8.73	18.32	30.1	42.5	50.5
175	0.96	14.15	4.96	8.93	18.49	29.5	42.4	49.9
176	1.15	13.24	4.94	8.89	17.63	28.8	42.6	49.7
177	1.46	14.07	5.56	10.00	17.94	28.7	42.2	50.0
				$\Delta T_i \cong 34.0$°C.				
178	1.79	28.21	9.57	17.23	33.98	28.5	51.0	67.0
179	1.46	28.01	8.97	16.15	34.05	27.8	51.0	65.7
180	1.90	25.30	9.03	16.25	34.53	26.7	50.6	64.2
181	1.86	25.67	9.06	16.31	34.50	26.8	50.7	64.6
182	2.21	25.74	9.58	17.24	34.12	26.7	50.7	64.6
				$\Delta T_i \cong 38.0$°C.				
183	2.06	30.27	10.49	18.88	38.38	26.8	52.9	69.1
184	2.09	30.62	10.62	19.12	38.43	26.9	53.0	69.8
185	2.21	27.95	10.14	18.25	37.89	27.1	53.1	69.2
186	2.26	28.32	10.30	18.54	37.73	26.8	53.2	68.9
187	3.12	27.85	11.28	20.30	38.71	26.6	53.4	68.9

Appendix Table 1D (continued)

$V_D/V_C \cong 1.0$

$V_D + V_C \cong 40$ ft/hr.

Run Number	Temperature Differences $T_{C1}-T_{D1}$ ΔT_1 °C.	$T_{C2}-T_{D2}$ ΔT_2 °C.	ΔT_{lm} °C.	ΔT_{lm} °F.	$T_{C1}-T_{D2}$ ΔT_i °C.	Room Temperature T_r °C.	Average Phase Temperatures, °C. Benzene T_{Da}	Water T_{Ca}
				$\Delta T_i \cong 18.3$°C.				
168	0.99	11.11	4.18	7.52	18.48	30.7	41.8	47.7
169	0.93	11.11	4.47	8.05	18.45	30.2	41.9	48.0
170	1.13	9.98	4.06	7.31	18.31	29.5	41.9	47.4
171	1.31	10.05	4.28	7.70	18.29	29.3	41.8	48.0
172	1.83	10.32	4.90	8.82	17.90	28.7	41.7	47.8
				$\Delta T_i \cong 34.0$°C.				
158	1.90	19.96	7.66	13.79	33.14	32.7	49.8	60.8
159	1.76	20.99	7.75	13.95	34.04	30.0	50.1	61.5
160	2.25	17.86	7.53	13.55	34.17	32.4	49.9	59.9
161	2.63	18.58	8.16	14.69	33.90	32.8	49.7	62.8
162	3.45	18.40	8.91	16.04	33.64	32.4	49.1	60.0
				$\Delta T_i \cong 43.4$°C.				
163	5.18	22.46	11.75	21.15	43.40	33.1	53.3	67.1
164	4.95	23.94	12.03	21.65	43.40	29.5	53.2	67.6
165	5.51	21.75	11.82	21.28	43.23	30.9	52.8	66.5
166	5.76	21.90	12.08	21.74	43.45	30.5	52.7	66.6
167	6.32	21.91	12.53	22.55	43.41	30.7	52.6	66.2
				Standard Runs $\Delta T_i \cong 18.1$°C.				
131	0.90	11.19	4.08	7.34	18.75	23.3	41.9	47.9
132	1.90	11.74	5.40	9.72	20.25	22.2	40.1	46.9
133	0.83	10.73	3.86	6.95	17.61	26.2	42.5	48.3
141	1.32	12.32	4.92	8.86	19.94	23.8	43.2	50.0
168	0.99	11.11	4.18	7.52	18.48	30.4	41.8	47.7

Appendix Table 1D (continued)

$V_D/V_C \cong 3.0$

$V_D + V_C \cong 40$ ft/hr.

Run Number	Temperature Differences $T_{C1}-T_{D1}$ ΔT_1 °C.	$T_{C2}-T_{D2}$ ΔT_2 °C.	ΔT_{lm} °C.	ΔT_{lm} °F.	$T_{C1}-T_{D2}$ ΔT_i °C.	Room Temperature T_r °C.	Average Phase Temperatures, °C. Benzene T_{Da}	Water T_{Ca}
				$\Delta T_i \cong 18.5$°C.				
147	3.31	2.05	2.62	4.71	18.99	30.4	39.3	42.0
139	5.84	2.24	3.76	6.77	17.92	24.8	39.2	43.5
145	4.63	2.42	3.40	6.12	18.93	29.0	38.6	42.1
146	3.94	2.81	3.34	6.01	18.61	30.1	38.8	42.2
135	4.11	2.96	3.49	6.28	16.61	32.5	39.0	42.5
138	5.99	2.48	3.98	7.16	17.57	24.8	39.1	43.3
144	5.42	3.75	4.53	8.15	18.75	28.7	38.6	42.7
136	4.47	2.13	3.15	5.68	16.67	23.3	39.2	42.4
142	5.18	3.51	4.29	7.72	18.63	24.6	38.1	42.4
137	4.26	2.01	3.00	5.39	16.61	23.1	39.3	42.4
143	5.18	5.57	5.29	9.52	19.24	24.9	38.5	43.9
140	5.40	4.26	4.76	8.56	18.55	25.9	38.9	43.7
				$\Delta T_i \cong 31.0$°C.				
153	9.33	3.67	6.05	10.89	32.94	30.0	44.4	50.8
154	10.63	4.87	7.35	13.23	32.99	30.1	43.8	51.6
155	9.31	4.61	6.69	12.04	30.58	30.4	43.5	50.2
156	10.69	5.74	7.96	14.32	32.28	30.2	43.5	51.6
157	10.32	6.32	8.15	14.67	29.97	29.5	42.5	50.8
				$\Delta T_i \cong 44.0$°C.				
148	11.72	4.22	7.33	13.19	42.50	32.8	48.2	56.2
149	15.70	4.80	9.18	16.53	45.85	32.8	47.9	58.2
150	14.65	7.80	10.85	19.53	47.08	32.9	49.3	60.5
151	15.35	8.00	11.27	20.29	46.77	32.0	48.7	60.4
152	17.25	10.74	13.72	24.69	46.61	34.2	48.1	62.1

Appendix Table 1D (continued)

Special Runs

Run Number	Temperature Differences $T_{C1}-T_{D1}$ ΔT_1 °C.	$T_{C2}-T_{D2}$ ΔT_2 °C.	ΔT_{lm} °C.	ΔT_{lm} °F.	$T_{C1}-T_{D2}$ ΔT_i °C.	Room Temperature T_r °C.	Average Phase Temperatures, °C. Benzene T_{Da}	Water T_{Ca}
188	0.43	5.98	2.11	3.79	9.91	30.0	35.6	38.8
189*	2.50	2.41	2.46	4.43	9.60	30.2	34.2	36.7
190	3.69	1.43	2.38	4.28	9.64	30.2	33.6	36.2
191	0.93	5.27	2.84	5.12	9.52	27.4	49.9	53.0
192	2.31	0.87	1.47	2.65	7.53	27.7	48.9	50.0
193⁂	3.15	1.76	2.38	4.29	7.09	27.7	47.9	50.0
194	1.57	5.49	3.13	5.63	10.59	27.5	62.7	66.2
195	2.86	0.68	1.51	2.73	8.26	27.4	61.6	63.4
196⁂	3.13	1.55	2.25	4.05	6.42	27.2	60.9	62.1
197	0.85	5.06	2.36	4.24	9.40	29.4	38.1	41.0
198	0.59	5.81	2.28	4.10	9.99	29.4	38.7	41.4
199	0.20	6.82	1.87	3.37	10.32	29.0	39.2	42.1
Reversed Direction of Heat Transfer Runs								
200	+0.15	-13.39			-15.67	28.3	40.3	33.7
202	-0.54	-11.65	3.61	6.51	-17.76	28.3	41.7	35.6
203	-0.26	-11.43	2.95	5.31	-17.78	28.8	41.5	35.7
204	-0.44	-12.05	3.50	6.31	-17.65	28.8	41.6	35.3
205	-0.48	-11.95	3.56	6.42	-17.49	28.7	41.6	35.3
206	-0.82	-11.84	4.12	7.42	-17.38	29.3	41.7	35.4
201	-5.20	- 5.24	4.34	7.81	-18.95	29.2	44.6	39.4

*Average value $(\Delta T_1+\Delta T_2)/2$

⁂Corrected value of water outlet temperature used in calculations.

Appendix Table 1E. Data of Barlage - Rates of heat transfer

$V_D/V_C \cong 0.38$

$V_D + V_C \cong 40$ ft/hr.

Run Number	Benzene Phase, Btu/hr. q_D	q_B	q_e	q_b^*	q_b	Water Phase, Btu/hr. q_C	q_L	q^*	q_c	q_a Btu/hr.	Results of Heat Balances Δq^* Btu/hr.	Δq Btu/hr.	% error
						$\Delta T_i \cong 18.4°C.$							
173	172	7	8	165	173	208	13	11	186	180	+ 21	+ 13	+ 7.2
174	147	7	23	140	163	195	13	14	170	167	+ 30	+ 7	+ 4.2
175	148	7	32	141	173	258	13	16	231	202	+ 90	+ 58	+28.7
176	154	7	37	147	184	275	14	19	244	214	+ 97	+ 60	+28.0
177	153	7	46	146	192	244	14	17	216	204	+ 70	+ 24	+11.8
						$\Delta T_i \cong 34.0°C.$							
178	293	16	42	277	319	361	25	24	314	320	+ 37	- 5	- 1.6
179	296	16	115	280	395	368	25	24	321	358	+ 41	- 74	-20.7
180	368	16	161	352	513	628	25	27	578	546	+226	+ 65	+11.9
181	361	16	197	345	542	728	25	27	678	610	+333	+136	+22.3
182	337	16	234	321	555	537	25	29	486	521	+165	- 69	+13.2
						$\Delta T_i \cong 38.0°C.$							
183	388	19	111	369	480	532	30	27	477	479	+108	- 3	- 0.6
184	356	19	162	337	499	523	30	26	469	484	+132	- 30	- 6.1
185	326	19	228	307	535	629	30	28	563	549	+256	+ 28	+ 5.1
186	319	19	268	300	568	604	30	29	547	558	+247	- 21	- 3.8
187	319	19	342	300	642	720	30	30	663	653	+363	+ 21	+ 3.2

In the calculation of the above rates of heat transfer, it was assumed that $q_{PF} = 0$ for both the benzene and water phases. For the water phase, q_w was assumed to be 2Btu/hr.

Appendix Table 1E (continued)

$V_D/V_C \cong 1.0$

$V_D + V_C \cong 40$ ft/hr.

Run Number	Benzene Phase, Btu/hr q_D	q_B	q_e	q_b^*	q_b	Water Phase, Btu/hr q_C	q_L	q^*	q_c	Results of Heat Balances q_a Btu/hr.	Δq^* Btu/hr.	Δq Btu/hr.	% error
						$\Delta T_i \cong 18.3°C.$							
168	280	7	11	273	284	313	9	14	292	288	+ 19	+ 8	+ 2.8
169	270	7	16	263	279	312	13	15	286	283	+ 23	+ 7	+ 2.5
170	261	7	23	254	277	358	13	16	331	304	+ 77	+54	+17.8
171	270	7	27	263	290	348	13	17	320	305	+ 57	+30	+ 9.8
172	244	7	33	237	270	325	13	24	291	281	+ 54	+21	+ 7.5
						$\Delta T_i \cong 34.0°C.$							
158	518	15	47	503	550	570	18	20	534	542	+ 31	-16	- 3.0
159	470	15	70	455	525	542	20	21	503	514	+ 48	-22	- 4.3
160	510	15	98	495	593	629	16	22	593	593	+ 98	- 0	0.0
161	440	15	115	425	540	610	18	22	582	561	+157	+42	+ 7.5
162	485	15	142	470	612	630	16	24	593	603	+123	-19	- 3.2
						$\Delta T_i \cong 43.4°C$							
163	630	20	96	610	706	844	22	25	799	752	+188	+92	+12.2
164	608	20	142	588	730	795	26	26	745	738	+157	+15	+ 2.0
165	570	20	200	550	750	834	23	26	787	769	+237	+37	+ 4.8
166	595	20	235	575	810	865	23	26	818	814	+243	+ 8	+ 1.0
167	581	20	291	561	852	888	23	27	841	847	+280	-11	- 1.3
						Standard Runs $\Delta T_i \cong 18.4°C.$							
131	283	7	11	277	288	324	16	26	284	286	+ 7	- 4	- 1.4
132	267	7	11	260	278	362	16	1	349	317	+ 89	+78	+24.6
133	266	7	11	259	270	296	13	10	275	273	+ 16	+ 5	+ 1.8
141	272	7	11	265	276	318	19	14	290	283	+ 25	+14	+ 4.9
168	280	7	11	273	284	313	9	14	292	288	+ 19	+ 8	+ 2.8

In the above calculations of rates of heat transfer, it was assumed that $P_{PF} = 0$ for both the benzene and water phases. For the water phase, q_w was assumed to be 2Btu/hr.

Appendix Table 1E (continued)

$V_D/V_C \cong 3.0$

$V_D + V_C \cong 40$ ft/hr.

Run Number	Benzene Phase, Btu/hr q_D	q_B	q_e	q_b^*	q_b	q_C	q_L	q^*	q_c	Water Phase, Btu/hr. q_a	Results of Heat Balances Δq^*	Δq	% error
										Btu/hr.	Btu/hr.	Btu/hr.	
						$\Delta T_i \cong 18.5°C.$							
147	407	5	3	402	405	404	6	8	392	399	-10	-13	- 3.2
139	338	5	4	333	337	380	12	17	353	345	+20	+16	+ 4.6
145	397	5	4	392	396	391	7	8	378	387	-14	-18	- 4.6
146	386	5	4	381	385	380	6	9	367	376	-14	-18	- 4.8
135	353	5	6	348	354	349	11	6	334	344	-14	-20	- 5.8
138	322	5	6	317	324	369	12	17	338	332	+21	+15	+ 4.5
144	361	5	6	356	362	344	8	10	328	345	-28	-34	- 9.8
136	343	5	9	338	347	369	12	8	352	350	+14	+ 5	+ 1.4
142	374	5	9	369	378	384	11	13	362	368	- 7	-16	+ 4.3
137	344	5	10	339	349	371	12	7	354	352	+15	+ 5	+ 1.4
143	372	5	10	367	377	346	12	14	320	349	-47	-57	-16.3
140	352	5	13	347	360	356	11	22	326	348	-21	-43	-12.4
						$\Delta T_i \cong 31.0°C.$							
153	688	10	10	678	688	735	12	15	710	699	+32	+22	+ 3.1
154	620	9	15	611	626	680	13	14	655	641	+44	+29	+ 4.5
155	584	8	21	576	597	625	13	14	600	599	+24	+ 3	+ 0.5
156	556	9	25	547	572	602	12	14	578	575	+31	+ 6	+ 1.0
157	495	8	31	487	518	531	13	16	505	512	+18	-13	- 2.5
						$\Delta T_i \cong 44.0°C.$							
148	842	14	27	828	855	866	14	13	842	854	+14	-23	- 2.7
149	870	13	39	853	892	933	15	14	906	899	+53	+14	+ 1.6
150	844	15	59	829	888	915	16	16	881	885	+52	- 7	- 0.8
151	800	15	69	785	854	877	17	16	846	850	+61	- 8	- 0.9
152	757	13	86	744	830	819	15	18	789	810	+45	-41	- 5.1

In the calculation of the above rates of heat transfer, it was assumed that $q_{PF} = 0$ for both the benzene and water phases. For the water phase, q_w was assumed to be 2Btu/hr.

Appendix Table 1E (continued)

Special Runs

Run Number	Benzene Phase, Btu/hr q_D	q_B	q_e	q_b^*	q_b	q_C	Water Phase, Btu/hr. q_L	q^*	q_c	Results of Heat Balances q_a Btu/hr.	Δq^* Btu/hr.	Δq Btu/hr.	% error
188	153	3	5	150	155	171	5	9	159	157	+ 9	+ 4	+ 2.5
189	171	2	3	169	172	174	3	7	166	169	- 3	- 6	- 3.6
190	184	2	2	182	184	187	3	5	181	183	- 1	- 3	- 1.6
191	141	9	22	132	154	186	17	27	144	149	+12	-10	- 6.7
192	128	7	11	121	132	155	17	34	106	119	-15	-26	-21.8
193	126	7	9	119	128	158	13	41	107	118	-12	-21	-17.8
194	142	17	82	125	207	210	26	36	150	179	+25	-57	-31.8
195	136	16	47	120	167	188	23	45	122	145	+ 2	-45	-31.0
196	105	14	28	91	119	151	22	48	83	101	+ 8	-36	-35.6
197	87	4	6	83	89	124	7	9	110	100	+33	+21	+21.0
198	148	4	7	144	151	179	7	11	163	156	+19	+12	+ 7.7
199	335	5	8	330	338	347	7	16	326	332	- 4	-12	+ 3.6

Reversed Direction of Heat Transfer Runs

200	140	1	3	141	138	147	3	9	139	142	- 2	+ 1	+ 0.7
202	255	1	2	256	254	268	4	1	271	263	+15	+17	+ 6.5
203	268	1	1	269	268	264	4	0	266	267	- 3	- 2	- 0.7
204	263	1	3	264	261	236	4	1	237	249	-27	-24	- 9.6
205	273	1	4	274	270	232	4	2	232	241	-42	-38	-15.1
206	259	1	5	260	255	232	4	10	224	240	-36	-31	-12.9
201	372	2	3	374	371	323	6	10	317	344	-57	-54	-15.7

In the calculation of the above rates of heat transfer, it was assumed that $q_{PF} = 0$ for both the benzene and water phases. For the water phase, q_w was assumed to be 2Btu/hr.

Appendix Table 1F. Data of Barlage

Calculated heat transfer responses

$V_D/V_C \cong 0.38$

$V_D + V_C \cong 40$ ft/hr.

Run Number	Number of Transfer Units: Benzene $\bar{N}_{OD}$	Number of Transfer Units: Water $\bar{N}_{OC}$	Heights of Transfer Units: Benzene HOU_{OD} ft.	Heights of Transfer Units: Water HOU_{OC} ft.	Overall Heat Trans. Coefficient U_a Btu/hr-°F-ft^3.
			$\Delta T_i \cong 18.4$°C.		
173	3.50	0.545	0.387	2.48	764
174	3.62	0.472	0.374	2.87	733
175	3.48	0.470	0.389	2.88	867
176	3.34	0.498	0.405	2.72	922
177	2.96	0.435	0.457	3.11	782
			$\Delta T_i \cong 34.0$°C.		
178	3.36	0.489	0.403	2.77	712
179	3.63	0.540	0.373	2.51	849
180	3.61	0.599	0.375	2.26	1287
181	3.60	0.483	0.376	2.80	1433
182	3.33	0.523	0.407	2.59	1158
			$\Delta T_i \cong 38.0$°C.		
183	3.46	0.564	0.391	2.40	972
184	3.42	0.501	0.396	2.70	970
185	3.50	0.490	0.387	2.76	1152
186	3.46	0.467	0.391	2.89	1153
187	3.16	0.426	0.428	3.18	1232

Appendix Table 1F (continued)

$V_D/V_C \cong 1.0$

$V_D + V_C \cong 40$ ft/hr.

Run Number	Number of Transfer Units: Benzene $\bar{N}_{OD}$	Number of Transfer Units: Water $\bar{N}_{OC}$	Heights of Transfer Units: Benzene $H\Theta U_{OD}$ ft.	Heights of Transfer Units: Water $H\Theta U_{OC}$ ft.	Overall Heat Trans. Coefficient U_a Btu/hr-°F-ft.^{3}
			$\Delta T_i \cong 18.3$°C.		
168	4.19	1.58	0.323	0.857	1467
169	3.92	1.42	0.345	0.954	1347
170	4.23	1.49	0.320	0.909	1593
171	3.97	1.49	0.341	0.909	1518
172	3.28	1.16	0.413	1.17	1221
			$\Delta T_i \cong 34.0$°C.		
158	4.21	1.68	0.322	0.806	1506
159	4.16	1.46	0.325	0.927	1412
160	4.24	1.76	0.319	0.769	1677
161	3.83	1.35	0.354	1.00	1463
162	3.39	1.31	0.399	1.03	1410
			$\Delta T_i \cong 43.4$°C.		
163	3.25	1.33	0.417	1.02	1362
164	3.20	1.24	0.423	1.09	1306
165	3.19	1.25	0.424	1.08	1384
166	3.12	1.22	0.434	1.11	1434
167	2.96	1.12	0.457	1.21	1439
			Standard Runs $\Delta T_i \cong 18.4$°C.		
131	4.38	1.85	0.309	0.732	1493
132	3.39	1.58	0.400	0.860	1250
133	4.34	1.78	0.312	0.760	1505
141	3.78	1.55	0.359	0.875	1224
168	4.19	1.58	0.323	0.857	1467

Appendix Table 1F (continued)

$V_D/V_C \cong 3.0$

$V_D + V_C \cong 40$ ft/hr.

Run Number	Number of Transfer Units: Benzene $\overline{N}_{OD}$	Number of Transfer Units: Water $\overline{N}_{OC}$	Heights of Transfer Units: Benzene $H\Theta U_{OD}$ ft.	Heights of Transfer Units: Water $H\Theta U_{OC}$ ft.	Overall Heat Trans. Coefficient U_a Btu/hr-°F-ft.^{3}
			$\Delta T_i \cong 18.5$°C.		
147	5.98	6.54	0.226	0.207	3246
139	3.21	4.12	0.422	0.329	1952
145	4.21	4.92	0.322	0.274	2423
146	4.39	4.80	0.308	0.282	2397
135	3.58	3.91	0.378	0.346	1841
138	2.80	3.90	0.483	0.347	2026
144	2.94	3.48	0.461	0.389	1846
136	3.86	4.60	0.351	0.294	1645
142	3.14	3.52	0.431	0.384	2482
137	4.10	4.85	0.330	0.280	1747
143	2.65	2.57	0.511	0.527	1401
140	2.76	3.00	0.491	0.451	1557
			$\Delta T_i \cong 31.0$°C.		
153	3.90	4.53	0.347	0.299	2459
154	3.04	3.48	0.445	0.389	1856
155	3.18	3.62	0.426	0.374	1906
156	2.71	3.07	0.500	0.441	1538
157	2.41	2.71	0.561	0.500	1337
			$\Delta T_i \cong 44.0$°C.		
148	4.20	5.00	0.322	0.271	2481
149	3.28	4.14	0.413	0.327	2084
150	2.99	3.31	0.453	0.409	1736
152	2.79	3.11	0.485	0.435	1605
152	2.14	2.42	0.632	0.560	1257

Appendix Table 1F (continued)

Special Runs

Run Number	Number of Transfer Units: Benzene $\bar{N}_{OD}$	Number of Transfer Units: Water $\bar{N}_{OC}$	Heights of Transfer Units: Benzene $H_{OU_{OD}}$ ft.	Heights of Transfer Units: Water $H_{OU_{OC}}$ ft.	Overall Heat Trans. Coefficient U_a Btu/hr-°F-ft.^{3}
188	4.46	1.67	0.304	0.811	1587
*189	2.89	2.87	0.468	0.471	1461
190	2.50	3.39	0.542	0.399	1638
191	3.02	1.14	0.448	1.19	1115
192	3.55	3.69	0.381	0.367	1721
**193	1.66	1.62	0.816	0.834	1054
194	2.88	1.10	0.470	1.23	1218
195	3.58	3.63	0.378	0.373	2035
**196	1.46	1.19	0.927	1.11	955
197	3.62	1.30	0.374	1.04	904
198	4.12	1.51	0.329	0.897	1458
199	5.41	1.81	0.250	0.748	3774

Reversed Direction of Heat Transfer Runs

200					
202	4.77	1.61	0.284	0.841	1548
203	5.94	2.18	0.228	0.621	1926
204	4.92	1.78	0.275	0.760	1512
205	4.78	1.83	0.283	0.739	1498
206	4.02	1.50	0.337	0.903	1239
201	3.15	3.63	0.430	0.373	1688

*Calculations made using average temperature driving force $(\Delta T_1+\Delta T_2)/2$.

**Calculations made from corrected water outlet temperatures.

Appendix Table 2A. Data of Li - Measured flow conditions

$$V_D/V_C \cong 1.0$$

$$V_D + V_C \cong 40 \text{ ft/hr.}$$

Run Number	Benzene: Vol. flow rate v_D ft^3/min.	Benzene: Sup. velocity V_D ft^3/hr-ft^2	Water: Vol. flow rate v_C ft^3/min.	Water: Sup. velocity V_C ft^2/hr-ft^2
		$\Delta T_i \cong 31.0^\circ C.$		
79	0.0057	17.8	0.0060	18.7
89	0.0069	21.5	0.0066	20.6
95	0.0060	18.7	0.0060	18.8
88	0.0067	20.9	0.0067	20.9
90	0.0069	21.5	0.0069	21.5
70	0.0066	20.6	0.0068	21.2
91	0.0067	20.9	0.0068	21.2
71	0.0060	18.7	0.0063	19.6
84	0.0064	19.9	0.0059	18.4
92	0.0068	21.2	0.0069	21.5
86	0.0059	18.4	0.0059	18.4
99	0.0066	20.6	0.0064	19.9
101	0.0066	20.6	0.0060	18.7
102	0.0061	19.0	0.0060	20.2
94	0.0066	20.6	0.0061	19.0
97	0.0060	18.7	0.0060	18.7
		$\Delta T_i \cong 23.0^\circ C.$		
74	0.0073	22.7	0.0073	22.7
73	0.0074	23.1	0.0068	21.2
75	0.0068	21.2	0.0073	22.7

Appendix Table 2B. Data of Li - Calculated flow conditions

$V_D/V_C \cong 1.0$

$V_D + V_C \cong 40$ ft/hr.

Run Number	Total Sup. Velocity $V_D + V_C$ $ft^3/hr\text{-}ft^2$	Diff. in Sup. Velocity $V_D - V_C$ $ft^3/hr\text{-}ft^2$	Pulse Pump Frequency F cpm.	Pulse Pump Amplitude A in.	FA Product FA in/min.	Average Phase Velocities ft/hr $\bar{u}_D$	$\bar{u}_C$	Ratio V_D/V_C
			$\Delta T_i \cong 31.0°C.$					
79	36.5	-0.9	23.8	0.20	4.76	49.8	45.5	0.95
89	42.1	-0.9	23.4	0.20	4.08	50.5	46.4	1.04
95	37.4	0.0	24.2	0.20	4.84	50.2	46.4	0.99
88	41.8	0.0	73.8	0.20	14.76	153	144	1.00
90	43.0	0.0	71.5	0.20	14.30	150	138	1.00
70	41.8	0.6	28.7	0.50	14.35	150	138	0.97
91	42.1	0.3	29.4	0.50	14.70	153	141	0.98
71	38.3	-0.9	46.6	0.63	29.36	308	279	0.95
84	38.3	1.5	47.3	0.63	29.80	310	283	1.08
92	42.7	-0.3	48.1	0.63	30.30	315	288	0.99
86	36.8	0.0	75.1	0.75	56.33	590	532	1.00
99	40.5	0.7	78.3	1.00	78.30	818	741	1.04
101	39.3	1.9	39.5	2.00	78.00	826	748	1.10
102	39.2	-1.2	64.0	1.50	96.00	1000	909	0.94
94	39.6	1.6	75.5	1.50	113.25	1180	1080	1.08
97	37.4	0.0	75.5	1.50	113.25	1180	1080	1.00
			$\Delta T_i \cong 23.0°C.$					
74	45.4	0.0	28.7	0.50	14.35	150	138	1.00
73	44.3	1.9	46.4	0.63	29.23	308	279	1.09
75	43.9	-0.3	74.3	0.75	55.73	582	528	0.93

Appendix Table 2C Data of Li - Measured temperature conditions

$V_D/V_C \cong 1.0$

$V_D + V_C \cong 40$ ft/hr.

Run Number	Benzene Temperatures (°C) T^*_{D2} (in)	T_{D2} (in)	T_{D1} (out)	Water Temperatures (°C) T_{C1} (in)	T_{C2} (out)
		$\Delta T_i \cong 31.0$°C.			
79	23.75	24.89	59.52	60.16	46.39
89	27.60	29.29	59.87	60.47	47.67
95	28.63	26.62	56.13	57.04	45.80
88	27.65	29.44	58.83	60.50	48.25
90	27.27	29.17	58.60	60.48	47.97
70	21.29	22.60	57.61	58.69	45.50
91	27.57	29.55	59.62	60.55	48.81
71	21.69	23.00	57.43	58.64	45.50
84	26.35	27.95	58.60	60.35	46.02
92	28.00	30.15	59.40	60.59	47.59
88	28.15	29.56	58.13	60.12	47.20
99	28.60	31.21	58.54	60.48	47.75
101	29.22	31.22	58.55	60.48	47.46
102	29.10	31.31	58.52	60.49	50.00
94	28.11	27.65	54.80	58.90	45.71
97	29.84	31.55	57.80	60.50	49.36
		$\Delta T_i \cong 23.0$°C.			
74	22.29	23.13	45.48	46.00	37.24
73	21.95	22.73	44.90	45.92	35.84
75	22.53	23.30	45.12	45.98	37.10

Appendix Table 2D. Data of Li

Calculated temperature conditions

$V_D/V_C \cong 1.0$

$V_D + V_C \cong 40$ ft/hr.

Run Number	Temperature Differences $T_{C1}-T_{D1}$ ΔT_1 °C.	$T_{C2}-T_{D2}$ ΔT_2 °C.	ΔT_{lm} °C.	ΔT_{lm} °F.	$T_{C1}-T_{D2}$ ΔT_i °C.	Room Temperature T_r °C.	Average Phase Temperatures, °C. Benzene T_{Da}	Water T_{Ca}
				$\Delta T_i \cong 31.0$°C.				
79	0.64	21.50	5.93	10.67	35.27	24.2	41.6	53.3
89	0.60	18.38	5.20	9.36	31.18	27.1	43.7	54.1
95	0.91	19.18	6.00	10.80	30.42	29.7	42.4	51.4
88	1.67	18.81	7.09	12.76	31.06	27.4	43.2	54.4
90	1.88	18.80	7.36	13.25	31.31	27.4	43.0	54.3
70	1.08	22.90	7.16	12.89	36.09	22.8	39.5	52.1
91	0.93	19.26	6.05	10.89	31.00	28.1	43.6	54.7
71	1.21	22.50	7.30	13.14	35.64	22.5	39.6	52.1
84	1.75	18.07	7.00	12.60	32.40	27.0	42.5	53.2
92	1.19	17.44	6.07	10.93	30.44	28.7	43.7	54.1
86	1.99	13.64	6.06	10.91	30.56	28.6	43.1	53.7
99	1.94	16.54	6.83	12.29	29.27	28.7	43.6	54.1
101	1.93	16.54	6.82	12.28	29.26	30.0	43.9	54.1
102	1.97	18.69	7.45	13.41	29.18	29.1	43.8	55.3
94	4.10	18.06	9.43	16.97	31.25	28.8	41.5	52.3
97	2.70	17.81	8.04	14.47	28.95	30.2	43.8	54.9
				$\Delta T_i \cong 23$°C.				
74	0.52	14.11	4.12	7.42	22.87	24.6	33.9	41.6
73	1.02	13.11	4.74	8.53	23.19	24.2	33.4	40.9
75	0.86	13.80	4.67	8.41	22.68	24.6	33.8	41.5

Appendix Table 2E. Data of Li

Recalculated rates of heat transfer

$V_D/V_C \cong 1.0$

$V_D + V_C \cong 40$ ft/hr.

Run Number	Benzene Phase, Btu/hr. q_D	q_B	q_e	Water Phase, Btu/hr. q_b^*	q_b	q_C	q_L	q^*	q_c	Results of Heat Balances q_a Btu/hr.	Δq^* Btu/hr.	Δq Btu/hr.	%error
						$\Delta T_i \cong 31.0°C.$							
79	502	10	14	492	506	556	19	16	523	515	+31	+17	+3.3
89	524	10	14	514	528	559	17	31	513	521	- 1	-15	-2.9
95	435	10	9	425	434	450	14	-15	453	444	28	+19	+4.3
88	489	10	24	479	503	544	17	30	499	501	20	- 4	-0.8
90	502	10	24	492	516	561	17	32	514	515	22	- 2	-0.4
70	568	10	22	558	580	595	19	22	556	568	- 2	-24	-4.2
91	496	10	29	486	515	549	17	32	485	500	- 1	-30	-6.0
71	507	10	32	497	529	549	19	19	514	522	+17	-15	-2.9
84	483	10	35	473	508	558	17	27	516	512	+43	+ 8	+1.6
92	493	10	38	483	521	550	17	38	497	509	+14	-24	-4.7
86	419	10	49	409	458	470	17	21	435	447	+26	-23	-5.1
99	450	10	48	440	488	535	17	39	481	485	+41	- 7	-1.4
101	445	10	48	435	483	505	16	32	460	472	+25	-23	-4.9
102	409	10	48	399	447	452	17	32	405	426	+ 6	-42	-9.8
94	446	10	46	436	482	533	16	42	477	480	+41	- 5	-1.0
97	392	10	66	382	448	447	16	25	409	429	+27	-39	-9.1
						$\Delta T_i \cong 23.0°C.$							
74	398	6	3	392	395	427	11	15	403	399	+11	+ 8	+2.0
73	403	6	6	397	403	451	11	8	434	418	+31	+31	+7.4
75	364	6	12	358	370	395	11	14	371	371	+13	+ 1	+0.3

In the above calculations for the rates of heat transfer, it was assumed that $q_{PF} = 0$ for both the benzene and water phases. For the water phase, q_w was assumed to be 2Btu/hr.

Appendix Table 2F. Data of Li

Recalculated calculated heat transfer responses

$V_D/V_C \cong 1.0$

$V_D + V_C \cong 40$ ft/hr.

Run Number	Number of Transfer Units: Benzene $\overline{N}_{OD}$	Number of Transfer Units: Water $\overline{N}_{OC}$	Heights of Transfer Units: Benzene $H\Theta U_{OD}$ ft.	Heights of Transfer Units: Water $H\Theta U_{OC}$ ft.	Overall Heat Trans. Coefficient U_a Btu/hr-°F-ft³
			$\Delta T_i \cong 31.0$°C.		
79	5.84	2.32	0.232	0.584	1692
89	5.88	2.46	0.230	0.552	2004
95	4.92	1.87	0.276	0.723	1450
88	4.15	1.73	0.327	0.784	1334
90	4.00	1.70	0.339	0.787	1301
70	4.89	1.84	0.277	0.737	1610
91	4.97	1.94	0.273	0.698	1630
71	4.72	1.80	0.287	0.753	1401
84	4.37	2.05	0.310	0.661	1311
92	4.83	2.14	0.281	0.634	1543
86	4.72	2.14	0.288	0.624	1109
99	4.00	1.87	0.339	0.725	1244
101	4.00	1.87	0.339	0.725	1254
102	3.65	1.41	0.372	0.961	1091
94	2.85	1.40	0.471	0.969	814
97	3.27	1.39	0.415	0.975	958
			$\Delta T_i \cong 23.0$°C.		
74	5.42	2.12	0.250	0.639	1916
73	4.68	2.12	0.290	0.639	1610
75	4.67	1.90	0.290	0.714	1447

Appendix Table 3A. Data of Gardner - Measured flow conditions

Run Number	Benzene		Water	
	Vol. flow rate v_D $ft^3/min.$	Sup. velocity V_D $ft^3/hr\text{-}ft2.$	Vol. flow rate v_C $ft^3/min.$	Sup. velocity V_C $ft^3/hr\text{-}ft^2$
104	0.0069	21.5	0.0071	22.1
103	0.0077	24.0	0.0070	21.8
110	0.0070	21.8	0.0067	20.9
105	0.0078	24.3	0.0072	22.4
106	0.0073	22.7	0.0072	22.4
123	0.0066	20.6	0.0078	24.3
107	0.0068	21.2	0.0068	21.2
108	0.0063	19.6	0.0069	21.5
109	0.0066	20.6	0.0070	21.8
115	0.0067	20.9	0.0067	20.9
114	0.0072	22.4	0.0069	21.5
124	0.0132	41.1	0.0078	24.3
122	0.0134	41.7	0.0079	24.6
120	0.0147	45.8	0.0070	21.8
117	0.0166	51.7	0.0079	24.6
112	0.0164	51.1	0,0076	23.7
116	0.0161	50.2	0.0070	21.8
111	0.0166	51.7	0.0069	21.5
113	0.0171	53.3	0.0072	22.4
125	0.0186	57.9	0.0065	20.2
121	0.0187	58.2	0.0066	20.6
118	0.0192	59.8	0.0062	19.3
119	0.0196	61.1	0.0060	18.7

Appendix Table 3B. Data of Gardner - Calculated flow conditions

Run Number	Total Sup. Velocity $V_D + V_C$ $ft^3/hr\text{-}ft^2$	Diff. in Sup. Velocity $V_D - V_C$ $ft^3/hr\text{-}ft^2$	Pulse Pump Frequency F cpm.	Pulse Pump Amplitude A in.	FA Product FA in/min.	Average Phase Velocities ft/hr $\overline{u}_D$	$\overline{u}_C$	Ratio V_D/V_C
104	43.9	- 0.6	28.8	0.50	14.4	150	135	0.97
103	45.8	2.2	71.5	0.20	14.3	150	136	1.10
110	42.7	0.9	28.3	0.50	14.2	149	132	1.04
105	46.7	1.9	28.5	0.50	14.3	150	136	1.08
106	45.1	0.3	71.7	0.20	14.3	149	134	1.01
123	44.9	- 3.7	28.6	0.50	14.3	148	137	0.85
107	42.4	0.0	71.7	0.20	14.3	150	135	1.00
108	41.1	- 1.0	29.4	0.50	14.7	152	138	0.91
109	42.4	- 1.2	29.1	0.50	14.6	152	138	0.94
115	41.8	0.0	30.3	0.50	15.2	157	144	1.00
114	43.9	0.9	26.4	0.50	13.2	138	124	1.04
124	65.4	16.8	27.4	0.50	13.7	147	122	1.69
122	66.3	17.1	27.7	0.50	13.8	147	122	1.70
120	67.6	24.0	26.6	0.50	13.3	145	118	2.12
117	76.3	27.1	65.9	0.20	13.2	146	114	2.10
112	74.3	27.4	71.7	0.20	14.3	159	124	2.16
116	72.0	28.4	26.4	0.50	13.2	146	114	2.30
111	73.2	30.2	28.3	0.50	14.2	157	121	2.40
113	75.7	30.9	71.7	0.20	14.3	157	121	2.38
125	78.1	37.7	27.4	0.50	13.7	154	117	2.87
121	78.8	37.6	26.6	0.50	13.3	153	113	2.83
118	79.1	40.5	65.2	0.20	13.0	150	108	3.10
119	76.3	42.4	26.6	0.50	13.3	151	108	3.27

Appendix Table 3C Data of Gardner

Measured temperature conditions

Run Number	Benzene Temperatures (°C) T^*_{D2} (in)	T_{D2} (in)	T_{D1} (out)	Water Temperatures (°C) T_{C1} (in)	T_{C2} (out)
104	26.85	27.40	34.42	34.58	31.63
103	26.70	27.42	34.14	34.53	31.36
110	23.70	28.08	40.36	40.69	35.03
105	24.78	25.94	38.61	39.12	33.13
106	24.56	25.63	38.52	39.32	33.66
123	30.80	31.50	46.85	47.64	41.41
107	25.98	27.15	43.12	44.23	37.01
108	26.15	26.72	42.87	44.00	36.50
109	24.01	28.41	48.22	49.30	40.63
115	30.30	30.92	58.66	60.31	48.30
114	30.90	31.57	59.41	60.61	48.15
124	30.20	30.50	44.35	46.15	34.88
122	29.60	30.19	60.49	63.60	38.81
120	29.60	28.83	56.21	59.89	35.96
117	29.30	29.58	56.77	60.01	84.56
112	26.85	30.66	45.81	49.30	34.86
116	29.90	30.13	57.49	60.22	35.46
111	26.83	28.52	46.20	49.02	31.40
113	26.85	30.82	46.23	49.25	33.90
125	31.00	30.36	41.76	45.92	31.40
121	29.80	30.04	54.52	60.06	31.91
118	29.50	29.66	51.16	59.80	31.90
119	29.70	29.83	51.43	59.30	31.62

Appendix Table 3D. Data of Gardner

Calculated temperature conditions

Run Number	Temperature Differences					Room Temperature	Average Phase Temperatures, °C.	
	$T_{C1}-T_{D1}$	$T_{C2}-T_{D2}$	ΔT_{lm}	ΔT_{lm}	$T_{C1}-T_{D2}$	T_r	Benzene	Water
	ΔT_1	ΔT_2			ΔT_i			
	°C.	°C.	°C.	°F.	°C.	°C.	T_{Da}	T_{Ca}
104	0.16	4.23	1.24	2.23	7.10	26.7	30.9	33.1
103	0.39	3.94	1.53	2.75	7.11	27.3	30.8	32.9
110	0.33	6.95	2.18	3.92	12.61	29.1	34.2	37.9
105	0.51	7.19	2.52	4.54	13.18	23.3	32.3	36.1
106	0.80	8.03	3.14	5.65	13.69	23.3	32.1	36.5
123	0.79	9.91	3.62	6.52	16.14	30.6	39.2	44.5
107	1.11	9.86	4.02	7.24	17.08	27.7	35.1	40.6
108	1.13	9.78	4.01	7.23	17.28	27.3	34.8	40.3
109	1.08	12.22	4.62	8.32	20.89	26.5	38.3	45.0
115	1.65	17.38	6.69	12.04	29.39	30.5	44.8	54.3
114	1.20	16.58	5.87	10.57	29.04	31.2	45.5	54.4
124	1.80	4.38	3.72	6.70	15.65	30.8	37.4	40.5
122	3.11	8.62	5.39	9.70	33.41	30.1	45.3	51.3
120	3.60	7.13	5.17	9.31	31.06	30.3	42.5	47.9
117	3.24	4.98	4.11	7.40	30.43	28.5	43.2	47.3
112	3.49	4.20	3.84	6.91	18.64	30.8	38.2	42.1
116	2.73	5.33	4.03	7.25	30.09	29.2	43.8	47.8
111	2.82	2.88	2.85	5.13	20.50	31.8	37.4	40.2
113	3.02	3.08	3.05	5.49	18.43	31.6	38.5	41.6
125	4.16	1.04	2.25	4.05	15.56	31.0	36.1	38.7
121	5.54	1.87	3.37	6.07	30.02	30.7	42.2	46.0
118	8.64	2.24	4.74	8.53	30.14	29.8	40.4	45.9
119	7.87	1.79	4.11	7.40	29.64	30.0	40.6	45.5

Appendix Table 3E. Data of Gardner

Rates of heat transfer recalculated

Run Number	Benzene Phase, Btu/hr. q_D	q_B	q_e	q_b^*	Water Phase, Btu/hr. q_b	q_C	q_L	q^*	Results of Heat Balances q_c	q_a	$\triangle q^*$	$\triangle q$	% error
									Btu/hr.	Btu/hr.	Btu/hr.		
104	119	1	2	118	120	141	4.2	9.3	130	125	+ 12	+ 10	+ 8.0
103	128	1	2	127	129	150	0.2	13.7	138	128	+ 11	+ 9	+ 7.0
110	213	3	3	210	213	256	6.0	76.0	176	195	- 34	- 37	-19.0
105	243	3	3	240	243	289	7.0	22.2	262	254	+ 22	+ 19	+ 7.5
106	232	3	3	229	231	273	8.5	19.2	247	239	+ 18	+ 15	+ 6.3
123	248	5	4	243	247	329	9.5	11.3	310	281	+ 67	+ 63	+22.4
107	267	4	4	263	267	329	8.2	19.5	303	285	+ 40	+ 36	+12.6
108	251	3	4	248	252	347	8.2	8.8	332	292	+ 84	+ 80	+27.4
109	320	6	8	314	322	408	13.0	71.0	326	324	+ 12	+ 4	+ 1.2
115	456	11	25	445	470	544	19.0	10.2	516	493	+ 71	+ 46	+ 9.3
114	493	12	24	481	505	582	19.0	11.8	553	529	+ 72	+ 48	+ 9.1
124	453	5	4	448	452	590	6.0	9.8	576	514	+128	+124	+24.1
122	1000	12	26	988	1014	1321	13.0	19.5	1290	1152	+302	+276	+24.0
120	994	10	15	984	999	1136	10.0		1128	1064	+144	+129	+12.1
117	1110	10	15	1100	1115	1360	12.0	11.4	1339	1227	+239	+224	+18.2
112	612	5	4	607	611	733	8.0	162.0	565	588	- 42	- 46	- 7.8
116	1085	8	16	1079	1093	1166	12.0	9.1	1147	1120	+ 70	+ 54	+ 4.8
111	725	5	5	720	725	818	13.0	69.2	738	732	+ 18	+ 13	+ 1.8
113	645	5	5	640	645	747	8.0	176.0	565	605	- 75	- 80	-13.2
125	524	3	3	521	524	636	7.9	7.3	623	574	+102	+ 99	+17.2
121	1131	9	11	1122	1133	1245	11.0		1236	1186	+114	+103	+ 8.7
118	1022	7	7	1015	1022	1162	11.0	7.6	1145	1084	+130	+123	+11.3
119	1043	7	8	1036	1044	1115	11.0	6.0	1100	1072	+ 64	+ 56	+ 5.2

In the calculation of the above data, it was assumed that $q_{PF} = 0$ for both the benzene and water phases. It was also assumed that q_w = 2Btu/hr.

Appendix 3F. Data of Gardner

Recalculated calculated heat transfer responses

Run Number	Number of Transfer Units: Benzene $\overline{N}_{OD}$	Number of Transfer Units: Water $\overline{N}_{OC}$	Heights of Transfer Units: Benzene $H\Theta U_{OD}$ ft.	Heights of Transfer Units: Water $H\Theta U_{OC}$ ft.	Overall Heat Trans. Coefficient U_a Btu/hr-°F-ft^3
104	5.66	2.38	0.239	0.569	2148
103	4.39	2.07	0.308	0.654	1783
110	5.63	2.60	0.240	0.520	1906
105	5.03	2.38	0.269	0.569	2144
106	4.10	1.80	0.330	0.752	1621
123	4.24	1.72	0.319	0.786	1651
107	3.97	1.80	0.341	0.752	1508
108	4.03	1.87	0.336	0.724	1547
109	4.28	1.88	0.316	0.720	1492
115	4.15	1.79	0.326	0.756	1569
114	4.74	2.12	0.286	0.638	1918
124	3.72	3.02	0.364	0.448	2939
122	5.62	4.59	0.241	0.295	4550
120	5.29	4.62	0.256	0.293	4379
117	6.61	6.19	0.205	0.219	6353
112	3.94	3.76	0.343	0.360	3260
116	6.78	6.14	0.200	0.200	5919
111	6.20	6.18	0.218	0.219	5467
113	5.04	5.02	0.269	0.270	5723
125	5.06	6.45	0.267	0.210	3623
121	7.25	8.35	0.187	0.162	5327
118	4.53	5.88	0.299	0.230	5612
119	5.25	6.73	0.258	0.201	5550

Since FA = 15.0 in/min, then from equation (82)

$$\overline{\Pi}a = (10)(15) = 150 \text{ ft/hr.}$$

and from Figure 9 it can be seen that,

$$q_{PF} = 0$$

Using equation (117), q* may be calculated as,

$$q^* = (0.00398)(0.425)(0.855)(33.61-31.10)(60)(1.8)(62.4)$$

or

$$q^* = 11 \text{ Btu/hr.}$$

Since T_R = 30.2 °C and T_{Ca} = 50.4 °C, then employing equation (116),

$$\Delta T_L = 50.4 - 30.2 = 20.2 \text{ °C,}$$

and from Figure 10,

$$q_L = 13 \text{ Btu/hr.}$$

From equation (97), the heat of evaporation, q_e, was found to be,

$$q_e = 8 \text{ Btu/hr.}$$

Thus from equation (110) and (111),

$$q_c = 208 + 2 - 13 - 11 = 186 \text{ Btu/hr.}$$

and

$$q_b = 172 - 7 + 8 = 173 \text{ Btu/hr.}$$

Also from equations (104) and (105),

$$q_a = (186 + 173)/2 = 180 \text{ Btu/hr.}$$

and

$$\% \text{ deviation} = (186 - 173)/180 \times 100 = +7.2\%$$

Calculation of Heat Transfer Responses

From equation (119), the ln-mean temperature difference may be calculated as

$$\Delta T_{lm} = \frac{(48.71-33.61)-(52.01-51.12)}{2.303 \log (48.71-33.61)/(52.01-51.12)}$$

$\Delta T_{lm} = 3.01\ ^{o}C.$

or

$\Delta T_{lm} = 9.02\ ^{o}F.$

Thus from equations (34) and (35),

$$\bar{N}_{OD} = (51.12-33.61)/5.01 = 3.50$$

and

$$\bar{N}_{OC} = (52.01-48.71)/5.01 = 0.545$$

and from equations (41) and (42),

$$H\Theta U_{OC} = 1.354/3.50 = 0.387 \text{ ft.}$$

and

$$H\Theta U_{CD} = 1.354/0.545 = 2.48 \text{ ft.}$$

The overall volumetric heat transfer coefficient, Ua, may be from equation (52) as,

$$Ua = 180/(0.0261)(9.02) = 764 \text{ Btu/(hr)}(^{o}F)(ft^{3}).$$